QUADRUPEDAL LOCOMOTION WITH A UNILATERAL BONE-ANCHORED TRANSTIBIAL PROSTHESIS IN THE CAT

A Dissertation
Presented to
The Academic Faculty

By

Joshua R. Jarrell

In Partial Fulfillment
Of the Requirements for the Degree
Doctor of Philosophy in
Applied Physiology

Georgia Institute of Technology
December, 2017

QUADRUPEDAL LOCOMOTION WITH A UNILATERAL BONE-ANCHORED TRANSTIBIAL PROSTHESIS IN THE CAT

Approved by

Dr. Boris Prilutsky, Advisor
School of Biological Sciences
Georgia Institute of Technology

Dr. T. Richard Nichols
School of Biological Sciences
Georgia Institute of Technology

Dr. Young-Hui Chang
School of Biological Sciences
Georgia Institute of Technology

Dr. Lee Childers
School of Biological Sciences
Georgia Institute of Technology

Dr. Johnna Temenoff
School of Biomedical Engineering
Georgia Institute of Technology

Date Approved: October 31, 2017

ACKNOWLEDGEMENTS

I owe a lifetime of gratitude to my wife, Rainey, and our children, Tessa, Abby, and Isaac, for all their love and support. You empower me to perform my best in all my endeavors. I would also like to thank both my Ph.D. committee and the leadership of Alpha Company, 1st Battalion, 20th Special Forces Group for their continued patience and support as I strove to fulfill my duties and opportunities as both a researcher and soldier. The military demands sacrifices of entire communities, and you all were always willing to assist in any way you could. Finally, I'd like to thank my advisor, Dr. Prilutsky, for his continued mentorship and guidance over these past few years, and my colleagues Dr. Ricky Mehta, Ted Oh, and Dr. Hangue Park for their teamwork and friendship.

TABLE OF CONTENTS

LIST OF TABLES

LIST OF FIGURES

SUMMARY

Bone-anchored limb prostheses offer numerous advantages over conventional socket-supported prostheses. As opposed to socket prostheses, loads on a bone-anchored prosthetic limb during natural activities are directly transmitted to the residual bone, which prevents damage of skin and other soft tissues. Despite this and other documented advantages, however, bone-anchored prostheses have been limited in their availability in the United States due to an increased risk of skin and deep tissue infection through the skin-implant interface. A novel porous titanium pylon, the skin- and bone-integrating pylon (SBIP), has been developed to promote deeper tissue integration with the percutaneous implant and thereby reduce the risk of infection (Farrell et al., 2014c; Pitkin et al., 2009; Pitkin, 2012). Further research is needed to examine if the SBIP can be utilized for anchoring a limb prosthesis in natural load bearing applications. In veterinary medicine, gait changes in animals after limb loss and subsequent prosthesis intervention have not been extensively investigated. In addition, it is not completely understood how the motor system adapts to a loss of sensory feedback from the distal leg and to a reduced ability to absorb and generate mechanical energy for locomotion. Currently, detailed biomechanical analyses of such adaptations are missing. Therefore, the overall goal of my research was to investigate the effects of walking with a unilateral, transtibial, bone-anchored via SBIP prosthesis on mechanics and stability of quadrupedal locomotion and on tissue integration with the SBIP implant. The general hypothesis tested was that the SBIP would provide secure, infection free anchoring of a transtibial prosthesis and that would permit the cats to adopt the prosthesis for stable quadrupedal locomotion. In Specific Aim 1, I examined the ability of the SBIP to serve as attachment for a unilateral, transtibial bone-anchored prosthesis during walking in the

cat. In Specific Aim 2, I investigated dynamic stability by analyzing margins of dynamic stability and changes in angular impulse during quadrupedal walking with a unilateral bone-anchored passive transtibial prosthesis. In Specific Aim 3, I determined the amount of skin and bone ingrowth into the SBIP after the residual tibia had been loaded during natural motor activities including level and slope walking. The results of these investigations showed purposeful adoption of the bone-anchored prosthesis into the animals' chosen gait strategies. More specifically, normal ground reaction forces produced by the prosthetic limb were of substantial magnitudes (at least 50% of the pre implantation level), and tangential ground reaction forces, while significantly reduced, were statistically greater than zero and in the appropriate direction and timing across the gait cycle. Frontal-plane stability metrics deviated from the intact values to a lesser extent than in similar studies in human prosthetic gait. The histological results revealed deep bone and skin integration highly correlated with the duration of implantation and exceeded ingrowth of in a non-locomotive subject of similar implantation times. This study has provided important new information about the ability of the novel SBIP implants to be utilized for anchoring limb prostheses and about how the motor system of a quadrupedal animal adapts to a partial loss of the limb's ability to absorb and generate mechanical energy for locomotion.

CHAPTER I

BONE-ANCHORED LIMB PROSTHESES: THE NEXT STEP IN PROSTHESIS ATTACHMENT TECHNIQUE

1.1 History of Limb Prostheses

Amidst the innovations in prosthetic technology, living aids, and rehabilitative care, a potentially revolutionary method of prosthesis attachment directly to the residual limb bone has been developed. Known as bone-anchoring, or osseointegration, this method of attachment secures a prosthesis to the residual limb via a percutaneous titanium pylon mounted in the medullary canal of a long bone at the site of amputation (Branemark et al., 2001). To better understand the advantages of this approach, let's first review the development of limb prostheses and their corresponding attachment techniques.

The oldest preserved prosthesis was discovered in an Egyptian tomb circa 15th century BC (Figure **1**, left panel) (Nerlich et al., 2000). These and other early examples of prostheses were predominantly held onto the residual limb by the friction of a tight fit over the residual limb, leather straps wrapped circumferentially around the residual limb, or body weight during walking and controlled by a modified crutch (Thurston, 2007). The first major advancement in attachment design was accomplished by the 16th century French surgeon Ambroise Paré. Paré served as the royal surgeon of four consecutive French kings, and was responsible for major advances in combat medicine, specifically in the treatment of then-new gunshot wounds and corresponding hemostatic vessel ligation. He was also the first known medical professional to promote limb amputation as a life-saving intervention after military trauma (Hernigou, 2013). Consequently, Paré also

invested substantial time in improving prosthetic design and functionality, and among his lasting influential advancements is a suspension attachment technique for lower limb (LL) prostheses (Figure **1**, right panel) (Thurston, 2007; Wilson, 1970).

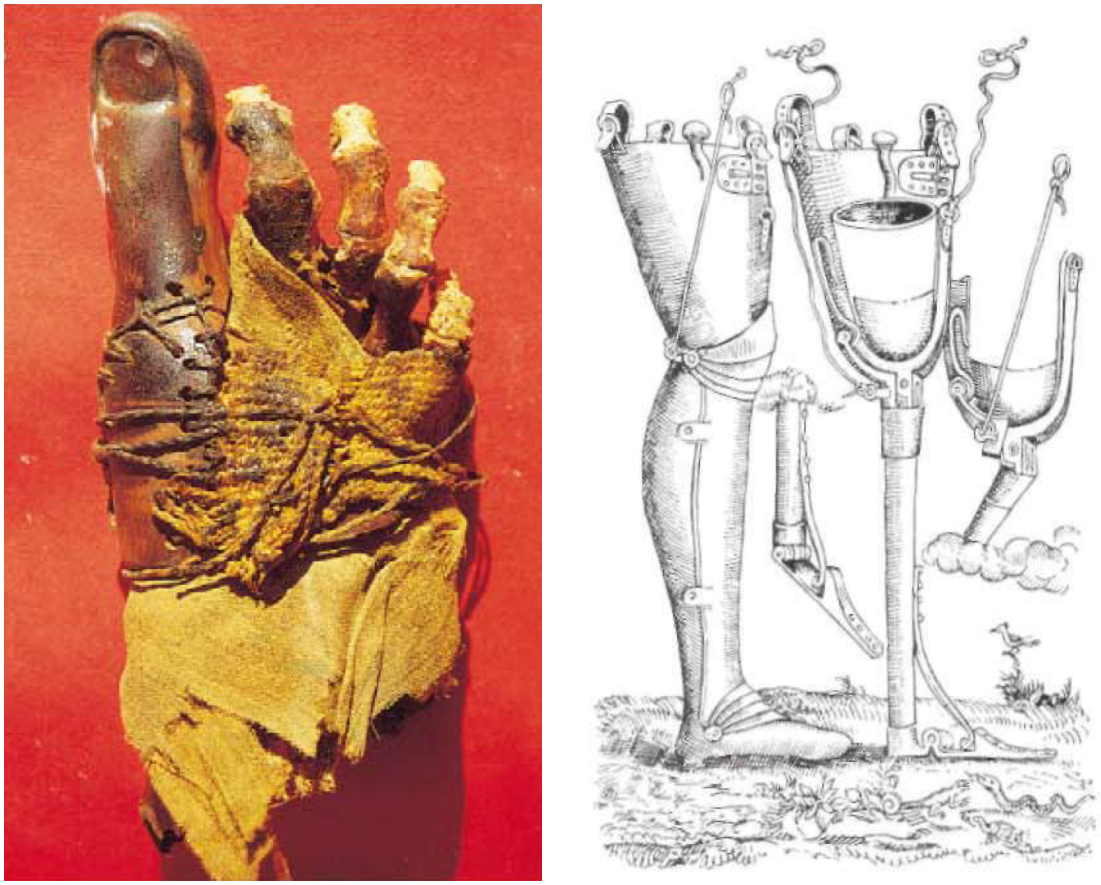

Figure 1: Early prosthetic attachment. Left: prosthetic hallux circa 1500 BC, attached to the forefoot with a primitive sleeve and lashings, from Nerlich, *et al*, 2000. Right: An artificial leg designed by Ambroise Paré, showing a novel suspension approach to prosthesis attachment, first published by Paré in *Oeuvres Completes*, 1940, referenced in Wilson, 1970.

The next significant advancement in LL prosthesis attachment was the use of atmospheric pressure (suction) in 1863 by Dubois Parmelee. However, this technique was not widely used until after WW2 (Fliegel, 1966). The development of patellar tendon

bearing sockets and elevated vacuum to improve liner fit (Board et al., 2001) aided in the reduction of common skin sores due to friction after residual limb volume changes during prosthetic use (Hachisuka et al., 1998; Zhang et al., 1998; Zhang et al., 1996).

Unfortunately, many skin, comfort, and functionality problems still exist with LL prostheses. The most commonly reported skin problems include pressure sores around bony prominences, bacterial and fungal infections, allergic reaction to the socket or liner material, and increased sweating or dryness inside the socket (Koc et al., 2008; Lyon et al., 2000; Meulenbelt et al., 2007). Many of these skin problems are attributed to the involvement of soft tissue in the residual limb-socket-prosthesis kinetic chain of load bearing (SilverThorn et al., 1996). In above-the-knee (AK) prostheses, the problems associated with socket-supported prostheses are even more intrusive, as AK amputees report higher rates of falls (Miller et al., 2001), back pain (Smith et al., 1999), and increased oxygen consumption and decreased gait speed (Jeans et al., 2011; Khiri et al., 2015).

1.2 Bone-Anchored Prostheses

Attempts to bypass the socket, as well as the load bearing skin of the distal residual limb, by anchoring a prosthesis into the bone of a residual limb have been attempted by many researchers over the past 150 years (Malgaigne, 2007; Murphy, 1973). Many such attempts were met with infection, avulsion, or implant marsupialization (von Recum, 1984). It was George Winter's work on percutaneous implants in the pig model in 1974 that described the process of downgrowth of epithelial cells along an interrupting percutaneous foreign object as marsupialization. He even suggested a porous layer around the percutaneous pylon in order to allow for tissue integration (Winter, 1974). To my knowledge, this is the first recommendation of porosity as a solution to the epithelial marsupialization problem of percutaneous implants. Interestingly, it is not in the context of

infection per se, but marsupialization. The same year, Dr. William Hall published a description of the marsupialization of buttons pressed into a human forearm after 7 months, which remains a seminal publication on the nature of epithelial cells (Hall, 1974).

Dr. Hall's publication touched upon additional questions regarding bone-anchoring a limb prosthesis, namely the security of the bone-anchor itself. He describes this issue using 3 different devices as percutaneous rods to anchor the prosthesis into the residual bone: sandblasted Vitallium, a more tightly-fitting Vitallium or steel rod, and a metal rod with a porous ceramic covering over the intramedullary portion. After being implanted into a caprine model, the first rod type became loose, the second was removed largely due to osteomyelitis, and the third came out mostly due to implant breaking (Hall, 1974). In addition to the skin integrity problems, one must also tackle the bone-implant interface problems as well. To adequately anchor limb prosthesis into the host's skeletal structure, the bone-implant interface must be secure and safe from infection, and the implant itself must be able to bear the forces that are expected during locomotion.

An important step towards a promising solution came from a Swedish doctor studying blood flow inside the bones of rabbit. In the 1950's, Dr. Per Ingvar Brånemark discovered bone cells' natural adhesion to implanted titanium (Rudy et al., 2008). While other researchers had described this titanium's unique property previously (Bothe, 1940), Brånemark was the first to push forward with new medical applications based specifically on this bone-titanium bonding. This developed into titanium-based dental implants anchored into the mandibular bone (Albrektsson et al., 1981; Manderson, 1972). With low infection rates (Adell et al., 1981) and the ability to withstand high forces of mastication (Haraldson and Carlsson, 1977), the first successful application of a percutaneous bone-anchored implant was established (Branemark, 1983; Zarb and Symington, 1983). Following dental implants, bone-anchored hearing aids were quickly researched and developed (Hakansson et al., 1985; Tjellstrom et al., 2001).

1.3 Advantages of Bone-Anchored Prostheses

Despite lingering infection risk (Branemark et al., 2014; Tillander et al., 2010), osseointegration has been performed on humans internationally since the 1990's (Aschoff et al., 2009; Aschoff and Juhnke, 2016; Branemark et al., 2001; Branemark and Thomsen, 1997; Juhnke and Aschoff, 2015; Ortiz-Catalan et al., 2014). Bone-anchored prostheses have been shown to offer many potential advantages over conventional socket-attached prostheses, due in large part to bypassing the residual limb distal soft tissue in locomotive loading. In a bone-anchored prosthesis, the forces of loading of the prosthetic limb from daily activities, including locomotion, are instead transmitted through the percutaneous pylon directly to the patient's skeletal system. By eliminating the need for soft tissue load bearing, individuals with bone-anchored prostheses report less residual limb skin problems (Hagberg and Branemark, 2009; Jonsson et al., 2011; Tranberg et al., 2011), improved comfort and confidence (Hagberg et al., 2008; Lundberg et al., 2011; Witso et al., 2006), easier donning and doffing of the prosthesis (Jonsson et al., 2011), as well as increased 6-minute walk distance and lower oxygen consumption (Van de Meent et al., 2013). Physiologically, a bone-anchored prosthesis increases range of motion and improves walking mechanics over socket-attached prostheses (Frossard et al., 2013; Hagberg et al., 2005; Tranberg et al., 2011), improves the user's perception of prosthesis loading, which has been termed osseoperception (Haggstrom et al., 2013a; Jacobs et al., 2000; Lundborg et al., 2006), and allows for improved myoelectric control of the prosthesis by providing a conduit through which implanted EMG or nerve cuff wires can connect directly to the prosthesis (Ortiz-Catalan et al., 2014; Pitkin et al., 2012a). Clinically, bone-anchored prostheses require fewer prosthetist visits than customary socket-attached prostheses (Haggstrom et al., 2013b).

Despite multiple advantages, however, bone-anchored prostheses have only recently become available to humans with limb amputations in the United States and only in limited applications (FDA, 2015). As detailed above, the two documented concerns preventing greater access to this technology are the high rate of skin infection/marsupialization at the skin-pylon interface (Isackson et al., 2011; Tillander et al., 2010) and the quality of implant integration inside the medullary canal (Dapunt et al., 2016; Shin et al., 2016; Tuan, 2011).

1.4 Problems of Skin Integration with Percutaneous Implants

High risk of skin infection (between 38 and 55%) at the skin-pylon interface has been reported in many studies, although in most cases this infection can be treated with antibiotics and rarely leads to deep bone infection and implant removal (Branemark et al., 2014; Tillander et al., 2010; Tsikandylakis et al., 2014). Nevertheless, there is a risk of deep infection, e.g. osteomyelitis (Montanaro et al., 2011), when a solid titanium pylon is used for attachment of a limb prosthesis to the bone. Therefore, implant design and procedures need to be continually improved to provide a stable skin-implant interface that can form a barrier to pathogens around the percutaneous implant. To this end, understanding of the mechanisms of skin infection associated with the percutaneous aspect of bone-anchored limb prostheses, and developing methods to mitigate this risk, has been the goal of several recent studies. Various animal models have been used in these studies, including rats (Farrell et al., 2014c; Pitkin et al., 2009), rabbits (Gerritsen et al., 2000; Jansen et al., 1990; Shevtsov et al., 2015), cats (Farrell et al., 2014b; Pitkin et al., 2009), dogs (Drygas et al., 2008; Fitzpatrick et al., 2011), sheep (Jeyapalina et al., 2014b; Shelton et al., 2011), goats (Hall, 1974), and pigs (Saunders et al., 2012).

Building on the original suggestion of porosity as a mechanism to prevent epithelial marsupialization (Winter, 1974), Dr. Catherine Pendegrass and her team investigated the properties of deer antlers, nature's own percutaneous bone-anchored implant (Pendegrass et al., 2006a; Pendegrass et al., 2006b), leading to many international labs attempting to anchor the epithelial layer in place via integration with the porous percutaneous pylon. In these and other studies, different implant designs and implantation strategies have been tested, including subdermal flanges mimicking natural antlers (Pendegrass et al., 2006b), thin porous titanium coating (Jeyapalina et al., 2012), pylon surface nano-modifications (Farrell et al., 2014c; Pendegrass et al., 2008), antimicrobial barrier pads (Perry et al., 2010), and deeply porous skin and bone integrated pylons with a perforated enforcing frame (Pitkin, 2013; Pitkin et al., 2012b; Pitkin et al., 2009). The latter pylon, the Skin- and Bone-Integrating Pylon (SBIP) has demonstrated deep skin ingrowth into the porous pylon (up to 60% of available volume within 6 weeks of implantation) and a low infection rate, 2.9%, in the rat model (Farrell et al., 2014c). These results suggest that integration of skin with a porous implant has the potential to form a barrier at the skin-pylon interface and reduce skin and deep tissue infection associated with bone-anchored prostheses.

While skin-pylon integration may hold important defense against infection, bone-pylon integration can protect against internal loosening or breaking of the anchoring implant. Pylon loosening or breaking represents a significant step backwards in rehabilitation and often requires extensive surgical revision (Aschoff et al., 2010; Chowdhary et al., 2011; Kramer et al., 2008; Tsikandylakis et al., 2014). Many techniques and pylon designs have been developed to increase stability of a bone-anchored percutaneous pylon (Aschoff et al., 2010; Gabler et al., 2014; Pitkin, 2013). Based on research of porosity promoting bone-pylon integration (Aschoff and Juhnke, 2016; Farrell

et al., 2014b; Jeyapalina et al., 2014b), the SBIP incorporates 40 – 100μm-sized pores with an overall porosity of 30-50% and volume size 40-45% (Pitkin et al., 2012b).

1.5 Limb Prosthetics in Veterinary Medicine

In veterinary medicine, trauma and osteosarcoma are the two most common indications for limb amputation (Galindo-Zamora et al., 2016; Szewczyk et al., 2015; Withrow and Hirsch, 1979). While much research has been done on limb-saving and alternative procedures (Kuntz et al., 1998; Lascelles et al., 2005; Liptak et al., 2006; Mitchell et al., 2016), amputation remains the standard of care for appendicular osteosarcoma (Mitchell et al., 2016; Szewczyk et al., 2015). Socket-supported prostheses have shown important but limited success in use in animals with a limb loss, especially in pursuit of chronic pain management (Adamson et al., 2005; Mich, 2014) resulting from tripedal gait adaptations (Fuchs et al., 2014; Galindo-Zamora et al., 2016; Kirpensteijn et al., 2000). Bone-anchored limb prostheses offer similar advantages in veterinary care as they do in human patients, with special emphasis on potential improvement in animal and owner compliance due to less restrictive and uncomfortable suspension equipment (Mich, 2014). Previous publications consistently report high rates of owner satisfaction and animal quality-of-life scores after limb amputation (Carberry and Harvey, 1987; Forster et al., 2010; Kirpensteijn et al., 1999; Withrow and Hirsch, 1979), although much concern still persists regarding long-term effects of chronically altered gait patterns and intact limb loading, especially for heavier animals (Dickerson et al., 2015; Kirpensteijn et al., 2000). While there has been much research on limb loading during tripedal gait in quadrupeds, little is known about full-body locomotor kinetic or kinematic changes after prosthesis intervention following limb amputation (Farrell et al., 2014b; Shelton et al., 2011). A better understanding of motor control adaptations following prosthesis attachment in quadrupeds

can support better-informed veterinary decisions regarding medical care and rehabilitation of animals suffering from debilitating limb pathologies.

The relationship between human medical research and veterinary medical research can be mutually supportive. Many medical devices, drugs, and procedures are first tested on non-human animals to ensure safety and efficacy before being used on humans (Jeyapalina et al., 2014a; Lu et al., 2010; Wanntorp, 1960). At the same time, many advances in human medicine, and rehabilitative research, are later tested for veterinary applications (Adams and Kurtz, 2006; Baggot and Giguere, 2013; Mich, 2014). A similar bidirectional relationship exists in biomechanics and motor control. While many studies have been published investigating fundamental motor control questions in quadrupeds and other animals (Gregor et al., 2006; Markin et al., 2016; Whelan, 1996), there is also a substantial amount of investigators committed to human studies of biomechanical changes after injury or pathology (Herr and Grabowski, 2012; Olney et al., 1991). Discoveries in one species or pathology can lead to new hypotheses and new investigations in other species or pathologies (Duysens and Pearson, 1998; Jahn et al., 2008). Therefore, prosthetic gait research in quadrupeds can simultaneously help shape rehabilitation and motor control theories in both quadrupeds and humans, while simultaneously borrowing from both human and quadruped biomechanical studies to shape the methods and hypotheses of future studies.

1.6 Evaluation of Pathological and Prosthetic Gait

Regarding human pathological gait as result of chronic disease, injury or aging, many researchers have contributed to the deepening understanding of the biomechanical changes (Chen et al., 2005; Ebersbach et al., 1999; Gutierrez et al., 2005; Hurley et al., 1990). These advances have helped improve protective devices of at-risk populations (Morone et al., 2016) and rehabilitative efforts for post-insult patients (Dobkin et al., 2006; Pan et al., 2017). In pursuit of this understanding, various metrics have been developed and analyzed in an effort to better assess gait stability and symmetry (Benedetti et al., 2013; Berg et al., 1992; Herr and Popovic, 2008; Hof et al., 2005). Such metrics may also help better predict falls (Lajoie and Gallagher, 2004; Verghese et al., 2009) and chronic injuries (Bateni and Maki, 2005; Devan et al., 2014). Two metrics used to quantify gait stability are dynamic stability and angular momentum.

Dynamic stability (DS) was developed by Hof (Hof, 2008; Hof et al., 2005) after identifying the limitations of static stability and improving the previous efforts to evaluate dynamic stability (Pai and Patton, 1997) during gait. DS has been used to study gait stability changes and limitations in persons with amputations (Curtze et al., 2016; Hof et al., 2007), stroke (Kajrolkar et al., 2014), spinal cord injuries (Gagnon et al., 2012), as well as multiple sclerosis (Peebles et al., 2016).

Whole-body angular momentum (H) refers to the rotational momentum of a body about its center of mass (CoM). In gait analysis, H is generally found to be relatively small, with little-to-no net change (cumulative angular impulse) over a complete stride (Bennett et al., 2011; Bruijn et al., 2011; Herr and Popovic, 2008). Previous investigations into the individual segment angular momentum during gait have reported evidence of H stability during swing and H modification during double-support phases of gait (Bennett et al., 2011; Robert et al., 2009). Likewise, H value at the onset of single-support was found to

correlate negatively with change in *H* during the same single support phase (Nott et al., 2014), supporting both the notion of *H* being a controlled variable and the adaptation occurring during single-support and swing phases. Accepted as a control variable, *H* has since been used to evaluate gait and control changes in persons with cerebral palsy (Bruijn et al., 2011), amputations (Gaffney et al., 2016; Sheehan et al., 2015), stroke (Nott et al., 2014; Vistamehr et al., 2016), at varying gait speeds (D'Andrea et al., 2014; Silverman and Neptune, 2011), and during walking on sloped surfaces (Pickle et al., 2016; Silverman et al., 2012).

While both *H* and DS have been studied extensively in human pathologic gaits, less research has been done evaluating the changes in these stability metrics in quadrupedal gait (Farrell et al., 2014a; Park, 2017). Investigating the stability changes in quadrupeds after amputation can help guide veterinary intervention and rehabilitation decisions in injured animals, as well as uncover similarities across mammalian motor control adaptations, giving rise to stronger support for motor control theories and future investigations.

1.7 Specific Aims

1.7.1 Goal of the study

Despite numerous advantages of bone-anchored limb prostheses, the infection rate at the interface between the skin and the skin-penetrating implant is the major challenge to this new technology (Branemark et al., 2014; Tillander et al., 2010). A porous titanium implant, the SBIP, has been developed as a percutaneous anchor for a bone-anchored limb prosthesis to resolve the issue of infection (Pitkin et al., 2012b; Pitkin et al., 2009). A previous study of the SBIP implanted in the skin of rats has demonstrated the potential for this pylon to improve skin-implant integration and reduce the skin infection

rate several fold (Farrell et al., 2014c). While the low infection rate in the rat model has been promising, the SBIP implants in that study were not subjected to loading associated with daily activities including walking. Further research is needed to examine if the SBIP can be utilized for anchoring limb prosthesis in natural load bearing applications. **The overall goal of my research was to investigate the effects of walking with a unilateral, transtibial, bone-anchored via SBIP prosthesis on mechanics and stability of quadrupedal locomotion and on tissue integration with the SBIP implant.** My work began with an investigation into the forces being applied to the SBIP during locomotion in order to confirm adoption of the prosthesis into chosen gait strategy and quantify changes in the moment and power production at the joints of each limb after implantation. My second aim focused on the whole-body stability changes after implantation and speaks to the broader efficacy of both bone-anchored prostheses, and specifically on a purposeful use of the SBIP as an anchoring pylon, in quadrupeds after limb amputation. The final phase of my work was to investigate the extent of skin and bone tissue ingrowth with the SBIP after the pylon has been loaded with the forces of daily locomotion. The histology work spoke to the potential of the SBIP to mitigate tissue infection and implant loosening by promoting deeper tissue integration with the porous SBIP. Here is each research aim in further detail:

1.7.2 Specific Aim 1

Examine the ability of the SBIP to serve as attachment for a unilateral, transtibial bone-anchored prostheses during walking in the cat. I tested the hypothesis that cats with an SBIP-attached unilateral transtibial prosthesis will utilize the prosthetic limb for walking, i.e. they will load the limb to at least 50% of pre-implantation values. In addition, I hypothesized that the decreased loading of the prosthetic limb (right hindlimb) will be compensated by increased loading, joint moments, and power in the

sound limbs, as reported for humans with a single limb loss (Barr et al., 1992; Fey et al., 2011; Segal et al., 2006).

After confirming prosthetic adoption in Aim1, I investigated how the bone-anchored prosthesis was used to provide coordinated and stable locomotion. Specifically, I studied the changes in lateral stability of walking after implantation with the SBIP-anchored limb prostheses.

1.7.3 Specific Aim 2

Determine lateral stability during quadrupedal walking with a unilateral bone-anchored passive transtibial prosthesis. The following hypotheses were tested. (1) The necessity to absorb and generate additional mechanical energy for propulsion by the contralateral hindlimb (CH) and greater loading of the contralateral limbs (Jarrell, 2014, 2016) will lead to a shift of the CoM towards the contralateral side and to a reduction of the margin of dynamic stability (MDS) on the contralateral side as reported in quadrupeds with anesthetized paws (Park, 2017). (2) The lack of paw cutaneous sensory feedback in the prosthetic limb will be compensated by a more lateral placement of the prosthesis to increase the MDS on the ipsilateral side, specifically during ipsilateral double-limb stance, as has been shown in humans with a unilateral prosthesis (Hof et al., 2007). (3) Cumulative angular impulse (cumulative change in H) will be zero after each stride but the range of angular impulse over the gait cycle will increase after implantation, specifically during contralateral stance phases of gait, as reported in human prosthetic gait (Sheehan et al., 2015).

After reporting evidence of adoption of the prosthetic limb into the subjects' daily gait strategies and quantifying changes in stability metrics, I next investigated the depth and extent of skin and bone integration with the porous SBIP. Previous histology studies

with the SBIP were promising, but were either not after loaded with daily locomotive forces (Farrell et al., 2014c), or solely qualitative (Farrell et al., 2014b).

1.7.4 Specific Aim 3

Determine the amount of skin and bone ingrowth into the SBIP after the residual tibia has been loaded during natural motor activities including locomotion. Two principle hypotheses were tested: (1) no signs of infection will be noted on the histological images and (2) the bone ingrowth in the SBIP after natural limb loading for 2-3 months will exceed the 20% ingrowth achieved in the implanted SBIP not subjected to daily locomotion loads (Pitkin et al., 2009). The first hypothesis was based on previous results of SBIP implantations in skin of rats demonstrating skin ingrowth into the SBIP of 60% within 6 weeks of implantation and a low infection rate of only 2.9% (Farrell et al., 2014c). Justification for the second hypothesis was the evidence that bone loading leads to bone remodeling and reinforcement (Bentolila et al., 1998; Burr et al., 1985; Lanyon and Rubin, 1984; Torcasio et al., 2008).

CHAPTER II

GENERAL METHODS

2.1 Percuataneous Bone-Anchoring Pylon

A completely porous pylon has been developed for use as a percutaneous skeletally mounted anchor for a bone-anchored limb prosthesis (Pitkin et al., 2007; Pitkin et al., 2009). The Skin- and Bone-Integrating Pylon (SBIP) consists of a solid cylindrical titanium core wrapped in titanium particles creating a matrix of 40-100 μm-sized pores with an overall porosity of 30-50% and volume size 40-45% (Pitkin, 2012). Implants were sized appropriately for the feline tibia: 5 cm long, 0.5 cm at the distal end and tapered to 0.3 cm at the proximal end to fit in the narrow tibial medullary canal. The pylon had porous cladding over its entire length with the exception of the most distal 0.7 cm that served as the attachment point for the ankle and paw prosthesis (Figure **2**) (Farrell et al., 2014b).

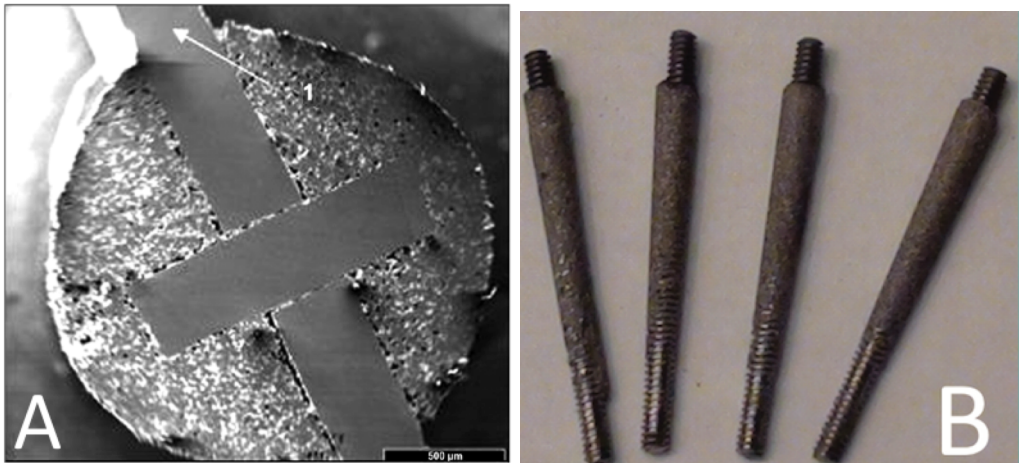

Figure 2: Skin- and Bone-Integrating Pylon (SBIP). A, cross-sectional image of the solid core and porous cladding, scale bar at bottom right represents 500μm, from Pitkin *et al*, 2009. B, images of intact SBIP implants of the kind used in this study.

2.2 Animals and Surgery

All experimental procedures have been in agreement with the US Public Health Service Policy on Humane Care and Use of Laboratory Animals and are approved by the Institutional Animal Care and Use Committees at both Georgia Institute of Technology and St. Joseph's Translational Research Institute (now known as T3 Labs).

Cats have been selected as an animal model of human locomotion because they exhibit patterns and normalized values of ground reaction forces during walking similar to those of humans (Lay et al., 2006; Prilutsky et al., 2011). In addition, cat segment inertial parameters are known (Hoy and Zernicke, 1985) and thus kinetic analysis of cat walking can be performed, e.g. (Farrell et al., 2014b; Gregor et al., 2006; Lavoie et al., 1995).

Eight adult purpose-bred cats (baseline mass range 2.8 to 3.6 kg, Table **1**) were used for this study. The cats were trained to walk along an enclosed walkway with 3 embedded force platforms (Bertec Corporation, Columbus OH, USA). The walkway was set at three slopes: 0% or 0^{o} (level), 50% or 27^{o} (upslope), and -50% or -27^{o} (downslope). These slopes were selected to impose different loading demands on the prosthetic limb, as forces exerted by hindlimbs on the ground increase from downslope to level and to upslope walking (Gregor et al., 2006; Prilutsky et al., 2011).

At the end of the training period, full-body kinematics and ground reaction forces were recorded by a 6-camera motion capture system (Vicon, UK) and the force platforms during level and sloped walking. Prior to implantation, sagittal and frontal plane X-ray images of the right tibia were taken to evaluate the size and shape of the medullary canal. Porous titanium SBIP implants were obtained from Poly-Orth International (Sharon, MA, USA). Implants were tapered to fit the tibial marrow cavity. After implantation surgery, performed in sterile conditions under isoflurane anesthesia, the residual limb with implant was casted for 10 weeks to prevent premature loading (Farrell et al., 2014b). During weeks

6 through 10 after implantation, the distal end of the protruding implant was loaded with gradually increased forces each week from ~4% to 45% of body weight, increasing by 10% each week. This process aimed to strengthen bone-implant integration and is similar in loading initiation time, duration, and magnitude to those used in individuals with press-fitted titanium implants for bone-anchored transfemoral prostheses (Aschoff et al., 2010; Juhnke and Aschoff, 2015). Starting with week 11, the cast was removed and the animal received a prosthesis. The cat was trained to stand and walk with food reward for four to six weeks. After the animal started walking with a J-shaped transtibial prosthesis, level and slope locomotion was recorded several days a week for at least four weeks. After locomotion data were collected, the animal was euthanized using deep anesthesia (an overdose of sodium pentobarbital, 120–180 mg/kg, IV) and the residual shank with the implant was harvested for histological analysis as described in Aim 3.

Table 1: Animal and Experimental Information

Cat	Base .mass (kg)	Term. mass (kg)	Implantation duration (days)	Walk w/ prosthesis	Aims Included	Reason for withdrawal
11GMQ51	2.8	3.0	7	No	3	Surgical complication
11GMJ42	3.6	4.0	33	No	3	Broke jaw – couldn't eat
11GLO43	3.2	3.0	173	No	3	Deep infection
11GMJ54	3.2	4.2	174	Partial	3	Broke pylon during collection
09NHT45	3.3	3.0	161	Yes	1, 2, 3	Study Completion
11NLS46	3.2	3.2	183	Yes	1, 3	Study Completion
QMV57	3.6	4.0	148	Yes	1, 2, 3	Study Completion
QM048	3.6	4.0	148	Yes	1, 2, 3	Study Completion

CHAPTER III

SPECIFIC AIM I

KINETICS OF INDIVIDUAL LIMBS DURING LEVEL AND SLOPE WALKING WITH A UNILATERAL TRANSTIBIAL BONE-ANCHORED PROSTHESIS IN THE CAT

3.1 Introduction

During overground walking, the body exerts forces on the ground to propel the body forward. Ground reaction forces (GRFs) can be measured by force plates during gait studies to quantify the amount of force exerted by individual limbs during locomotion (Sutherland, 2001). This approach has been used extensively for over 100 years (Lu and Chang, 2012) to evaluate differences in gait between species (Corbee et al., 2014), between different gaits within the same subjects (Pontzer et al., 2014; Segers et al., 2013), and between able-bodied and pathological gait within the same species (Bowden et al., 2006; DeVita et al., 1998; Dimiskovski et al., 2017). In this study, I recorded the GRFs exerted by the limbs of a cat during full-bodied and prosthetic walking. With these force values and the body position reconstructed via a motion capture system, I was able to perform inverse dynamics and calculate the moments, powers, and work performed by each limb. Previous publications on changes in kinetics in human amputees show a decrease in GRF produced by the prosthetic limb. In animal studies, two prosthetic walking studies showed a similar decrease in GRF through the prosthetic limb (Farrell et al., 2014b; Shelton et al., 2011), while these and tripedal, post-amputation, studies show

compensatory increases of the GRFs in the remaining sound limbs (Fuchs et al., 2014; Galindo-Zamora et al., 2016; Kirpensteijn et al., 2000).

The goal of this study was to examine the ability of the Skin- and Bone-Integrating Pylon (SBIP) to serve as an attachment point for a bone-anchored prosthesis during walking in the cat. We hypothesized that cats with an SBIP-attached unilateral transtibial prosthesis would utilize the prosthetic limb for walking, i.e. they would load the limb to at least 50% of pre-implantation values. In addition, I hypothesized that the lower loading of the prosthetic limb would be compensated by increased loading, joint moments, and power in the sound limbs.

3.2 Methods

3.2.1 Inverse Dynamics Analysis and Prosthesis Properties

A full-body inverse dynamics analysis in the sagittal plane was performed to determine the resultant moments at hindlimb and forelimb joints, their negative and positive power and work (Prilutsky and Klishko, 2011; Prilutsky et al., 2005) before implantation and during prosthetic walking. Negative values of joint moments corresponded to extension except the knee moment that had positive extension moments. Inertial properties of the prosthesis were determined using measurements of prosthesis weight, as well as suspension and geometric methods (Farrell et al., 2014b). Mass of the prosthesis was smaller than the estimated mass of the foot and distal third of the tibia that the prosthesis substituted (Table **2**).

3.2.2 Kinetic Variables Investigated

The time-dependent kinetic variables (tangential and normal ground reaction forces, GRFx and GRFz, respectively, and resultant joint moments and joint powers) were

time-normalized to the duration of the stride of the corresponding limb. Moments and powers were computed for individual joints of each limb: metatarsophalangeal, ankle, knee, and hip joints for hindlimbs and metacarpophalangeal, wrist, elbow and shoulder joints for forelimbs. Each time-normalized variable was averaged at each percent of the cycle across cycles of the corresponding limb and across cats. Total negative and positive work of each limb were obtained from the total limb power computed as the sum of powers in individual joints. All kinetic variables were also amplitude-normalized to subject's body mass. In addition, the mean walking speed in the cycle and the limb duty factor (the ratio of the stance to cycle duration) were calculated for each limb and cycle.

Sagittal-plane angle of the GRF generated by the IH paw was computed during able-bodied walking and prosthetic walking using the tangential (x) and normal (z) GRF components. Large angle fluctuations secondary to very low recorded tangential GRF magnitudes at stance onset and offset were mitigated by ignoring the first and last 10% of the stance period for each trial, in both the able-bodied and prosthetic walking conditions. Using this protocol, early-stance GRF angle was defined as the angle calculated at 10% of the stance phase of the gait cycle, late-stance GRF angle calculated at 90% of the stance phase, and the GRF range was calculated as the difference between the minimum and maximum GRF angles between 10% and 90% of stance. Range was only used during level walking, however, while in sloped walking it was substituted with average GRF calculated between 10% and 90% of the stance phase. The average GRF was used during sloped walking because the GRF ranges were very small in these conditions and changes in the GRF range were less informative than changes in average direction of the GRF vector.

3.2.3 Statistical Tests

IBM SPSS Statistics software, v20 (IBM SPSS, Chicago IL, USA) was used for statistical tests. To test for significant differences in peaks of kinetic variables (peaks of positive and negative GRF, extension and flexion moments, positive and negative power) between intact and prosthetic walking, limbs, and slopes, a mixed linear model analysis was used. Walking condition (intact, prosthetic), limb (ipsilateral hindlimb, IH; ipsilateral forelimb, IF; contralateral hindlimb, CH; contralateral forelimb, CF), and walking slope (level, downslope, upslope) were set as fixed factors. Cats were considered a random factor. To account for a possible influence of the walking speed on kinetic variables (Lelas et al., 2003), the cycle time of the corresponding limb was used as a covariate. The cycle time was considered a better covariate than speed due to interlimb variability of cycle time.

To compare patterns of kinetic variables within the walking cycle between intact and prosthetic walking, the wavelet-based functional ANOVA (wfANOVA) analysis was used (McKay et al., 2013; Potocanac et al., 2016). This method reveals differences in the shape and magnitude of time-dependent variables with both high temporal resolution and high statistical power (McKay et al., 2013). Significance level in all statistical tests was set at 0.05.

Table 2: Subject Information

Cat Characteristics	09NHT4 (Cat #5)	11NLS4 (6)	QMV5 (7)	QM04 (8)	Mean ± SD
Baseline mass, kg	3.2	3.2	3.0	3.2	3.15±0.10
Terminal mass, kg	3.4	2.8	4.0	4.0	3.55±0.57
Estimated mass of the foot and distal third tibia, g	52.5	49.5	51.2	54.1	51.8±2.0
Estimated moment of inertia of the foot and distal third tibia, gcm^2	326	279	281	290	294±22
Baseline walking speed, m/s					
Level	0.46±0.02	-	0.54±0.04	0.67±0.06	0.56±0.10
Downslope	0.55±0.06	0.58±0.10	-	0.75±0.14	0.61±0.13
Upslope	0.40±0.07	0.71±0.20	-	0.56±0.21	0.55±0.20
Terminal walking speed, m/s					
Level	0.39±0.03	-	0.40±0.03	0.50±0.07	0.44±07*
Downslope	0.32±0.08	0.59±0.07	-	0.61±0.07	0.47±0.16*
Upslope	0.41±0.09	0.42±0.04	-	0.54±0.14	0.47±0.12*

Notes: The term 'Terminal' designates measurements taken several days before euthanasia. Mass of the prosthesis and moment of inertia with respect to the frontal axis through the prosthesis center of mass were similar across 4 cats: 17.0±2.1 g and 164.5±10.6 gcm^2. Asterisks '*' indicate significant difference ($p<0.05$) between intact and prosthetic walking. Data for slope walking in cat QMV5 were not collected. Data of cat 11NLS4 for level intact walking were of poor quality and could not be analyzed. Since there were no intact control data for this cat during level walking, prosthetic level walking was not collected. Number of analyzed cycles per limb in each slope condition were as follows (intact/prosthesis walking condition): Level walking: Ipsilateral hindlimb (IH) – 14/15, Contralateral hindlimb (CH) – 12/13, Ipsilateral forelimb (IF) – 14/21, Contralateral forelimb (CF) – 13/15; Downslope walking: IH – 12/14, CH – 17/11, IF – 14/15, CF – 19/13; Upslope walking: IH – 17/14, CH – 16/13, IF – 13/10, CF – 13/12.

3.3 Results

No signs of discomfort or pain were observed (the absence of limb withdrawal during the post-surgical pylon loading in weeks 6 through 10, see Chapter 2: General Methods). Behavioral observations of the prosthesis use indicated that the cats engaged the prosthesis for standing, walking, and, occasionally, jumping. The animals investigated in the locomotion experiments did not have clinical signs of skin infection at the skin implant interface, i.e. no skin redness, swelling, or pus were observed.

3.3.1 Walking Speed and Duty Factor

Walking speed decreased significantly during prosthetic walking compared to intact walking in all three slope conditions (Table **2**): by 22% in level ($F_{1,97} = 13.4$, $p<0.001$), by 23% in downslope ($F_{1,99} = 11.9$, $p<0.001$), and by 14% in upslope ($F_{1,99} = 5.2$, $p=0.025$) walking. The duty factor of the prosthetic hindlimb significantly decreased compared to the pre-surgery values during downslope (by 22%, $F_{1,313} = 33.8$, $p<0.001$) and upslope (by 11%, $F_{1,313} = 9.0$, $p=0.003$) walking, but not during level walking ($F_{1,313} = 1.7$, $p=0.191$). The duty factor of the contralateral hindlimb and forelimb increased in all slope conditions by 10%-17% ($F_{1,313} = 8.5 – 25.0$, $p\leq0.004$), whereas there was no significant change in the duty factor of the ipsilateral forelimb in any slope condition ($F_{1,313} = 0.001 - 1.5$, $p=0.214 – 0.973$).

3.3.2 Ground Reaction Forces

GRFz applied to the prosthetic hindlimb was significantly lower than in the same hindlimb before surgery in level, downslope and upslope conditions throughout most of the stance phase (wfANOVA, $p<0.05$; Figure **3**). GRFz of the contralateral hindlimb and forelimb increased during prosthetic walking in various periods of the stance phase of all

slope conditions (wfANOVA, $p<0.05$), whereas small (level walking) or no changes (downslope, upslope) occurred in the ipsilateral forelimb GRFz (Figure **3**). Peaks of GRFz of the prosthetic hindlimb decreased by 30%, 45%, and 46% during level, downslope, and upslope walking, respectively ($F_{1,312}$ = 27.1 - 90.5, $p < 0.001$). The GRFz peak of contralateral hindlimb and forelimb increased during prosthetic walking in all slope conditions in the range of 16%-60% ($F_{1,312}$ = 11.1 - 68.0, $p \leq 0.001$). A small significant increase in GRFz peak of ipsilateral forelimb occurred during prosthetic level walking (10%, $F_{1,313}$ = 4.5, $p = 0.035$).

GRFx values of the prosthetic hindlimb were lower after implantation throughout most of the stance phase duration in all slope walking conditions (as revealed by the wfANOVA, $p<0.05$, shaded areas in Figure **4**). GRFx values in the contralateral hindlimb and forelimb were higher in substantial portions of stance during prosthetic walking (wfANOVA, $p<0.05$). Compared to intact walking, ipsilateral forelimb GRFx during prosthetic walking was slightly but significantly higher in the terminal period of stance in upslope condition, and it was lower in the initial and terminal periods of stance in level condition. No difference in ipsilateral forelimb GRFx between prosthetic and intact walking was observed in downslope condition ($p>0.05$; Figure **4**). GRFx peaks in the prosthetic hindlimb were lower than during intact walking in level (acceleratory force by 59%: $F_{1,316}$ = 25.7, $p < 0.001$; braking force by 52%: $F_{1,316}$ = 14.9, $p < 0.001$), downslope (braking force by 66%: $F_{1,316}$ = 133.3, $p < 0.001$), and upslope conditions (acceleratory force by 54%; $F_{1,316}$ = 181.8, $p < 0.001$). GRFx peaks of the contralateral hindlimb and forelimb were higher in downslope (braking force by 22 - 33%: $F_{1,316}$ = 31.2 – 47.7, $p < 0.001$) and upslope (acceleratory force by 21 – 85%: $F_{1,316}$ = 29.4 – 143.8, $p < 0.001$) conditions of prosthetic walking (Figure **4**). All peak GRFx values in all cats were significantly greater

than zero, however, with the exception of acceleratory force in downslope walking (all three cats with sloped walking data) and level walking braking force in Cat 5 (Table **3**).

Table 3: Normal and tangential tests against zero. P-values less than 0.05 represent average values significantly greater than or less than zero.

All values are means ± SD (N/kg)	09NHT4 (Cat #5)	11NLS4 (6)	QMV5 (7)	QM04 (8)
		Normal Ground Reaction Force (GRFz)		
Level	4.30±0.132 p<0.001		3.99±0.215 p<0.001	2.07±0.400 p<0.001
Downslope	3.60±0.703 p<0.001	1.35±0.218 p<0.001		1.01±0.146 p=0.007
Upslope	2.66±0.892 p=0.003	3.39±0.250 p<0.001		2.23±0.658 p=0.007
		Acceleratory Ground Reaction Force (+GRFx)		
Level	0.418±0.035 p=0.002		0.510±0.178 p=0.001	0.280±0.047 p<0.001
Downslope	0.033±0.044 p=0.167	0.030±0.032 p=0.07		0.047±0.037 p=0.160
Upslope	1.13±0.603 p=0.014	1.38±0.247 p<0.001		1.24±0.438 p=0.011
		Braking Ground Reaction Force (-GRFx)		
Level	-0.338±0.201 p=0.100		-0.480±0.098 p<0.001	-0.209±0.049 p<0.001
Downslope	-1.18±0.308 p=0.001	-0.267±0.050 p<0.001		-0.277±0.037 p=0.006
Upslope	-0.265±0.122 p=0.008	-0.086±0.045 p=0.013		-0.171±0.052 p=0.007

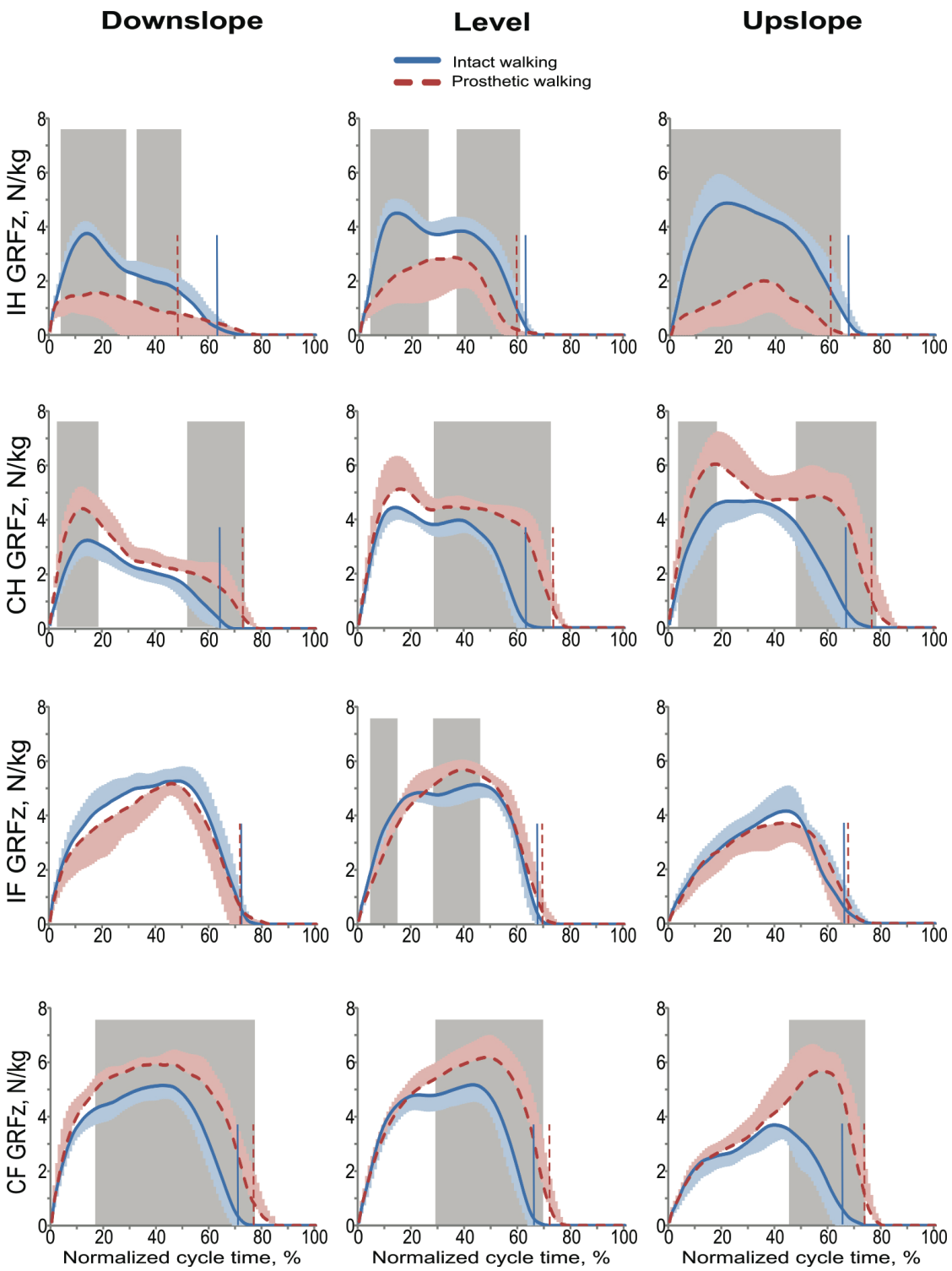

Figure 3: Normalized normal ground reaction forces (GRFz) during the cycle of intact (before surgery) and prosthetic (after surgery) walking in downslope (-27°), level (0°), and upslope (+27°) conditions. Mean (+SD or -SD) data of 4 animals. The vertical dashed and solid lines separate stance and swing phases for prosthetic and intact walking, respectively. The shaded areas in each panel indicate significant difference ($p<0.05$) between the intact and prosthetic walking determined using wfANOVA analysis. CH, contralateral hindlimb; IH, ipsilateral hindlimb (prosthetic limb in Post condition); IF, ipsilateral forelimb; CF contralateral forelimb.

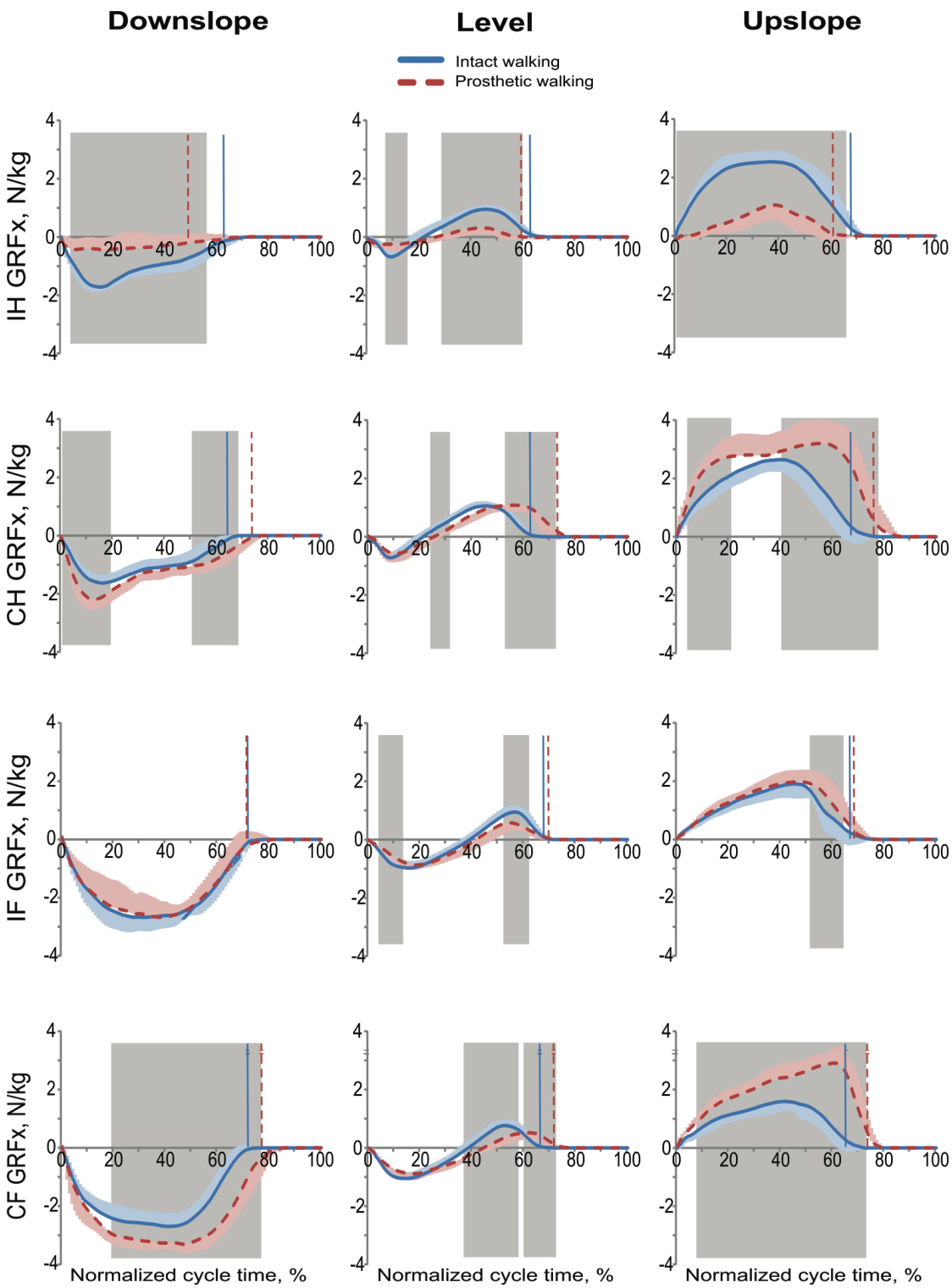

Figure 4: Normalized anterior-posterior ground reaction forces (GRFx) during the cycle of intact (before surgery) and prosthetic (after surgery) walking in downslope (-27°), level (0°), and upslope (+27°) conditions. Mean (+SD or -SD) data of 4 animals. The vertical dashed and solid lines separate stance and swing phases for prosthetic and intact walking, respectively. The shaded areas in each panel indicate significant difference ($p<0.05$) between the intact and prosthetic walking determined using wfANOVA analysis. CH, contralateral hindlimb; IH, ipsilateral hindlimb (prosthetic limb in Post condition); IF, ipsilateral forelimb; CF contralateral forelimb.

The sagittal-plane angle of the IF GRF vector also revealed significant changes. During level walking, late-stance GRF angle decreased from 17.3±2.4° anterior to 3.3±13.4° anterior ($F_{1,29}$=26.8, p<0.001) and the average GRF angle in the middle 80% of stance decreased from 5.6±2.9° anterior to 0.18±4.7° anterior ($F_{1,33}$=16.9, p<0.001). During downslope walking, the early-stance GRF angle decreased from 23.4±3.5° posterior to 14.4±7.4° posterior ($F_{1,51.3}$=8.23, p=0.006), the late-stance GRF angle decreased from 18.0±8.8° posterior to 3.4±19.9° posterior ($F_{1,51.1}$=4.11, p=0.048), and the average GRF angle during the middle 80% of stance decreased from 24.6±3.1° posterior to 11.0±4.9° posterior ($F_{1,51.1}$=42.8, p<0.001). During upslope walking, early-stance GRF angle decreased from 23.3±5.0° anterior to 1.8±13.0° posterior ($F_{1,51.9}$=82.7, p<0.001), late stance GRF angle decreased from 28.1±7.0° anterior to 1.9±28.1° anterior ($F_{1,51.8}$=18.7, p<0.001), and average GRF angle during the middle 80% of stance decreased from 28.7±3.1° anterior to 14.6±9.5° anterior ($F_{1,51.4}$=59.4, p<0.001).

Differences between GRF angle and leg angle during level walking. During downslope walking, late-stance angle difference decreased significantly from -37.2±8.2° to 0.55±24.9° ($F_{1,51.1}$=20.4, p<0.001). A negative angle difference means the GRF angle was more posteriorly oriented than the leg angle. The average angle difference decreased significantly from -17.3±5.4° to 6.3±6.9° ($F_{1,51.7}$=35.8, p<0.001). During upslope walking, the early-stance angle difference decreased significantly from 33.1±6.4° to 2.9±19.5° ($F_{1,53}$=56.4, p<0.001), late-stance angle difference from -17.6±5.5° to 2.0±14.9° ($F_{1,51.4}$=8.5, p=0.005), and average angle difference from 12.9±5.0° to -0.17±17.5° ($F_{1,52.8}$=13.2, p=0.001).

3.3.3 Joint Moments

The peaks of the ipsilateral knee extension moment decreased during prosthetic walking by 37% ($F_{1,313} = 26.0$, $p < 0.001$), 63% ($F_{1,313} = 65.9$, $p < 0.001$), and 38% ($F_{1,313} = 29.5$, $p < 0.001$) in level, downslope and upslope conditions, respectively (Figure **5**). The knee extension moment of the contralateral hindlimb was higher in late stance of prosthetic walking than during intact walking in all slope conditions (wfANOVA, $p<0.05$). The peaks of the contralateral extension moment were also higher during prosthetic level and upslope walking (Figure **5**). The resultant moment at the ipsilateral knee during both intact and prosthetic walking was mostly extension in the stance phase of all slope conditions, although moment values were substantially reduced during prosthetic walking (wfANOVA, $p<0.05$), except at the early stance in upslope condition (Figure **6**).

The hip moment in the prosthetic limb during the stance phase was mostly extension in level and downslope conditions, and was close to zero in upslope condition (Figure **6**). Before implantation, the hip moment in the same limb changed direction from extension to flexion in the stance phase. As a result, peaks of hip extension moment of the prosthetic limb were smaller than those at the same joint during intact upslope walking, whereas the peak flexion moments were lower in downslope condition ($F_{1,313} = 48.6$, $p < 0.001$; Figure **5**).

The elbow moment in ipsilateral and contralateral forelimbs were mostly extension in both intact and prosthetic walking in all slope conditions (Figure **7**). The elbow extension moment magnitudes were greater during prosthetic walking in level conditions in both forelimbs and in upslope condition in the contralateral forelimb (wfANOVA, $p<0.05$; Figure **5**, Figure **7**). The extension elbow moment in the contralateral forelimb was lower during the stance phase of downslope prosthetic walking (wfANOVA, $p<0.05$; Figure **5**, Figure **7**). There was a much larger flexion moment in the contralateral elbow during the

terminal stance phase of prosthetic downslope walking than before the implantation surgery (wfANOVA, $p<0.05$).

Shoulder flexion moments were substantially greater in the contralateral forelimb during prosthetic walking than in the intact condition (wfANOVA, $p=0.05$; Figure **5**, Figure **7**). Shoulder moments in the contralateral and ipsilateral forelimbs were mostly flexion during prosthetic and intact level and downslope walking; in upslope conditions, the moment sign switched from extension to flexion in mid stance (Figure **7**).

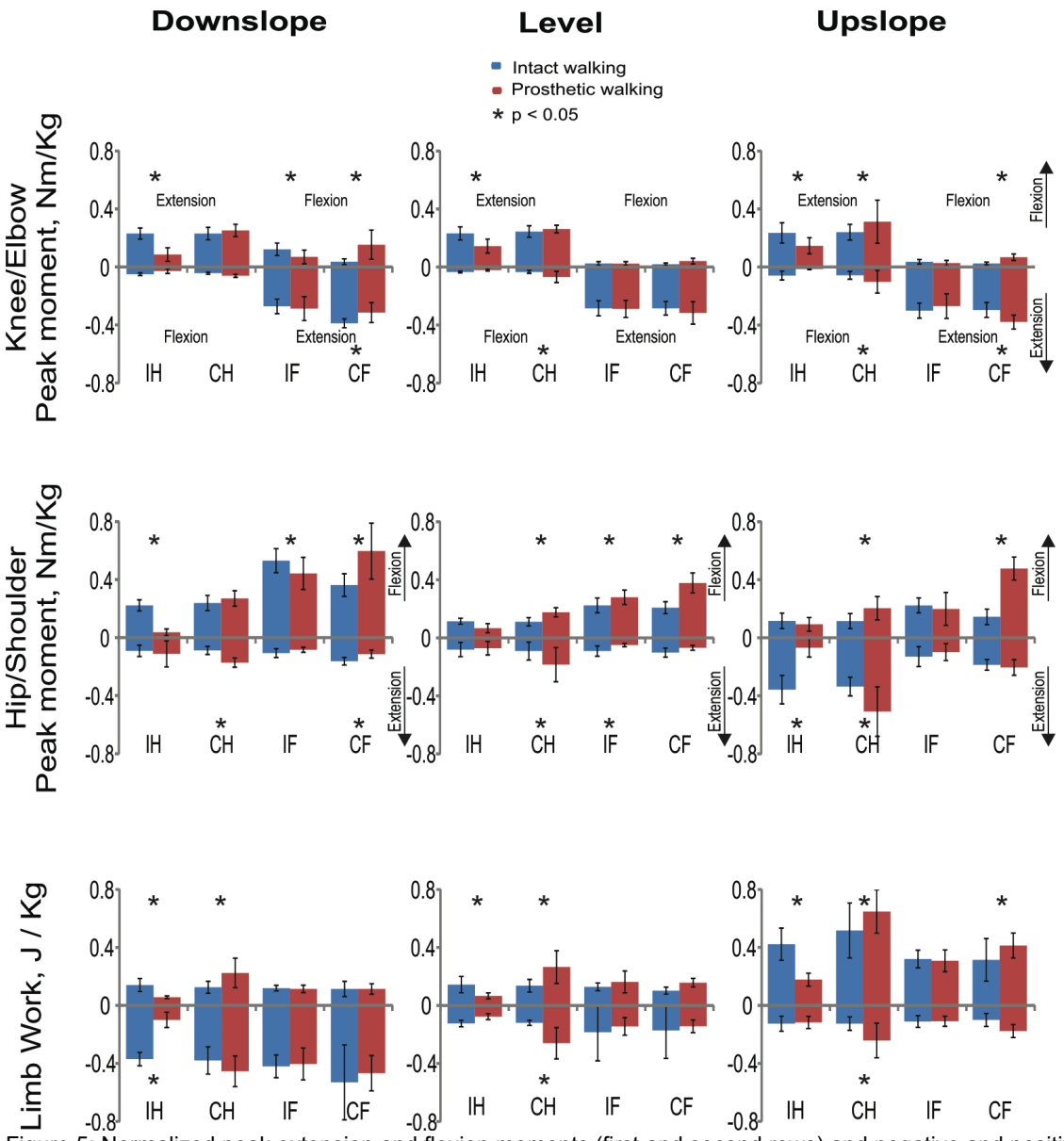

Figure 5: Normalized peak extension and flexion moments (first and second rows) and negative and positive work done by four limbs (third column) during the cycle of intact (before surgery) and prosthetic (after surgery) walking in downslope (-27°), level (0°), and upslope (+27°) conditions. Mean (+SD or -SD) data of 4 animals. CH, contralateral hindlimb; IH, ipsilateral hindlimb (prosthetic limb in Post condition); IF, ipsilateral forelimb; CF contralateral forelimb.

Asterisks indicate significant differences ($p<0.05$) between pre and post implantation conditions.

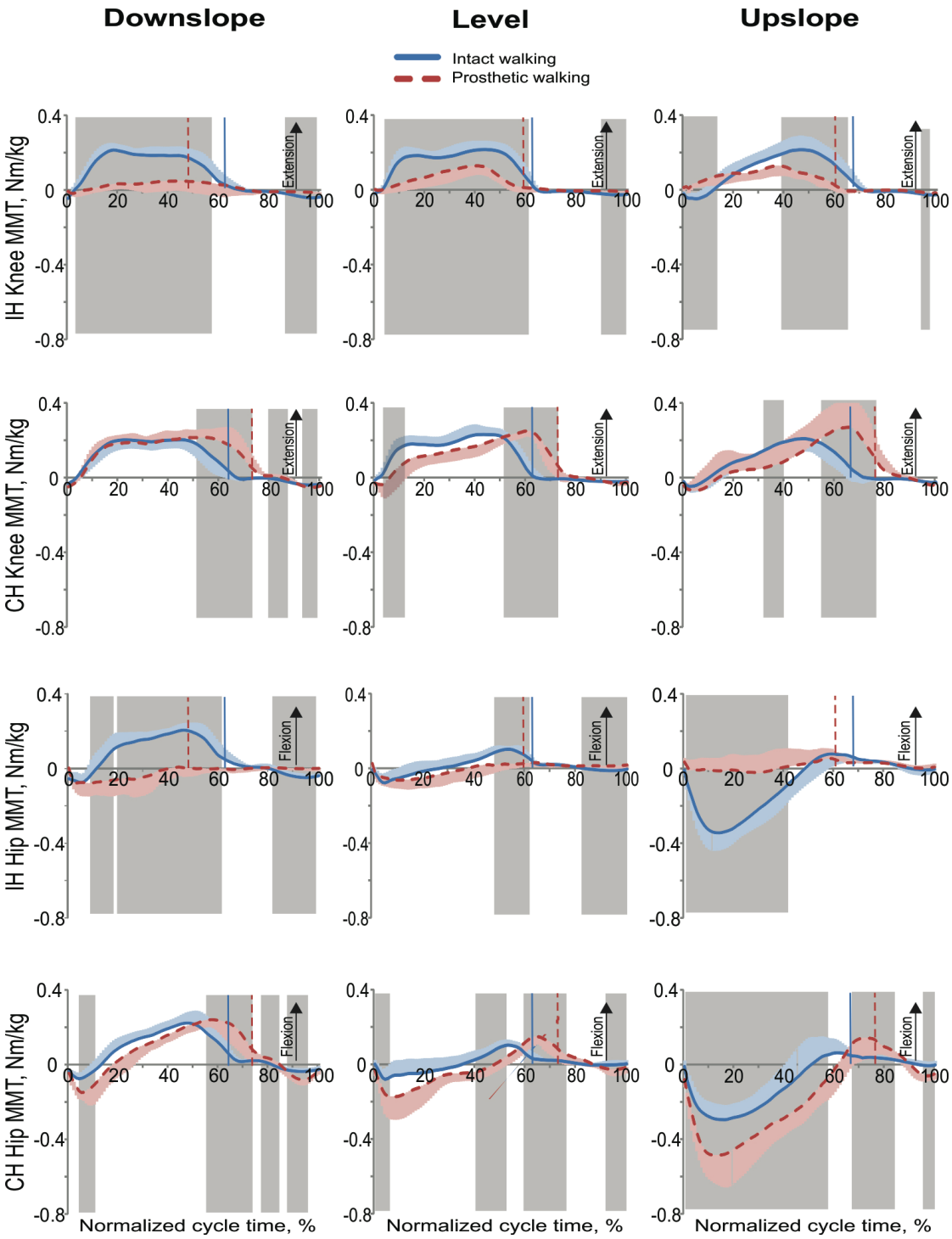

Figure 6: Normalized resultant moments at the knee and hip joints during the cycle of intact (before surgery) and prosthetic (after surgery) walking in downslope (-27^{o}), level (0^{o}), and upslope (+27^{o}) conditions. Mean (+SD or -SD) data of 4 animals. The vertical dashed and solid lines separate stance and swing phases for prosthetic and intact walking, respectively. The shaded areas in each panel indicate significant difference ($p<0.05$) between the intact and prosthetic walking determined using wfANOVA analysis. CH, contralateral hindlimb; IH, ipsilateral hindlimb (prosthetic limb in Post condition); IF, ipsilateral forelimb; CF contralateral forelimb.

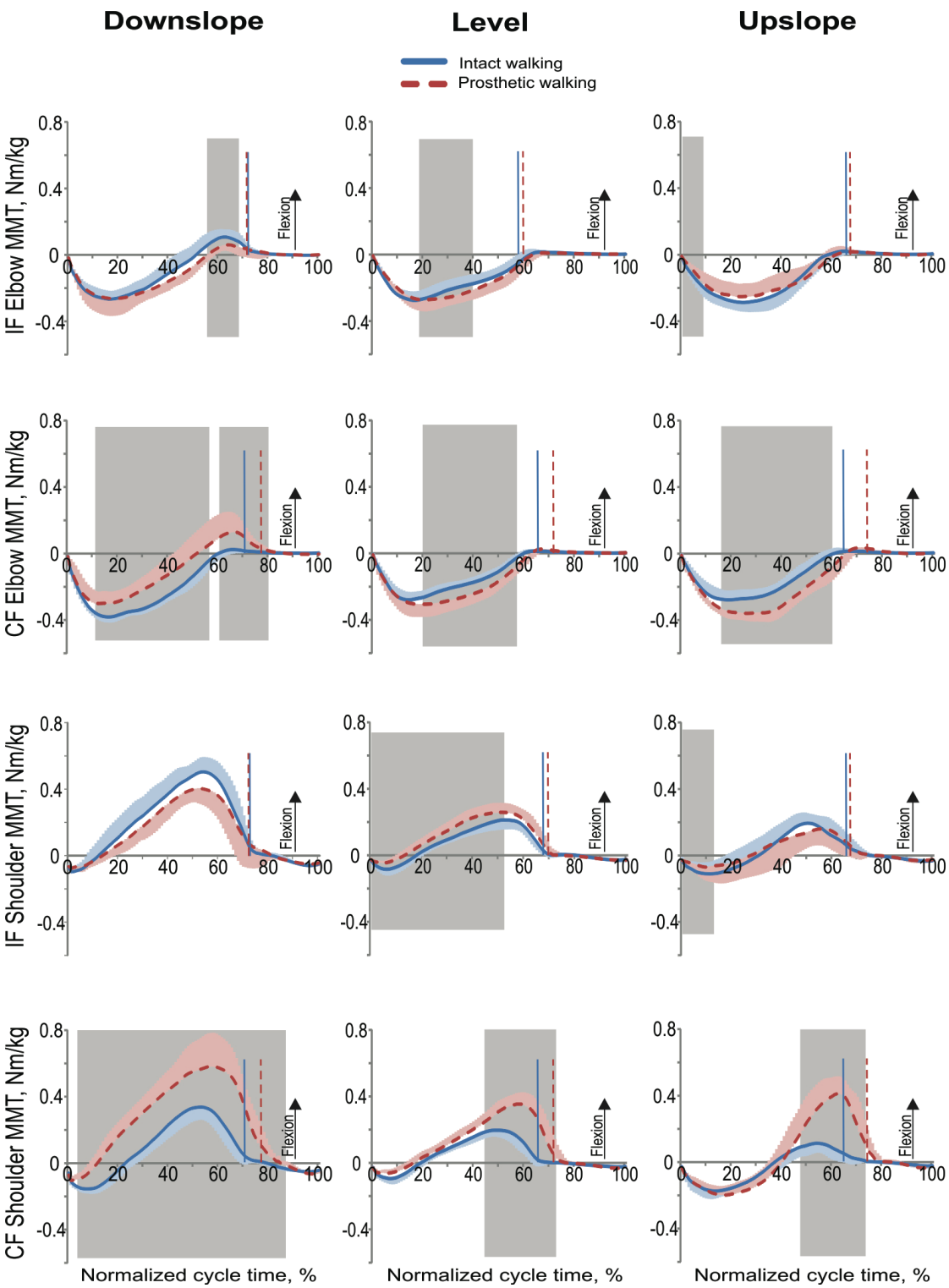

Figure 7: Normalized resultant moments at the elbow and shoulder joints during the cycle of intact (before surgery) and prosthetic (after surgery) walking in downslope (-27°), level (0°), and upslope (+27°) conditions. Mean (+SD or -SD) data of 4 animals. The vertical dashed and solid lines separate stance and swing phases for prosthetic and intact walking, respectively. The shaded areas in each panel indicate significant difference ($p<0.05$) between the intact and prosthetic walking determined using wfANOVA analysis. CH, contralateral hindlimb; IH, ipsilateral hindlimb (prosthetic limb in Post condition); IF, ipsilateral forelimb; CF contralateral forelimb.

3.3.4 Total Limb Power and Work

Little power was generated and work was done by the prosthetic hindlimb in all slope conditions (Figure **5**, Figure **8**). During intact walking, the same hindlimb produced negative power (absorbed mechanical energy) in the stance phase of downslope walking and first third of stance of level walking; positive power (energy generation) was produced in last two thirds of the stance phase of level walking and during the entire stance of upslope walking. The contralateral hindlimb produced higher negative and positive power and work during prosthetic walking in all slope conditions (wfANOVA, p=0.05; Figure **5**, Figure **8**).

Forelimbs produced primarily negative power and did negative work during intact walking in downslope and level conditions. During prosthetic level walking, both contralateral and ipsilateral forelimbs generated mostly positive power and work. During prosthetic downslope walking, the contralateral forelimb produced more negative power in the end of stance (wfANOVA, p=0.05; Figure **8**). There was less difference in power generation and work done between prosthetic and intact walking in the ipsilateral forelimb (Figure **5**, Figure **8**).

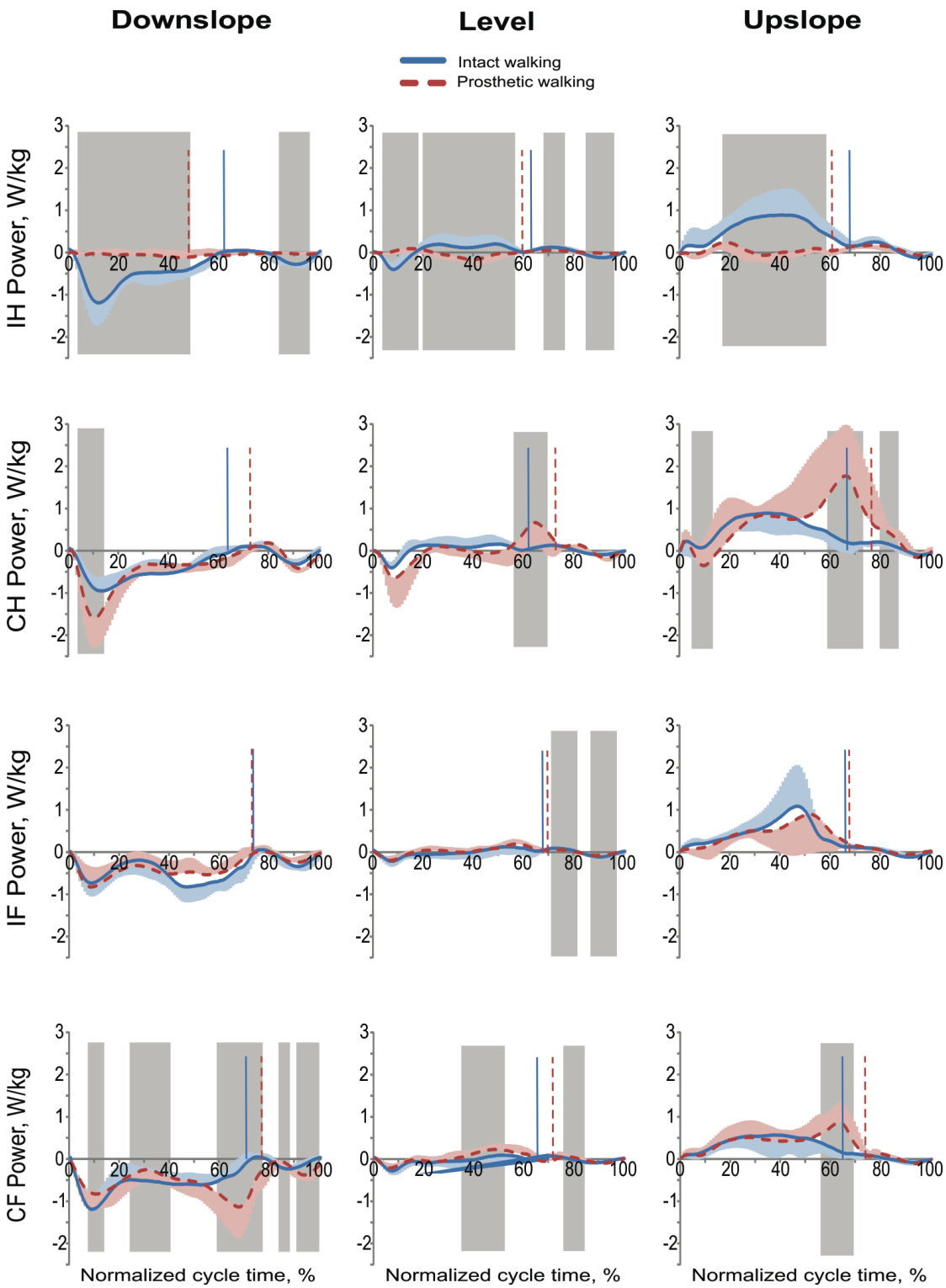

Figure 8: Normalized power of each limb during the cycle of intact (before surgery) and prosthetic (after surgery) walking in downslope (-27°), level (0°), and upslope (+27°) conditions. Mean (+SD or -SD) data of 4 animals. The vertical dashed and solid lines separate stance and swing phases for prosthetic and intact walking, respectively. The shaded areas in each panel indicate significant difference ($p<0.05$) between the intact and prosthetic walking determined using wfANOVA analysis. CH, contralateral hindlimb; IH, ipsilateral hindlimb (prosthetic limb in Post condition); IF, ipsilateral forelimb; CF contralateral forelimb.

3.4 Discussion

3.4.1 Ground Reaction Forces

The results of the study partially supported the hypothesis that cats with a SBIP-attached unilateral transtibial prosthesis would load the limb to at least 50% of pre-implantation values. The normal GRFz applied to the prosthesis during walking exceeded 50% of the intact walking values. Peak GRFx values, however, were only between 34% (braking force in downslope walking) and 48% (braking force in level walking) of the intact values. One possible explanation for the bigger decrease in GRFx compared to GRFz forces exerted by the prosthetic limb could be the reduced ability of the animal with a passive ankle to exert substantial tangential forces without slipping. The requirement to prevent slipping during stance might have forced the animal to reduce the ratio of the tangential to normal forces, known as the required coefficient of friction (Redfern et al., 2001).

There were no observed clinical signs of discomfort or pain while loading the implant and prosthesis and no signs of infection on x-ray and histological images at the end of the study (discussed in detail in Chapter 5). Therefore, it is unlikely that the reduced loading of the prosthetic limb was caused by discomfort or pain. Another possible explanation for the reduced loading might be the non-optimal length, alignment of the prosthesis and shape of the rocker bottom. These parameters were selected to approximately match the hindlimb length and orientation during the stance phase of normal cat walking (Farrell et al., 2014b). Also, the decreased loading of the prosthetic limb may reflect the limited ability of the cat with the transtibial prosthesis, which lacks an active ankle joint, to generate a sufficient amount of mechanical energy for propulsion. Note that the intact ankle in the cat does approximately 35% of total hindlimb positive work during level and upslope walking (McFadyen et al., 1999; Prilutsky and Klishko, 2011).

Changes in GRF angles after implantation show a significant reduction in early-stance posterior angle, late-stance anterior angle, and average angle throughout stance. All these changes are towards a more vertically-oriented GRF corresponding to a disproportionately greater reduction in tangential GRF than normal GRF during prosthetic walking. Furthermore, the significant magnitude decreases in GRF-leg angle difference reveals a GRF more closely aligned with the angle of the limb. Previous studies have suggested a decrease in GRF-leg angle difference may be an attempt to reduce moments about the knee (Chang et al., 2000), which may be a greater necessity during pathologic gait in which limb control is reduced. An additional motive for the decrease in GRF angles during prosthetic gait could be an attempt to prevent slipping, as a major factor in friction and slipping is the ratio of shear forces to normal force (Zatsiorsky, 2002), which is represented in this study by GRF angle. Further investigation is needed to determine whether the changes in GRF angle are the result of purposeful strategy to reduce joint moments or simply a byproduct of physiological changes that effect the tangential forces to a greater degree than the normal forces.

3.4.2 Moments and Power

I also hypothesized that the lower loading of the prosthetic limb would be compensated by increased loading, joint moments, and power in the sound limbs. This hypothesis was supported, as GRF, joint moments and power, as well as limb work generally increased in the contralateral hind- and forelimb during prosthetic walking (Figures 3-8).

The reduced loading of the prosthetic limb and greater loading of the sound contralateral fore- and hindlimb found in this study agreed well with previous results of dog locomotion with hindlimb lameness (Weishaupt et al., 2004) or hindlimb amputation (Fuchs et al., 2014), and of sheep prosthetic locomotion (Shelton et al., 2011).

3.4.3 Comparison Between Human and Quadruped Prosthetic Gait

Individuals with unilateral transtibial amputation also show unloading of the affected leg and increased loading of the contralateral leg during prosthetic walking (Barr et al., 1992; Fey et al., 2011; Segal et al., 2006). As discussed above, these changes in prosthetic walking may be needed to compensate for the lack of energy generation by the passive prosthetic ankle joint. This suggestion is supported by the fact that during prosthetic walking in humans, moments and power at the contralateral knee increase (Beyaert et al., 2008). However, in human walking with a passive transtibial prosthesis, hip moments and power in the affected limb also increase to compensate for the lack of ankle muscles (Silverman et al., 2008; Winter and Sienko, 1988), which is not the case in cat prosthetic walking (Figures 5, 6, and 8). This discrepancy could be explained by the differences in the number of limbs available for locomotion and in prosthesis design between human and cat subjects.

Several limitations of this study should be mentioned. The limited number of subjects tested was caused by the complexity of the procedures. Although the small sample size limits my ability to generalize the results, the study nevertheless provides evidence that the SBIP porous titanium pylons can serve for anchoring transtibial limb prostheses and that the animals can adopt the prosthesis for walking. The observed large reduction in loading and utilization of the prosthetic limb during walking could be partially caused by a relatively short duration of the study. It is possible that if the study was longer, the loading and use of the prosthetic limb may have increased, and walking kinetics might have shifted more toward intact patterns as the cats became more familiar with the prostheses. There was uncertainty in the positioning of the markers on the prosthesis to specify the location of the metatarsophalangeal and ankle joints. This uncertainty should not have affected substantially the calculated knee and hip moments reported here.

CHAPTER IV

SPECIFIC AIM 2

FRONTAL PLANE STABILITY DURING WALKING WITH A PASSIVE BONE-ANCHORED TRANSTIBIAL PROSTHESIS IN THE CAT

4.1 Introduction

Stability during gait has been defined, redefined, measured, and compared for decades (Berg et al., 1992; Laskomccarthey et al., 1990; Murray et al., 1975; Oddsson et al., 2004). The goal of quantifying rehabilitative progress (Day et al., 2012), intervention efficacy (D'Andrea et al., 2014; Morone et al., 2016), and risk of falling (Lajoie and Gallagher, 2004; Verghese et al., 2009) has driven the evolving field of research ever forward. Two metrics of recent development and exploration of gait stability are dynamic stability and whole-body angular momentum (*H)*.

Dynamic stability was defined and investigated after the limitations of static stability were identified during locomotive studies (Hof, 2008; Hof et al., 2005; Pai and Patton, 1997). Dynamic stability has since been used to help identify compensation strategies in different pathologic gait, such as amputation (Curtze et al., 2016; Hof et al., 2007) and stroke (Kajrolkar et al., 2014). In quadrupeds, studies have shown increased margins of dynamic stability (MDS) on the side of the impaired limb (Peebles et al., 2016), often in conjunction with an increased lateral placement of the impaired foot (Park, 2017). MDS, as it is defined, can also be used as a descriptor of the changes in relative distance

between the center of mass (CoM) and foot placement during single-limbed stance, which is considered the least stable phase of gait (Winter and Sienko, 1988).

Angular momentum refers to the amount of rotation about a body's CoM. Not only has this been evaluated across many pathologies, including human limb amputation (Gaffney et al., 2016; Sheehan et al., 2015), stroke (Nott et al., 2014; Vistamehr et al., 2016), and cerebral palsy (Bruijn et al., 2011), it has also been used to measure stability in jumping insects (Burrows et al., 2015) and in lizards after tail amputations (Gillis et al., 2009). In larger quadrupeds, angular momentum has been used to track gait changes during arboreal (Lammers and Zurcher, 2011) and narrow-support (Galvez-Lopez et al., 2011) walking, hence it is a stability metric with substantial cross-species and cross-gait strategy application. The common expectation in stable gait is a net-zero change in *H* over a gait cycle (Bennett et al., 2011; Bruijn et al., 2011; Herr and Popovic, 2008). Reported changes in pathologic gait center on increases in the range of *H* across the gait cycle, as the body is less able to efficiently control its stability (D'Andrea et al., 2014; Sheehan et al., 2015).

The goal of this study was to determine lateral stability during quadrupedal walking with a unilateral bone-anchored passive transtibial prosthesis. The following hypotheses were tested: (1) the necessity to absorb and generate additional mechanical energy for propulsion by the contralateral hindlimb (CH) and greater loading of the contralateral limbs will lead to a shift of the CoM towards the contralateral side and to a reduction of the margin of dynamic stability (MDS) on the contralateral side as reported in quadrupeds during walking on a split-belt treadmill with the ipsilateral belt moving faster (Park, 2017), (2) the lack of paw cutaneous sensory feedback in the prosthetic limb will be compensated by a more lateral placement of the prosthesis to increase the MDS on the ipsilateral side, specifically during ipsilateral double-limb stance, as has been shown in humans with a unilateral prosthesis (Hof et al., 2007) and (3) cumulative angular impulse (cumulative

change in *H*) will be zero after each stride but the range of angular impulse over the gait cycle will increase after implantation, specifically during contralateral stance phases of gait, as reported in human prosthetic gait (Sheehan et al., 2015).

4.2 Methods

4.2.1 Cats Included in Study

This study focused on frontal-plane stability during level walking, and only 3 cats provided enough level-ground prosthetic walking data to be included in this study. In this study, Cat 8 refers to QM04, Cat 5 refers to 09NHT4, and Cat 7 refers to QMV5. Detailed information about each cat can be seen on Table **1** and Table **2** in Chapter 2 and Chapter 3, respectively.

4.2.2 Stepping Patterns

The stance, swing and cycle durations for each limb were determined based on ground reaction forces from Chapter 3. Determination of the stepping patterns began with averaging the ratio of stance to cycle time, or duty factor (DF), of each limb separately across all trials for each cat in each walking condition (able-bodied or prosthetic). For the purposes of this study, the gait cycle was defined as the time between the two consecutive stance onset instances of the affected (ipsilateral) hindlimb. The gait cycle duration was time normalized to 100%. The average normalized stance onset for other limbs were determined with respect to the cycle onset (first stance onset of the ipsilateral hindlimb).

Establishing the stepping patterns in each walking condition allowed for quantification of the relative cycle time the cats spent in the ipsilateral two-limbed support and in diagonal ipsilateral hindlimb-contralateral forelimb support (diagonal two-limbed support). Quadrupeds are considered dynamically unstable when in two-limbed stance

(Farrell et al., 2014a; Farrell et al., 2015), so investigating stability in these phases during prosthetic walking could uncover strategies to minimize the less-stable gait conditions involving the compromised limb.

4.2.3 Dynamic Stability

Dynamic stability in the frontal plane was computed by calculating the extrapolated center of mass (XCoM) and subtracting it from the computed center of pressure (CoP) (Hof et al., 2007). To calculate the XCoM, I first determined the position of whole body CoM in the frontal plane. The XCoM positions in the medial-lateral (y) and vertical (z) directions were defined as

$$\boldsymbol{CoMy} = \frac{\sum_{i=1}^{18} \boldsymbol{m_{iy} CoM_{iy}}}{\boldsymbol{m}} \quad (1)$$

$$\boldsymbol{CoMz} = \frac{\sum_{i=1}^{18} \boldsymbol{m_{iz} CoM_{iz}}}{\boldsymbol{m}} \quad (2)$$

where m_i and CoM_i refer to the mass and y- and z-positions of the CoM for each of the 18 limb segments; m is the cat body mass. After determining the whole-body CoM position for each animal at each time frame, I computed the XCoM position in the medial-lateral direction:

$$\boldsymbol{XCoMy} = \boldsymbol{CoMy} + \frac{\boldsymbol{v_y}}{\sqrt{\boldsymbol{g}/\boldsymbol{l}}} \quad (3)$$

where v_y is the instantaneous velocity of the whole-body CoM in the medial-lateral direction, g is the gravitational constant, and l is the hip height as measured from the ground and averaged across the gait cycle. To determine the CoP at each time instant in the gait cycle, I established a standard coordinate system, the origin of which for each trial was set in the position of the ipsilateral hindpaw (or prosthetic foot) at the gait cycle onset. The positions of the other paws, as well as the CoM position, were then recalculated with respect to this coordinate system. In this coordinate system, x increases from the posterior

to anterior direction in the sagittal plane, while *y* increases from the ipsilateral to contralateral direction in the frontal plane. With this standardized coordinate system in place, I proceeded with calculating the CoP in the medial/lateral dimension, as defined by

$$\boldsymbol{CoPy} = \frac{\sum_{i=1}^{4} \boldsymbol{P_{y_i} * Fz_i}}{\sum_{i=1}^{4} \boldsymbol{F_{z_i}}} \quad (4)$$

where P_{yi} refers to the medial/lateral position of the *i*-th limb; Fz_i is the *i*-th limb vertical force value. For limbs whose ground reaction force was not available during a trial, the average vertical force component, averaged across cycles for that limb, cat and walking condition, was substituted into this trial data so CoP could be estimated for each trial. Using these equations, the difference ($XCoM_y - CoP_y$) was calculated at each time instant of the cycle. The ipsilateral and contralateral MDS were determined as the magnitude of this difference at the stance onset of the contralateral and ipsilateral hindpaws, respectively, as the end of ipsilateral double-support is the onset of the contralateral hindpaw, and vice-versa.

4.2.4 Angular Impulse

To determine the angular impulse (change in *H*, ΔH), I first determined the resultant moment of the ground reaction forces exerted by the four limbs about the CoM during the gait cycle (M_{COM}) at each time instant:

$$\boldsymbol{M_{CoM}} = \sum_{i=1}^{4} (\boldsymbol{p_{com,y}} - \boldsymbol{p_{i,y}}) \boldsymbol{F_{i,z}} - (\boldsymbol{p_{com,z}}) \boldsymbol{F_{i,y}} \quad (5)$$

where $p_{\mathrm{i,y}}$ is the y-position of the *i*-th paw; $p_{com,y}$ and $p_{com,z}$ are y- and z-positions of COM; $F_{i,z}$ and $F_{i,y}$ are z- and y-components of the *i*-th ground reaction force in the frontal plane.

The resultant moment M_{COM} was then time-integrated over the duration of the cycle to determine the angular impulse of the body or the change in angular momentum

in each trial, ΔH. The range of the angular impulse was determined as the difference between the maximum and minimum value of cumulative angular impulse over the whole cycle. Angular impulse curves were averaged for each cat in each walking condition. All calculations were performed with a custom MATLAB (MathWorks, Inc., USA) code.

4.2.5 Statistical Tests

Statistical tests were performed using IBM SPSS Statistics software, v20 (IBM SPSS, Chicago, IL, USA). A linear mixed model was used to compare dependent values between full-bodied and prosthetic walking. For each dependent variable, cycle time was used as a covariate, and walking condition the fixed factor. Results were split by subject eliminating the need for a subject random variable. Correlations were bivariate, two-tailed, Pearson's correlations. Significance for all tests was set at $p<0.05$.

4.3 Results

4.3.1 Limb Support Pattern

Relative stance time spent on the prosthetic limb decreased significantly in Cat 5 from 66.08 ± 1.63% to 57.50 ± 1.71% ($F_{1,6}$=53.021, $p<0.001$) and in Cat 7 from 70.03 ± 6.00% to 57.06 ± 4.01% ($F_{1,6}$=12.888, $p=0.012$), while Cat 8 did not change significantly (61.86 ± 3.97% to 62.38 ± 5.22%, $F_{1,8}$=0.031, $p=0.864$) during able-bodied and prosthetic gait. Relative stance time of the contralateral hindlimb increased significantly in all three cats: Cat 5 (65.20 ± 2.36% to 73.69 ± 2.99%, $F_{1,6}$=19,842, $p=0.004$), Cat 7 (65.92 ± 1.68% to 74.00 ± 2.23%, $F_{1,6}$=33.548, $p=0.001$), and Cat 8 (62.44 ± 2.58% to 77.92 ± 5.18%, $F_{1,8}$=35.739, $p<0.001$). Contralateral forelimb duty factor increased significantly in Cat 8 (65.16 ± 4.37% to 72.00 ± 3.16%, $F_{1,8}$=8.035, $p=0.022$), but only approached a significant increase in Cats 5 and 7 ($p=0.078$, and 0.057, respectively). The ipsilateral forelimb duty

factor also increased significantly in Cat 8 (66.53 ± 2.61% to 72.20 ± 3.45%, $F_{1,9}$=7.360, p=0.03), while remaining unchanged in the other two cats (p>0.5 in each). The contralateral forelimb shared-stance duration across all cats significantly increased from 58.9% ± 7.3 to 63.5% ± 11.0 ($F_{1,22}$=4.291, p=0.050), while neither the ipsilateral forelimb shared-stance duration nor the difference between the two (used to measure relative change) changed significantly; see Figure **9**.

Hindlimb step width decreased significantly in Cat 5 in the first step (35.4±11.9 mm to 12.2±10.5 mm, $F_{1,11}$=13.93, p=0.003), with no significant change in the other cats. The second rear step width decreased significantly in both Cat 5 (31.7±14.4 mm to 10. 6±10.8, $F_{1,11}$=9.19, p=0.011) and Cat 7 (48.8±8.17 mm to 30.34±8.79 mm, $F_{1,9}$=13.03, P=0.006).

Only Cat 8 demonstrated significant changes in the forelimb step width. The first step increased from 29.7±6.2 mm to 50.2±3.4 mm ($F_{1,9}$=49.75, p<0.001), while the second fore step increased from 33.4±12.0 mm to 49.7±6.6 mm ($F_{1,9}$=8.14, p=0.019). Distance between either of the forelimbs and the CoM did not significantly change for any cat: p-values for IF ranged between 0.197 and 0.721, while p-values for CF ranged between 0.155 and 0.574.

The average distance between the CoM and the contralateral hindpaw during the contralateral hindpaw stance significantly decreased in Cat 5 (22.2±8.44 mm to 5.7± 10.0 mm, $F_{1,11}$=10.093, p=0.009) and Cat 7 (25.6±7.6 mm to 12.2± 6.7 mm, $F_{1,9}$=9.397, p=0.013), and increased in Cat 8 (10.9±9.1 mm to 24.0 mm ± 7.7, $F_{1,9}$=6.705, p=0.029). The average distance between the CoM and the ipsilateral hindpaw during the ipsilateral hindpaw stance did not significantly change for any of the cats. Maximum (farthest from ipsilateral hindpaw) and minimum position of CoM with respect to the ipsilateral hindpaw did not change significantly for any cat after implantation, nor did the timing of the CoM extrema during the gait cycle.

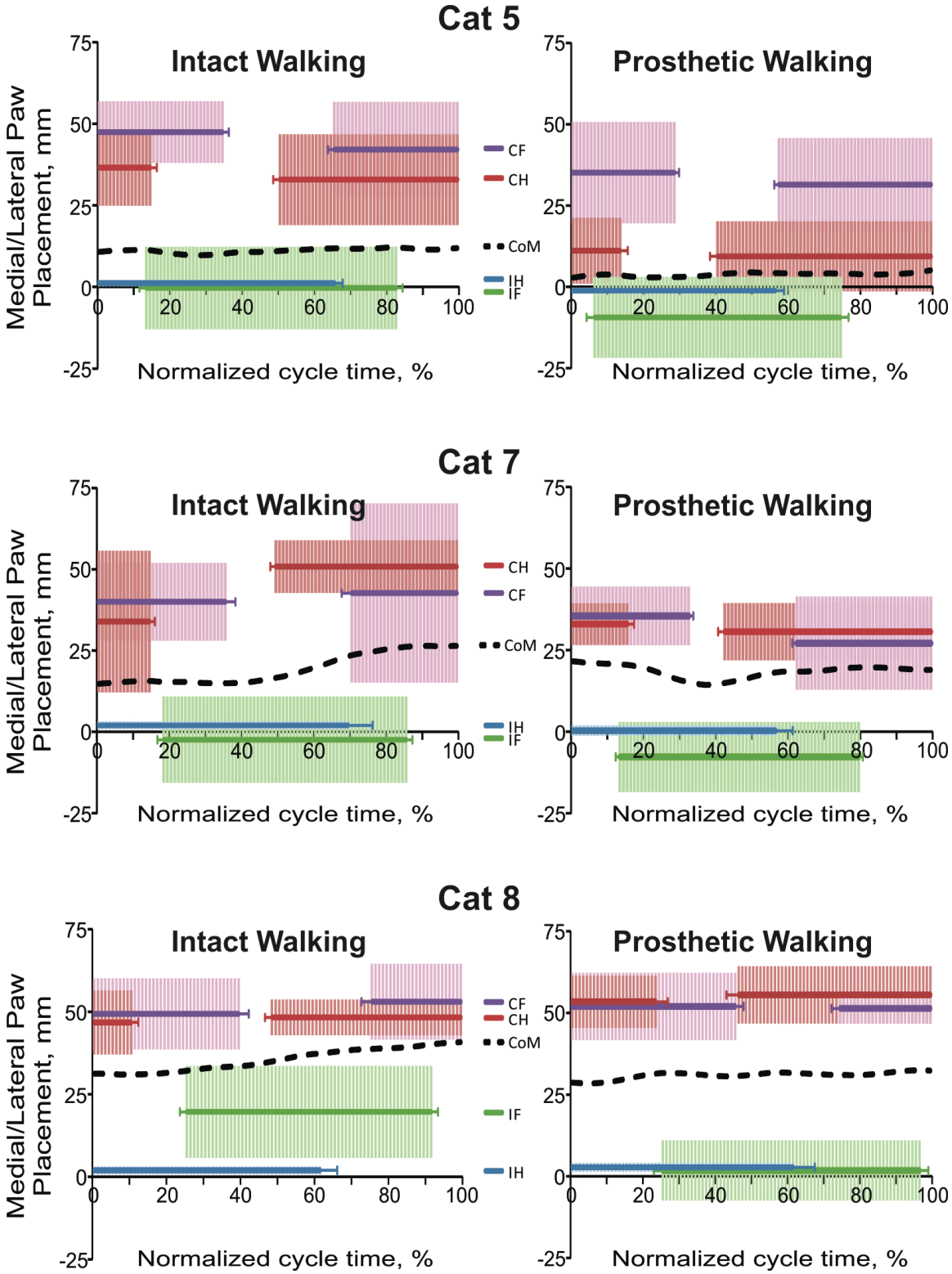

Figure 9: Medial/lateral paw placement and timing across the gait cycle ± standard deviations and average center of mass (CoM) trajectory for each condition. CH, contralateral hindlimb; IH, ipsilateral hindlimb (prosthetic limb in Post condition); IF, ipsilateral forelimb; CF contralateral forelimb.

4.3.2 Dynamic Stability

The ipsilateral margins of lateral dynamic stability during ipsilateral double-support stance did not significantly change in any cat. Cat 5: 13.9 ± 4.6 mm to 12.4 ± 9.7 mm ($F_{1,11}$=0.119, p=0.736), Cat 7: 20.6 ± 12.3 mm to 23.2 ± 10.1 mm ($F_{1,9}$=0.143, p=0.714), and Cat 8: 26.7 ± 13.8 mm to 28.9 ± 6.5 mm ($F_{1,9}$=0.126, p=0.731). The contralateral margins of lateral dynamic stability during contralateral double support decreased significantly in Cat 7 (23.9±4.1 mm to 15.5±7.6 mm, $F_{1,9}$=5.502, p=0.044), and approached a significant reduction in Cat 5 (32.1±5.2 mm to 22.7±10.7 mm, $F_{1,11}$=3.903, p=0.074). See Figure **10** and Figure **11**a.

Correlation between the contralateral and ipsilateral margins of dynamic stability was significant and negative in Cat 5 (-0.603, p=0.029) and Cat 8 (-0.626, p=0.039), and approached significance in Cat 7 (-0.582, p=0.06). The range of dynamic stability in the frontal plane after amputation decreased significantly in Cat 5 (46.0±6.6 mm to 35.0± 4.8 mm, $F_{1,11}$=12.21, p=0.005) and increased significantly in Cat 8 (42.9±7.7 mm to 54.1±5.5 mm, $F_{1,9}$=7.943, p=0.02), while Cat 7 did not change significantly: 44.5 ± 11.4 mm to 38.7 ± 3.5 mm, ($F_{1,9}$=1.186, p=0.304).

4.3.3 Angular Impulse

The net angular impulse over the gait cycle reached or approached zero in 5 of the 6 conditions (able-bodied and prosthetic walking for 3 subjects): both full-bodied and prosthetic walking for Cat 5 and 7, and Cat 8 full-bodied walking (see Figure **11**c). Final cumulative angular impulse over the complete stride was not significantly different from zero for the same 5 conditions, via one-sample t-test compared to zero (Figure **11**b). Pre and post net angular impulse change for Cat 5 was 0.015 ± 0.017 Nms/kg (p=0.078) and -0.025 ± 0.036 Nms/kg (p=0.118), respectively. Cat 7 averaged -0.014 ± 0.041 Nms/kg

(p=0.446) before implantation and 0.0012 ± 0.015 Nms/kg (p=0.868) after implantation. The remaining condition, Cat 8 prosthetic walking, showed a downward pointing waveform, suggesting the medial-lateral angular momentum was increasingly rotating towards the ipsilateral side of the animal. The net angular impulse after a stride with the prosthetic limb was significantly less than zero (mean=-0.0367 ± 0.0202 Nms/kg, p=0.007).

The maximum range of the angular momentum *H* was estimated by the range of change in angular impulse. The obtained range of *H* decreased in Cats 5 and 7, and increased in Cat 8 after implantation. None of these changes reached significance, however. Range of angular impulse during the ipsilateral double support and diagonal double-support phases was only available in Cats 5 and 7, as Cat 8 reduced its use of ipsilateral and diagonal double-support to a single frame total. Cat 5 demonstrated a significant reduction in range of angular impulse during ipsilateral and diagonal double-support phases (0.0192 ± 0.0059 Nms/kg to 0.0121 ± 0.0034 Nms/kg, $F_{1,11}$=7.475, p=0.019), while Cat 7 did not significantly change its ipsilateral and diagonal double-support phase range of angular impulse (from 0.0039 ± 0.0019 Nms/kg to 0.0054 ± 0.0025 Nms/kg, $F_{1,9}$=1.236, p=0.295).

Correlation between the range of dynamic stability and range of angular impulse was non-significant in all cats, but a significant positive correlation was found between the range of dynamic stability and the angular impulse range during the ipsilateral double-support phase in Cat 5 (r=0.555, p=0.049) and Cat 7 (r=0.622, p=0.041). Correlation between the ipsilateral dynamic stability and the angular impulse range during the ipsilateral double-support only significant in Cat 3 (R=0.899, p<0.001).

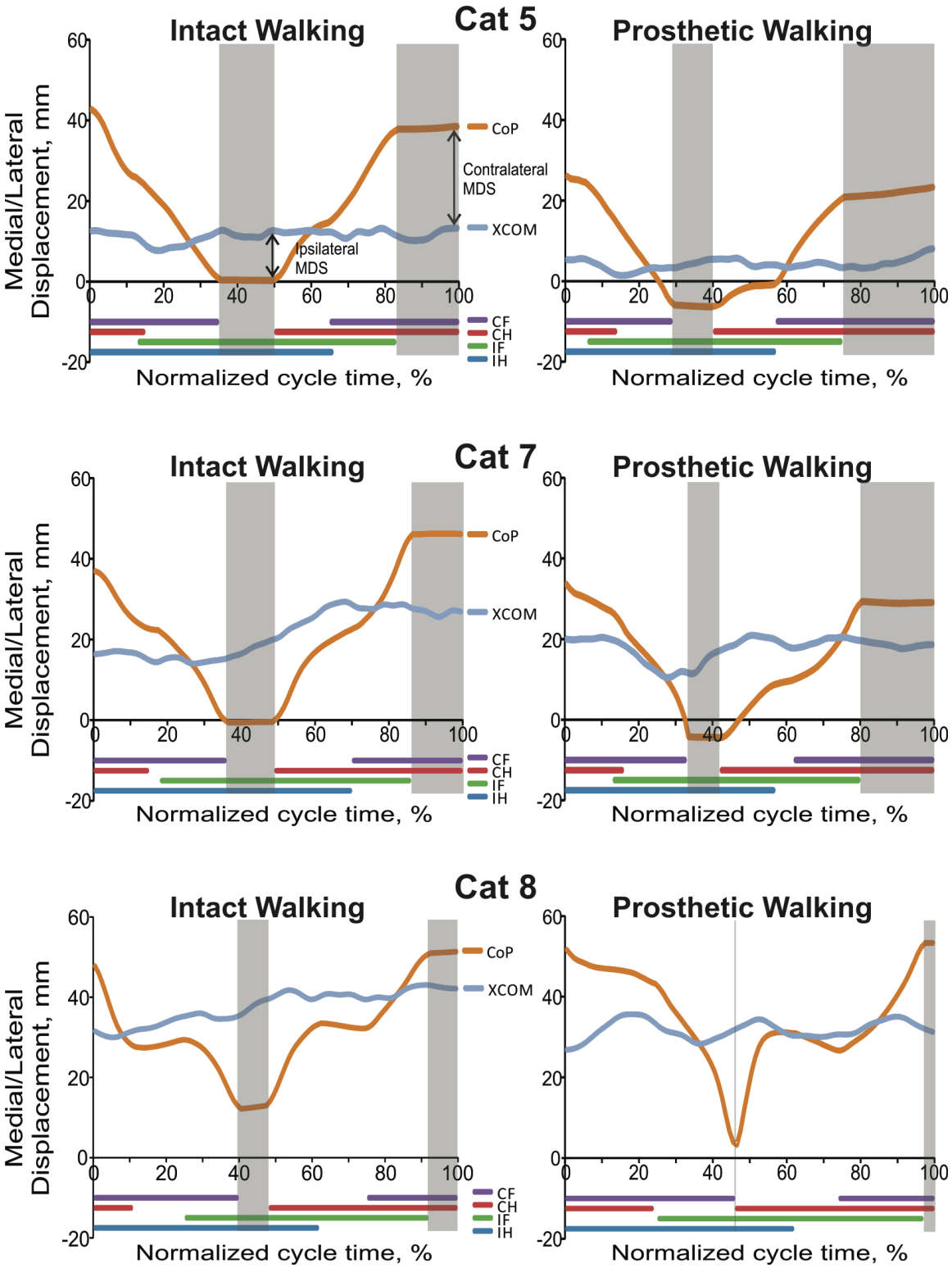

Figure 10: Dynamic stability, measured as the difference between the average center of pressure (CoP) and extrapolated center of mass (XCOM) for each animal and condition. Shaded areas represent ipsilateral (mid cycle) and contralateral (end of cycle) double support phases. Vertical arrows in top left frame illustrate the margin of dynamic stability (MDS) during ipsilateral and contralateral double support. CH, contralateral hindlimb; IH, ipsilateral hindlimb (prosthetic limb in Post condition); IF, ipsilateral forelimb; CF contralateral forelimb.

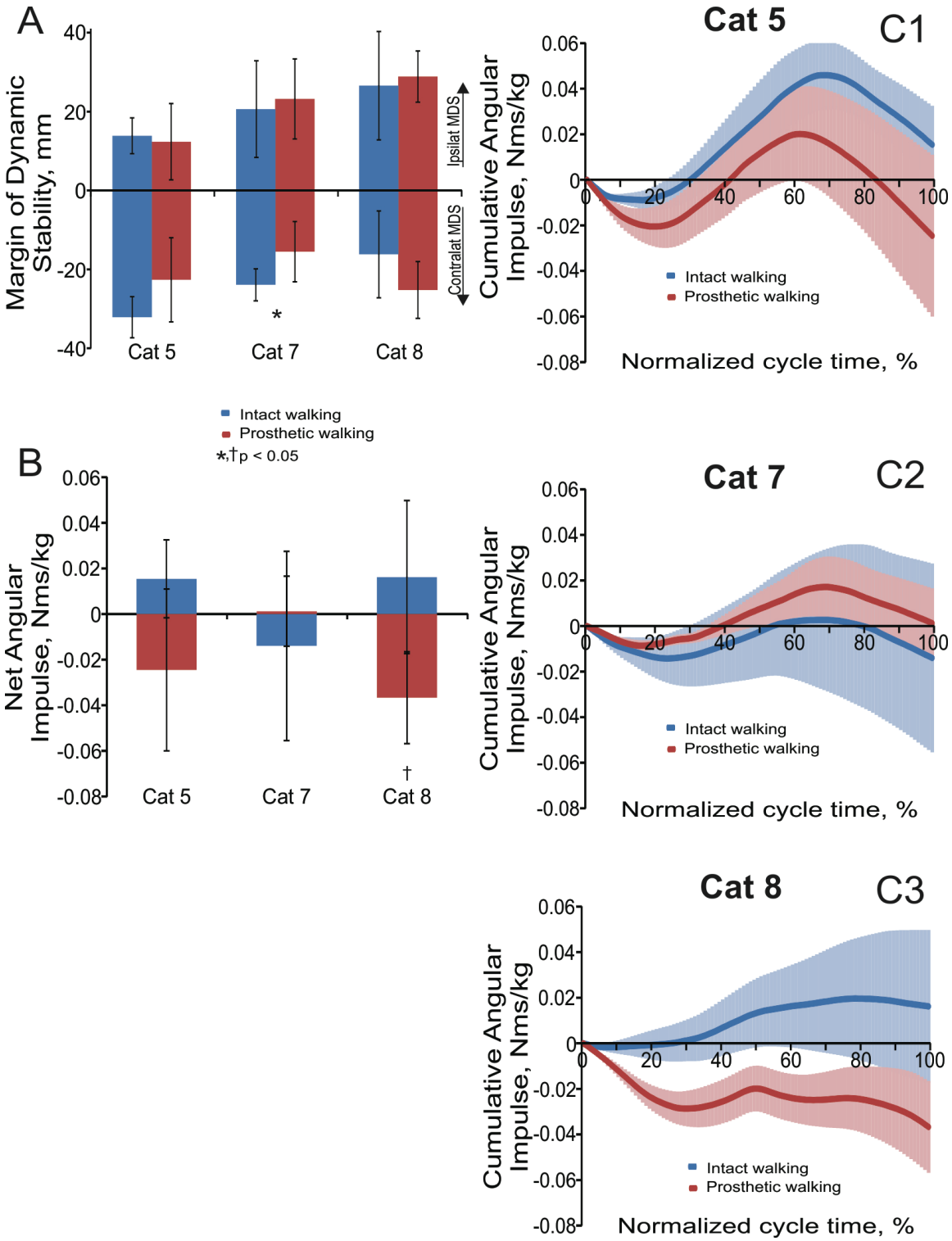

Figure 11: Margins of dynamic stability and angular impulse. A, the margin of dynamic stability (MDS) measured as the difference between center of pressure and extrapolated center of mass at the onset of the opposite-side hindpaw. * indicates significant differences ($p<0.05$) between pre- and post-implantation conditions. B, the net change in angular impulse across the gait cycle for each cat in each condition. † indicates significant differences ($p<0.05$) between value in that condition and zero. C, the cumulative angular impulse over the gait cycle, with standard deviations, for each cat in each condition.

4.4 Discussion

4.4.1 Limb Support Pattern

My first hypothesis was that the cats would shift their CoM toward the contralateral, sound side to match the shift in vertical GRF previously reported (Jarrell, 2017). Two of the three cats demonstrated significant reductions in the average distance between the CoM and the contralateral hindpaw during the stance phase of the contralateral hindlimb, as hypothesized. Both these cats also demonstrated the significantly reduced overall hindlimb stance width. The remaining cat demonstrated a significant increase in the lateral placement of the contralateral hindpaw relative to the CoM, but without a corresponding change in the hindlimb step width. Thus, the first hypothesis was partially supported as the majority of the subjects did shift their CoM toward the contralateral side.

4.4.2 Dynamic Stability

A similar investigation of the average distance between the CoM and the ipsilateral hindpaw during the ipsilateral hindlimb stance did not uncover any significant changes in any cat. I conclude, therefore, that the significant reduction in hindlimb step widths in Cats 5 and 7 was primarily the result of a more medially placed contralateral hindpaw, and not a more laterally placed ipsilateral hindpaw. As such, I have to reject the first half of my second hypothesis stating that the prosthetic foot would be placed more laterally during prosthetic gait. This suggestion was based on observations made in studies on cats walking on a split-belt treadmill (Park, 2017) and human prosthetic gait studies (Hof et al., 2007; Jaegers et al., 1995; Ramstrand and Nilsson, 2009). The second half of the second hypothesis stated that the more lateral paw placement would result in a greater margin of dynamic stability on the prosthetic side. This I must also reject, as the only change in the dynamic stability was a significant decrease on the contralateral side, with no significant

changes being exhibited in any of the cats on the prosthetic side. However, the significantly negative correlation between the MDS on each side, combined with the lack of increase in step width suggests any changes in MDS on one side was compensated by a reduction in MDS on the opposite side. This correlation suggests that the significant decrease in MDS on the contralateral side would be coupled with an increase in MDS on the prosthetic side. Increasing the number of trials and subjects in a future investigation may resolve these two findings.

One potential source for the discrepancy between the lack of a prosthetic-side MDS increase in my quadruped results and the increased prosthetic-side MDS in published human results is the additional support limbs available for compensation in quadrupeds. Shifting weight and CoM forward during prosthetic walking may provide additional compensation after implantation that could minimize or mask any contralateral shifts I have investigated here. In Chapter 3, I have reported an increase in the magnitude of ground reaction forces exerted by the contralateral fore- and hindlimb, whereas the force magnitude of the prosthetic limb decreased after implantation; see also (Jarrell, 2017). Since the compensation for the loss of body-weight support, propulsive, and braking forces in the prosthetic limb were redistributed both contralaterally and anteriorly, the shift in CoM may also be lateral and anterior. Further investigation into the sagittal plane CoM kinematics is warranted to identify additional compensatory mechanisms.

4.4.3 Angular Impulse

The relatively small, periodic oscillations of the changes in angular momentum about the x-axis suggest the momentum may be a controlled variable during walking. Small changes in angular momentum supports the first half of my third hypothesis: the net change in angular momentum would be zero over the walking cycle. This hypothesis was upheld in 5 of the 6 cases (2 walking conditions in 3 cats) as net angular momentum

change over the complete stride did not significantly differ from zero. In one condition, Cat 8's prosthetic walking, the change in angular momentum oscillated at a steady negative slope and was cumulatively different from zero at the end of the stride. Examination of the cumulative angular impulse in each of Cat 8's prosthetic walking trials shows a consistent curve with no outlying curves or points. Increasing the number of trials per subject session, as well as the number of sessions and subjects, may help shine light on the nature of this unique result.

The second half of my third hypothesis, that the range of angular impulse will increase during prosthetic gait, must be rejected. Neither across the whole stride, nor specifically during prosthetic double-support phases, did the range of angular impulse significantly increase in any cat. While this is only an estimation of the range of angular momentum (*H*) changes found in other studies (D'Andrea et al., 2014; Sheehan et al., 2015), increased changes in the range of *H* would be revealed in peak values in the cumulative angular impulse curves. These peak values themselves, the distance between them, and the rate of change of the angular impulse during both contralateral and ipsilateral hindlimb stance phases were all found to be not significantly different after implantation in at least 2 of the 3 cats.

4.4.4 Additional Findings

The cats' stepping pattern changes after implantation included a number of anticipated changes. Relative time during the gait cycle the cats spent in prosthetic stance decreased, while the two contralateral limbs increased their duty factors more consistently than the ipsilateral forelimb. This mirrors the changes in ground reaction forces reported in Chapter 3. These findings support the previously published studies demonstrating a decrease in time spent on an impaired limb, and an increase in time spent on the sound contralateral limb(s) in humans (Barnett et al., 2009; Jaegers et al., 1995) and quadrupeds

(Farrell et al., 2014b; Park et al., 2016), presumably in an effort to reduce the time spent in the least stable phases of walking (Farrell et al., 2015).

The positive correlations found between the range of angular impulse during ipsilateral double-support and both the range of dynamic stability and ipsilateral dynamic stability is interesting considering increases in the range of angular momentum is found in less-stable human populations (D'Andrea et al., 2014; Nott et al., 2014). But specifically in human amputees, the increase in this range was only found during intact contralateral stance, not during prosthetic-side stance (Sheehan et al., 2015). The explanation given by Sheehan and his team was that humans are less able to adjust their angular momentum during prosthetic stance, and must provide an increased amount of change through the intact limb during contralateral stance. In quadrupeds, it may be that the shared-stance limbs simultaneously perform the increased angular momentum adjustments during prosthetic stance. This may further explain the lack of a significant increase in the range of angular impulse as seen in the human pathologic gait studies. The ability for simultaneous compensation through additional limbs may offer a natural mitigation of gait deviation in single-limb pathologies that is unavailable to humans. Further investigation is needed of the partial-phase contribution of each limb to angular momentum during quadrupedal prosthetic walking.

4.5 Conclusion

Much is still unknown regarding gait and stability control strategy development in humans and other animals. Ever-deepening investigations into motor control networks and stability measurements provide increasing insight into stability patterns and deviations during able-bodied and impaired gait. In this study, in addition to quantifying the changes in stepping pattern in cats after they were fitted with a transtibial bone-anchored

prosthesis, I calculated and compared the changes in two widely-used gait stability metrics: margins of dynamic stability and changes in angular momentum. While a number of my results were unexpected, the deviations from previously published studies were always towards able-bodied results. The findings suggest that the cats were able to sufficiently control their frontal-plane stability while using the SBIP-anchored osseointegrated prosthesis.

CHAPTER V

SPECIFIC AIM 3

BONE AND TISSUE INGROWTH IN POROUS TITANIUM PYLON IN CATS WITH A TRANSTIBIAL OSSEOINTEGRATED PROSTHESIS

5.1 Introduction

Persistent risk of skin infection at the skin-pylon interface has limited the availability of bone-anchored limb prostheses in the United States (Branemark et al., 2014; FDA, 2015; Tillander et al., 2010; Tsikandylakis et al., 2014). As bone-anchored limb prostheses have been scientifically and clinically investigated (Aschoff et al., 2009; Aschoff and Juhnke, 2016; Drygas et al., 2008; Hagberg and Branemark, 2009; Jonsson et al., 2011; Palmquist et al., 2008), new percutaneous pylons have been developed to implement features shown to potentially reduce the risk of skin infection, including pylon porosity (Farrell et al., 2014c; Pendegrass et al., 2006a; Pitkin et al., 2012b). Porosity has been shown to decrease infection rates when applied to percutaneous pylons in rats (Farrell et al., 2014c; Pitkin et al., 2007; Pitkin et al., 2009), cats (Farrell et al., 2014b), sheep (Jeyapalina et al., 2012), and goats (Barrere et al., 2003). Porosity is believed to anchor the skin in place to prevent epithelial downgrowth (Jeyapalina et al., 2012; Pendegrass et al., 2006a), which is believed to be a major cause of skin infection among bone-anchored prosthetic users (Chehroudi et al., 1989; Vonrecum, 1984).

Skin and bone integration with the Skin- and Bone-Integrating Pylon (SBIP) has been histologically analyzed in previous studies. Farrell *et al* (Farrell et al., 2014c) reported

a 60% skin ingrowth when SBIPs were percutaneously implanted in the dorsal skin of rats for 6 weeks. Pitkin *et al (Pitkin et al., 2009)* reported "near-uniform filling of the internal-device pores with dense fibrous tissue or bone" of an SBIP implanted in the distal tibia of a single cat subject without pylon locomotive loading. While both these studies offered preliminary support of viable tissue integration with the SBIP, neither study involved subjecting the implanted porous pylons to loads of daily activity.

This study expands upon the body of knowledge established by these previous studies and reports the quantitative tissue ingrowth results after a prosthesis anchored in the distal tibia via an SBIP has been utilized for 2-3 months during daily activities, including locomotion, after surgical implantation. Chapter III reported the cats utilized the prosthesis for walking, demonstrating peak normal ground reaction forces exceeding 50% of pre-implantation values in level and sloped walking, and Chapter IV reported the maintenance of frontal-plane stability during the prosthesis-adopted gait. The purpose of this study was to investigate the skin and bone integration with the SBIP after the pylons were subjected to daily activity and locomotion loading.

Two principle hypotheses were tested in this study: (1) no signs of infection will be noted on the cross-sectional (XS) bone ingrowth slides or the longitudinal tissue ingrowth slides, and (2) the bone ingrowth achieved after loading the SBIP for 2-3 months will exceed the 20% ingrowth achieved in the tibia-implanted SBIP not subjected to loads of daily locomotion (Pitkin et al., 2009). Justification for the second hypothesis is based on evidence that force transmission through bone stimulates bone remodeling (Bentolila, 1998; Robling, 2006), and increases bone ingrowth into implant pore space (Burr et al., 1985; Lanyon and Rubin, 1984; Torcasio et al., 2008).

5.2 Methods

5.2.1 Implant Harvesting and Slide Preparation

After completion of the prosthetic walking data collection used in the previous chapters, the animals were euthanized via deep anesthesia, specifically an overdose of sodium pentobarbital, and the implant with surrounding residual shank was harvested for slide preparation. The harvested implants from Cats 1-6 were prepared, digitized, and analyzed by Alizée Pathology, LLC (Thurmont, MD). Slides were prepared by fixating the implant and residual limb in methylmethacrylate (MMA) then cut into three 50μm-thick sections (proximal and distal cross-sections, and one longitudinal cut; Figure 14A), which were polished and stained with hematoxylin and eosin (H/E) and digitized at 25x magnification.

Harvested shanks and implants from Cats 7 and 8 were prepared by T3 Labs. After being fixed in MMA, multiple 100μm-thickness sections were cut from each sample using the Exakt system (EXACT Technologies Inc., Oklahoma City, OK, USA), beginning at approximately the middle of the implant and advancing distally in 2 mm increments. The sections were then stained with H/E to distinguish tissue ingrowth from SBIP titanium. The slides were photographed with a 21-megapixel digital camera under 25x magnification and reassembled digitally with Adobe Photoshop CC (Adobe Systems Inc, Seattle, WA).

5.2.2 Slide Analysis

Color values of stained tissue in each slide were determined with ImageJ image software (NIH, Bethesda, MD). The hue, brightness, and saturation values of marked bone in the qualitative lab report were recorded. These values were used in a custom Matlab program (Farrell et al., 2014c) to differentiate between tissue, titanium, and empty space for each pixel inside the porous titanium zone in each slide. Comparisons under 100x

magnification were made for each slide between the qualitative lab report images and the resultant quantitative image to ensure accurate inclusion of targeted tissue ingrowth and exclusion of inflammatory or other fibrous connective tissue ingrowth.

Analysis of each XS slide was broken down into twelve regions, oriented so the division between area one and area twelve marks the rostral direction of each animal (Figure 12C). Regions were further grouped into anatomical quadrants: Anterior, Posterior, Medial, and Lateral. Longitudinal slides were divided between bone-implant integration for the length of implant within the tibia, and tissue-implant integration for the length of implant between the distal end of the tibia and the external border of the skin.

Longitudinal slides were broken into three sections (Figure 12D): bone tissue (BT) encapsulating the porous titanium space from the proximal edge of the image to the distal tip of the residual tibia, dermal tissue (DT) consisting of the porous titanium space between the distal tibia and the external border of the epidermal skin, and external tissue (ET) consisting of all stained tissue distal to the epidermis. Analysis in each section was performed separately for the left and right porous titanium spaces, broken down into 100 smaller rectangular regions, and compiled to provide a single ingrowth value for each tissue in that subject. The intra-medullary regions were divided into four sub-regions of equal length to better fit the rectangular zone of analysis onto the tapering pylon, and to allow for BT ingrowth comparisons as a factor of longitudinal location. Any region that, due to the slightly irregular external border of the porous titanium, extended outside the porous space was not included in the ingrowth calculation. Apposition was determined by measuring the linear distance of bone-pylon contact on the longitudinal slides, and normalizing that value by the intramedullary length of porous pylon. Normalizing the apposition value allowed me to include Cats 7 and 8 in the longitudinal correlations despite being unable to determine the precise location along the pylon from which the slides were made. See Figure **12** for an illustrative guide to XC and longitudinal analysis.

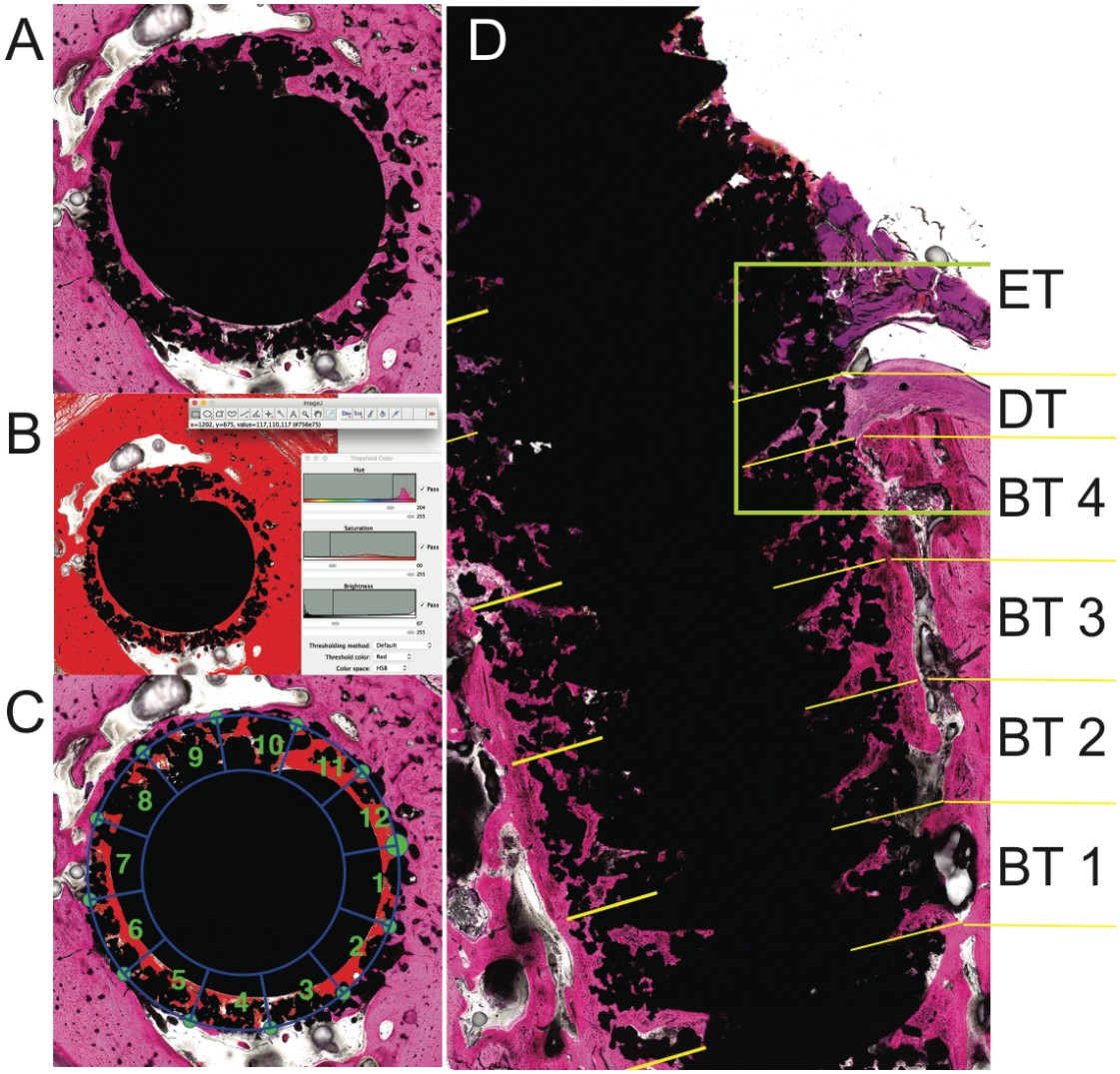

Figure 12: Example of hisotological analysis. A: Example of a cropped cross-sectional (XS) digitized slide. Black = titanium SBIP, white = empty space among porous titanium and between bone and pylon, pink = stained organic tissue. B: Color thresholds selected to highlight bone tissue according to the qualitative lab report. C: Color thresholds applied to the original slide and process through custom MATLAB program. D: Longitudinal slide breakdown before region analysis. BT1-4 = Bone Tissue regions 1-4, DT = Dermal Tissue region, ET = External Tissue region

5.2.3 Statistical Tests

Statistical analysis was performed using IBM SPSS Statistics software, v20 (IBM SPSS, Chicago IL, USA). One-way ANOVA was performed to test for significant differences between XS regions and quadrants. Mixed-model ANOVA was used to determine differences in BT ingrowth between subjects withdrawn early (33 days or less after implantation) and subjects who completed the full duration of the study (over 100 days). Pearson's correlation coefficients were computed in partial correlations to quantify correlation between bone-pylon apposition and ingrowth percentage while controlling for implantation duration and, in the XS slides, relative distal distance of slide from knee joint.

Data grouping for statistical analysis was based on relative location of XS slide and known length of residual tibia in longitudinal slides. While all eight subjects were included in apposition correlations, intergroup comparisons of the ingrowth of different tissues was restricted to Cats 1-6: early withdrawal (Cats 1 and 2), infection (Cat 3), and full duration implantation of over five months (Cats 4-6). Cats 7 and 8 were analyzed but reported separately. This was due to a lack of accurate information regarding where the XS slides were taken in Cats 7 and 8, as well as a lack of a length reference scale in their longitudinal or XS images. Efforts to determine longitudinal origin of the XS slides resulted in substantial intra- and inter-investigator variance.

5.3 Results

5.3.1 Implantation Duration and Animal Outcomes

Of the eight animals originally enrolled in the study, six animals were implanted with the SBIP for the intended five- to six-month duration of the study. Two cats (Cats 7 and 8) were implanted for 148 days under the same protocol to obtain pilot data before the rest of the animals were implanted. Cat 1 was removed from the study after seven

days of implantation due to a complication from a previously unknown heart condition occurring during routine bandage change under anesthesia. Cat 2 was removed early after 33 days of implantation when the animal suffered a jaw injury while chewing on the cast protecting the healing limb. Cat 3 was implanted for the duration of the study but was not fitted with a prosthesis, and therefore did not subject the implant with loads of locomotion, due to the development of an infection secondary to the surgery itself. At the conclusion of the study, or at time of withdrawal from the study, all eight implanted SBIPs were harvested and examined under 25x magnification for structural defects or fractures. Of the eight implanted pylons, one (Cat 4) broke it during prosthetic walking training, while another (Cat 7) broke it at the conclusion of prosthetic walking data collection. The other six pylons showed no signs of structural damage or fracturing. In total, six of the eight cats were implanted for the planned duration of their corresponding study, five of which loaded the pylon during locomotion.

5.3.2 Infection

Seven of the eight cats, including five of the six animals implanted for more than four months (Cats 4-8), exhibited no clinical signs of infection, such as erythema, edema, warmth, tenderness, crepitus, or visible necrosis (Rajan, 2012). The remaining cat implanted for over four months (Cat 3) did present with limb withdrawal during implant loading, as well as minor bleeding from the skin-pylon interface during standing training. The cat was treated for infection, and while blood samples did not reveal evidence of systemic infection, was not fitted with a prosthesis in order to protect the compromised limb. Histology analysis revealed chronic inflammation inside the medullary canal of the distal residual tibia (Figure **13**), and tissue culture at euthanasia revealed heavy growth of Meth-resistant staph bacteria.

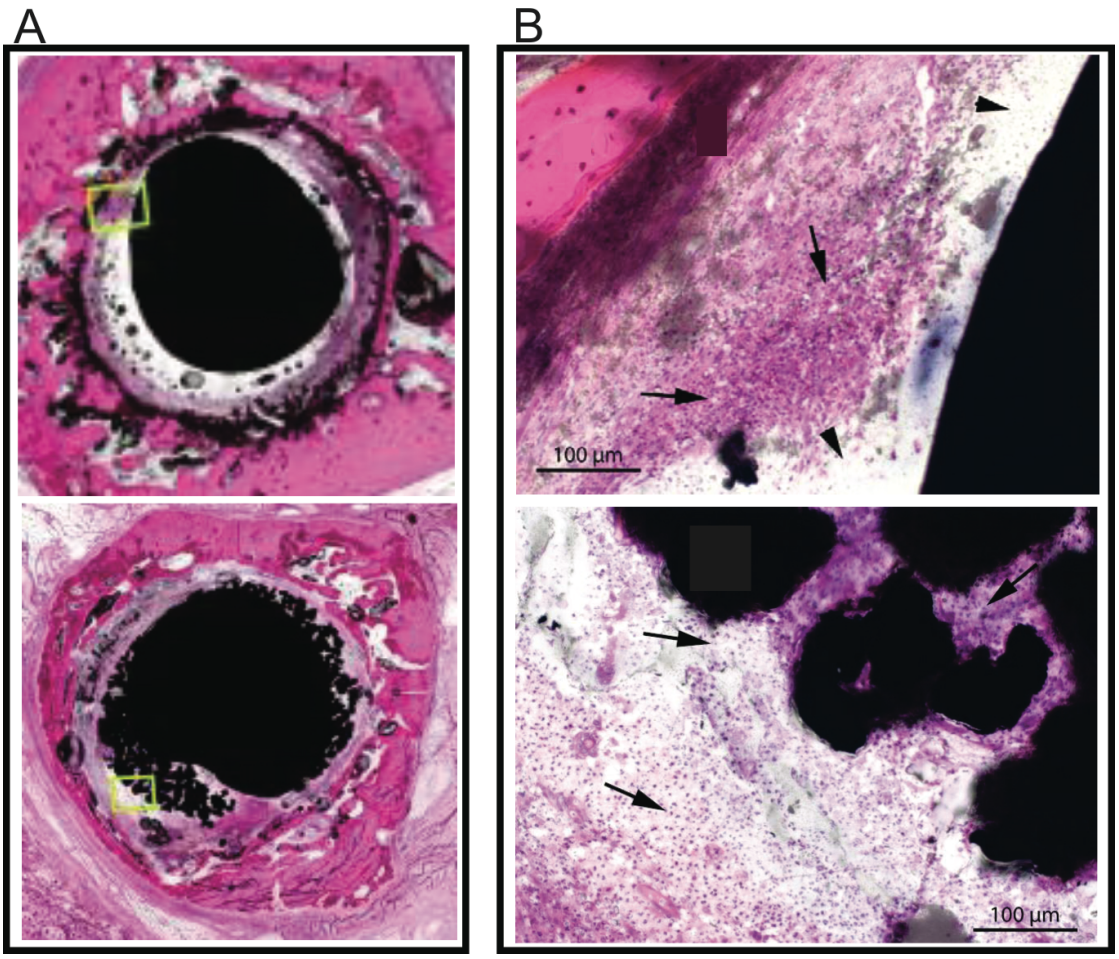

Figure 13: Chronic inflammation in Cat 3. A: XS slides taken from Cat 3. B: Magnified portions of previous slides. Arrows identifying chronic inflammation tissue.

5.3.3 Bone Ingrowth

Comparison of BT ingrowth percentage showed no significant difference among the anatomical regions ($F_{11,185}$=0.530, p=0.881) or quadrants ($F_{3,193}$=0.784, p=0.504) in the XS slides. These results supported using a single total ingrowth percentage for each individual XS slide. While another ingrowth comparison between the distal and proximal XS slides of each animal also technically did not reach significance ($F_{1,113}$=3.656, p=0.058) I kept the two values separate due to their near-significance and in order to have two

different ingrowth values for each animal. Similarly, no BT ingrowth difference was found among the longitudinal intramedullary regions in the longitudinal slides ($F_{3,21}$=0.813, p=0.501).

The average BT ingrowth demonstrated in the XS slides for each of the loaded pylons implanted for over five months (Cats 4-6) was 75.7%±7.8, and 89.6%±4.0% from the intramedullary zones on the longitudinal slides. For comparison, the BT ingrowth results in a previous study (Pitkin et al., 2009) consisting of a single cat implanted with an SBIP for 120 days, but without locomotive loading, was 20.3%, determined by running images of slides prepared from the previous study through my protocols for this study. It is important to note that unlike the loaded pylons from our current study, this non-loaded pylon from the prior study displayed substantial tissue ingrowth described as dense fibrous tissue that was distinguishable from woven bone ingrowth and filled an additional 53.2% of the total pore space. In our current study, another pylon was implanted for over five months but with no locomotive loading due to its development of osteomyelitis. The BT ingrowth results from this pylon reached 36.3% in the XS slides and 26.0% on the longitudinal slide. It is important to note that this animal suffered from healing complications, and cannot be directly compared to the healthy non-loading animal just described. See Figure **14** for examples of BT analysis.

Cats 7 and 8 exhibited XS BT ingrowth values of 13.0%±7.8%, and longitudinal BT ingrowth of 6.1%±2.2%. Reasons for the low ingrowth results despite long implantation and regular loading are elaborated upon in the Discussion section.

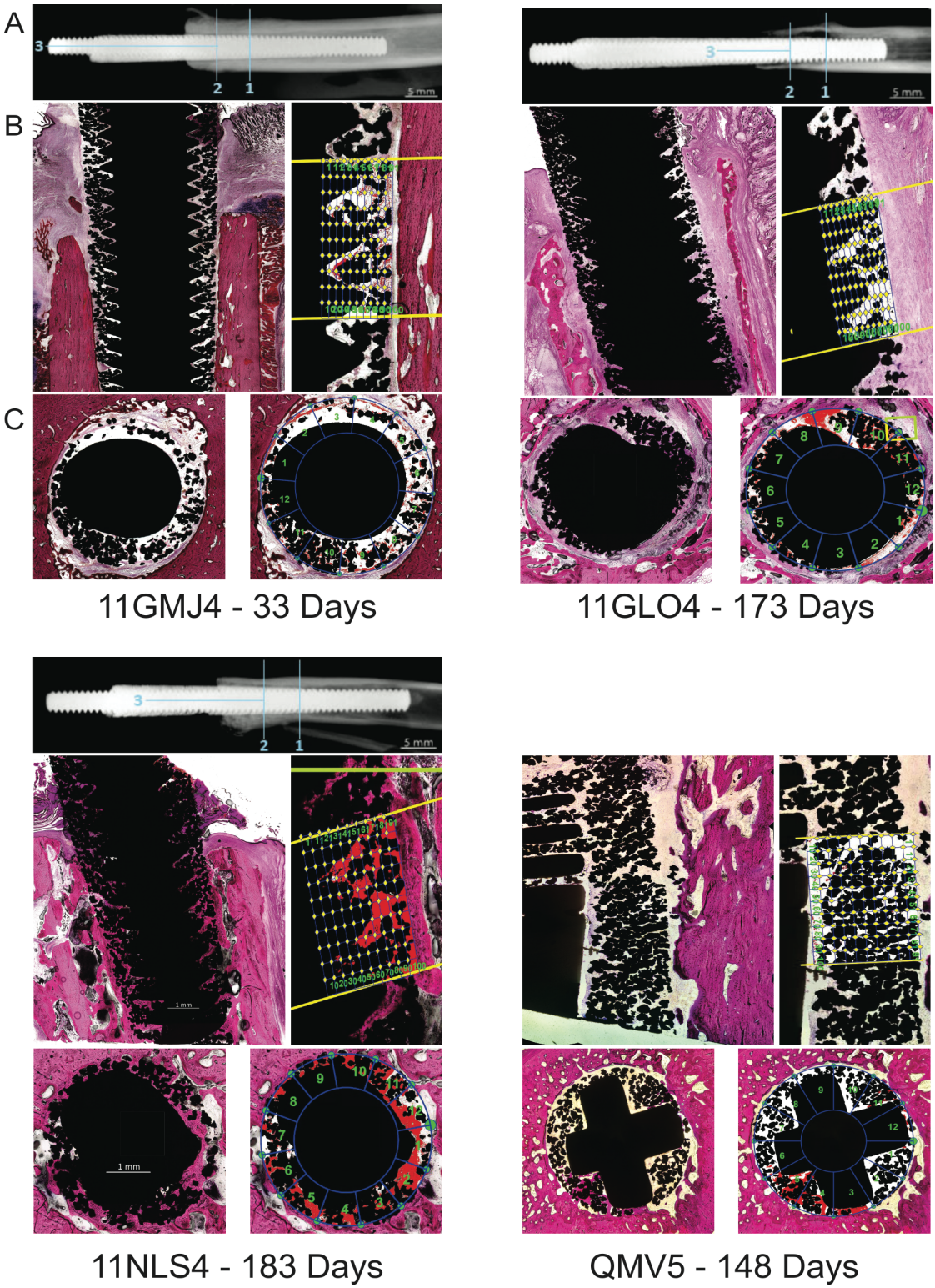

Figure 14: Cross-sectional and longitudinal bone-tissue integration analysis. Top left: Cat 2 withdrawn after 33 days. Top right: Cat 3 exhibited clinical signs of infection. Bottom left: Cat 6 implanted for 183 days and subjected pylon to daily loading. Bottom right: Cat 8 implanted for 148 days and loaded the pylon with daily activity, but positions of XS slides along harvested pylon were unavailable. A: X-ray images showing locations of XS and longitudinal slides taken from harvested pylon. B: Longitudinal images, original and analyzed. C: XS Images, original and analyzed.

Grouping the cats and their slides into Early Withdrawal (EW, Cats 1 and 2) and Full Duration (FD, Cats 3 through 6) and comparing bone ingrowth revealed significantly increased bone ingrowth in the XS slides of cats with implantation durations greater than 100 days (16.1±4.4% in EW and 69.1±17.5% in FD, $F_{3,65}$=11.638, p=0.031).

Qualitatively, the 5 infection-free cats implanted for greater than 100 days displayed robust bone ingrowth into implant and a marked absence of inflammatory tissue inside the medullary space, as well as bone-implant apposition at even the most distal aspect of the bone-implanted pylon.

5.3.4 Skin Ingrowth

DT ingrowth values for the pylons implanted for over five months and regularly loaded (Cats 4-6) averaged 75.4%±8.7%. The pylons implanted for 7 and 33 days reached 9.4% and 20.1%, respectively. The pylon implanted for 173 days and harvested with evidence of infection reached 21.6% ingrowth. DT ingrowth for Cats 7 and 8 implanted for 148 days averaged 18.5% ± 6.6%. Correlation between longitudinal BT and DT ingrowth, controlling for apposition and implantation duration, for all eight subjects was a non-significant 0.710 (p=0.114).

Due to a break in the external pylon in one animal, only two pylons were available among the subjects implanted over 5 five months for ET analysis. Additionally, the longitudinal slide made from harvested implant of Cat 8 did not include exterior portion, preventing ET ingrowth analysis in that subject. The two implants with over five months of implantation averaged 60.0%±6.3%. The early withdrawn subjects demonstrated a wide range of ET ingrowth, from 5.1% in Cat 1 after seven days of implantation and 43.3% in Cat 2 with 33 days of implantation, while the subject with an infection exhibited ET ingrowth of 40.4%, and Cats 7 reached 44.4%. The duration- and apposition-controlled correlation

between BT and ET ingrowth among all six subjects with ET analysis was a non-significant 0.600 (p=0.400).

Determining the breakdown of the specific tissue types in the dermal and exterior layer were outside the scope of this study, due to a non-specific organic tissue staining with H/E. Qualitatively, the DT zones showed complete or near-complete superficial epithelial apposition among the animals with the longest implantation durations (Cats 4-8), along with minimal inflammation tissue and no epithelial downgrowth. The subjects withdrawn early (Cat 1 and 2) as well as the subject with an infection (Cat 3) all presented with an epithelial layer extending from the original skin-pylon border proximally along the lateral borders of the porous pylon. See Figure **15** for an example of skin-tissue integration analysis.

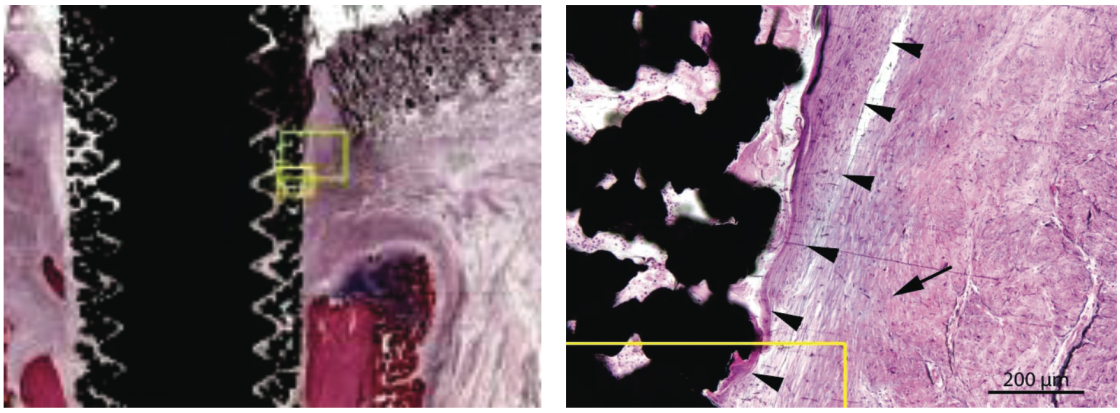

Figure 15: Example of skin-tissue integration qualitative analysis. Top row: epithelial layer downgrowth in apposition to SBIP after 33 days of implantation. Middle row: epithelial layer downgrowth without porous space infiltration after 173 days in presence of infection. Bottom row: epithelial infiltration into porous titanium space without downgrowth after 183 days of implantation. Black arrow heads identify epithelial layer.

5.4 Discussion

5.4.1 Infection and Bone Ingrowth

The goal of this study was to investigate the skin and bone integration with the SBIP after the pylons have been subjected to daily activity and locomotion loading. My first hypothesis, that no signs of infection will be noted on the XS bone ingrowth slides or the longitudinal tissue ingrowth slides, was mostly upheld as only one animal, Cat 3, exhibited any clinical signs or histological evidence of tissue infection. My second hypothesis, that the bone ingrowth achieved after loading the SBIP for 2-3 months will exceed the 20% ingrowth achieved in the tibia-implanted SBIP not subjected to loads of daily locomotion, was also upheld as all three full duration implantation animals (Cats 4-6) with matching locations of analyzed XS slides exhibited substantially increased BT ingrowth, averaging 75.7% and all exhibiting at least 62% ingrowth.

The post-loading BT ingrowth results in Cats 4-6 support the importance of force transmission through bone in stimulating bone remodeling and increasing bone ingrowth into implant pore space. Specifically, the significantly improved bone-pylon integration in these cats compared to both the non-loaded pylon from the previous study (Pitkin et al., 2009) and the infected pylon from this study, both of which had similar implantation durations but did not subject the implant to daily loading.

The effect of loading on bone remodeling has been well documented (Bentolila et al., 1998; Lanyon and Rubin, 1984; Torcasio et al., 2008), while simultaneously being challenged and refined (Cowin et al., 1991; Dunlop et al., 2009; Pearson and Lieberman, 2004; Ruff et al., 2006). On the cellular level, mechanical loading has been shown to inhibit bone resorption *in vitro* (You et al., 2008), although *in vivo* investigation of the pathways of post-loading bone resorption remains challenging to researchers (Brown et al., 2016). The most widely supported mechanism of bone adaptation initiation at the cellular level is

oscillatory fluid flow in the osteocyte canaliculi (Tami et al., 2002; Weinbaum et al., 1994; You et al., 2000; You et al., 2001). Mechanoreceptors sensitive to changes in intra-canicular fluid flow and pressure trigger the release of intracellular calcium and secondary messengers (Dalagiorgou et al., 2010), causing a cascade of wide-ranging effects (Thi et al., 2003) through hormonal (White and Wallis, 2001) and neural (Flier, 2002) mechanisms. The combined consequence of this cascade is an increase in bone remodeling activity and new calcified bone matrix (Robling et al., 2006).

Cats 7 and 8 displayed substantially lower BT ingrowth despite being implanted for 148 days and loading the pylon daily during locomotion. Despite the lower BT ingrowth values, the subjects successfully adopted the implant-anchored prosthesis into their gait strategies and ambulated daily with the prosthetic limb as demonstrated in Chapter III. The most likely cause of the decreased ingrowth values in these two subjects is an inconsistent pylon location at which the sample slides were taken. As the tibial medullary canal narrows distally, the highest percentage of bone-pylon apposition occurs in the distal portion of the tibia. Samples taken proximal to this zone of tightest fit will therefore likely exhibit decreased ingrowth values.

The necessity to remove 2 cats from the study at or before 33 days of implantation gave us the unplanned opportunity to compare tissue ingrowth differences between Early Withdrawal subjects and Full Duration subjects. This quantification was an investigation into the effect of increased implantation duration on tissue-implant integration. While the difference in BT ingrowth was significantly higher for the Full Duration subjects, differentiating between the effects of increased duration and the effect of pylon loading is difficult given that the study was not originally designed for this investigation. However, the results of the analysis of the non-loaded pylon (Pitkin et al., 2009), which showed only 20.3% BT ingrowth despite being implanted for over 100 days, also showed 53.2% dense fibrous tissue ingrowth for a total of 73.5% porous space filled with viable non-

inflammatory tissue. As a whole, these results seem to support implantation duration affecting tissue infiltration, while pylon loading increases bone formation. A new study with planned early pylon withdrawals, or a mechanism of quantifying pylon integration externally, would shine more light on the differing effects of implantation duration and pylon loading.

Initial implant-bone contact is another important factor in preventing aseptic implant loosening (Raphel et al., 2016; Sundfeldt et al., 2006). While initial apposition between tibial bone and implant was not measurable in my study design, apposition at time of implant harvesting was computed and included as a covariate in the mixed model to help isolate the effects of implantation duration on bone ingrowth.

5.4.2 Skin Ingrowth

The epithelial layer along the outer surface of the skin is of special importance in skin integration studies. In my analysis, epithelial downgrowth is more evident in the early withdrawal and infected subjects than in the full duration implantation subjects. While incomplete epithelial healing on a single side of the skin-pylon interface in Cats 4 and 5, no sign of epithelial downgrowth was noted on these study-complete subjects.

5.5 Conclusion

Six of eight subjects in this work were implanted with an SBIP for at least 148 days. Of the six full-duration subjects, only one presented with any clinical or histological evidence of infection. Despite the small sample size, these results support the potential of SBIP implants to mitigate infection risk, perhaps due to the dermal tissue integration shown to improve over time after pylon implantation.

The ingrowth and correlation results support the notion that force transmission, time after implantation, and bone-pylon apposition are important factors in maximizing tissue-pylon integration.

CHAPTER VI

DISCUSSION AND CONCLUSIONS

The goal of this project was to investigate the effects and efficacy of SBIP-anchored, osseointegrated, transtibial limb prostheses as an intervention after limb amputation in the cat. My study began by confirming the adoption of the prosthesis by quantifying the kinetics of the prosthetic limb during level and sloped walking, followed by investigation of the resulting frontal-plane stability metrics during walking with a bone-anchored prosthesis. Finally, after confirming both adoption of the prosthetic limb and stable walking, I investigated the extent of tissue-SBIP integration by quantifying the SBIP pore space infiltrated by host tissue. The results of each aim were encouraging of the potential use of SBIP-anchored, osseointegrated prostheses as rehabilitative interventions after limb amputation. However, each aim also revealed shortcomings, either of the structure of the investigation, or follow-up questions that need to be pursued.

My results in Aim 1 support purposeful adoption of the prosthetic limb into quadrupedal gait. The peak normal and tangential GRFs exerted by the prosthetic limb were significantly greater than zero and, for the tangential GRFs, exerted in the appropriate direction at the corresponding phases of the gait cycle. It was found that compensatory increases in GRFs, as well as most other tested kinetic variables, were shared by both of the contralateral limbs, while the kinetic variables of the ipsilateral forelimb changed very little from pre-implantation values. The extra limb involvement in compensation may help explain the lack of the moment and power increases in the intact hip of the prosthetic limb as seen in humans (Silverman et al., 2008; Winter and Sienko, 1988). As to why the contralateral forelimb increased its kinetic values, as opposed to the

ipsilateral forelimb, was an unanswered question. One explanation for the forelimb discrepancy in compensation could be a discrepancy in shared stance time between the contralateral forelimb and the prosthetic limb. While not an explicit hypothesis for my Aim 2 work, I expected an increased shared-stance duration between the contralateral forelimb and ipsilateral hindlimb than between the ipsilateral forelimb and ipsilateral hindlimb.

Another discrepancy discovered in Aim 1 was the relatively larger decrease in peak tangential force compared to peak normal forces exerted through the prosthetic limb. In my initial discussion in Aim 1, I referenced a potential decrease in the coefficient of friction as a limiting factor in producing tangential forces with the prosthetic limb during early and late stance. Regardless of the differences in the paw-ground interface and prosthesis-ground interface, the decreases in tangential GRFs would likely be associated with a decrease in leg angle with respect to the vertical at initial contact and toe-off during prosthetic walking. Further investigation is needed to identify the specific leg angle changes and to determine if this causes or is caused by decreases in tangential GRFs.

Aim 2 presented me with an opportunity to compare the changes in kinetics reported in Aim 1 with changes in stepping pattern and stability. While not explicit hypotheses within Aim 2, these comparisons can be supportive or discouraging of the expectations regarding stepping patterns formed after analyzing the kinetic results from Aim 1. The first such comparison arose out of the observed discrepancy in compensatory increases in kinetic values between the contralateral and ipsilateral forelimbs. I expected the prosthetic stepping pattern to reflect the contralateral compensation strategy by demonstrating an increase in shared-stance duration between the contralateral forelimb and prosthetic hindlimb relative to the shared-stance duration between the ipsilateral forelimb and prosthetic hindlimb. The results showed that the contralateral forelimb shared-stance duration significantly increased from 58.9% ± 7.3 to 63.5% ± 11.0 ($F_{1,22}$=4.291, p=0.050), while neither the ipsilateral forelimb shared-stance duration nor

the difference between the two (used to measure relative change) changed significantly. While this may be related to the contralateral forelimb compensation strategy, more research is needed. Further investigation into potential correlation between the shared-stance duration changes and the relative change in force production by each forelimb may be warranted in future work.

The changes in both the kinetic (Aim 1) and the stability (Aim 2) variables are presented here as the differences between the able-bodied walking and walking with a unilateral, bone-anchored, transtibial prosthesis. Hence, there are actually two major changes to the animals' bodies: first the loss of the natural limb, and second the attachment of the bone-anchored prosthesis. A potentially valuable additional comparison would be between the prosthetic walking reported here and tripedal walking of the same animals without their attached prosthetics. This comparison could help isolate the effects of the prosthetic intervention from the amputation, thereby better highlighting the efficacy of this approach on restoring function post-limb amputation in quadrupeds.

The effects of limb amputation alone on quadrupedal gait can be loosely divided into the loss of feedback from ascending, or afferent, sensory sources, and the loss of descending, or efferent, neural pathways along with muscular detachment between the residual motor control system and the implanted limb prosthesis. I say "loosely" divided because while I group muscular detachment with efferent neural bisection, muscular detachment not only results in the loss of power production capabilities, but also results in afferent sensory deficits by eliminating the muscle spindle and Golgi tendon organ contribution to the limb's proprioceptive calculus. While my study did not attempt to segregate the specific physiological causes from the gait effects, it is my forward-pointing hypothesis that the detachment of the shank muscles is the most consequential physiological change undergone during amputation in our subjects.

Regarding shank muscle detachment, one can quickly see how the effects on the kinetic variables produced by the prosthetic limb are directly affected by the lack of a power producing ankle. Aim 1 reported, among other kinetic variables, the decreased power generated by the prosthetic limb compared to the intact RH paw before implantation. However, changes in power production, limb loading, duty factor and stepping pattern are likely significantly affected by the removal of muscle-based afferent feedback, i.e. muscle spindles and Golgi tendon organs (GTOs). Muscle spindles are thought to play an important role in limb position and movement sensation (Proske and Gandevia, 2012). GTOs are believed to play significant role in stance-to-swing transition (Pearson, 2008) and limb loading feedback, especially when lacking paw cutaneous feedback such as the cats with amputations in my study (Duysens et al., 2000).

While parsing the effects on gait of the loss of cutaneous afferents, muscle spindle and GTO afferents, and muscular power was beyond the scope of my work, I believe there is substantial opportunity moving forward to restore a portion of these lost functions. In studies involving powered ankle prostheses, the effects due to power loss may be mitigated, and the residual gait deficits may be more attributable to afferent loss, given the right study controls and ankle power settings.

Aim 3 reported tissue integration with the SBIP after daily loading of the pylon with forces of locomotion. The results support the importance of time and residual bone loading in improving tissue integration. Attempts to correlate the bone ingrowth results from Aim 3 with the kinetic results from Aim 1 were unsuccessful due to the inability to identify the specific location along the pylon at which ingrowth slides were taken for two of the four ambulating subjects. Ensuring the same protocol for histology slide preparation in future SBIP studies can enable more direct ingrowth-functional return comparisons. Additionally, creating cross-sectional bone slides at the proximal end of the amputated hindlimb immediately after the initial surgery would have given me a close approximation of the

initial cross-sectional bone shape and condition. This in turn could have improved my ability to detect changes in the shape and density of the cortical wall around the porous implant. In the completed study, I was forced to limit my analysis solely to the porous space as no baseline cross-sectional images were available for comparison.

This project represents an investigation into the adoption and integration of a unilateral, transtibial, bone-anchored prosthesis mounted via a porous percutaneous pylon. My work shows that the cats stably adopted the prosthesis into their chosen gait strategies, with extensive skin and bone tissue ingrowth after daily implant loading. While limited by the low number of subjects, this work supports the potential use for the SBIP as a percutaneous anchor for osseointegrated prostheses in quadrupeds.

REFERENCES

Adams, C.L., Kurtz, S.M., 2006. Building on existing models from human medical education to develop a communication curriculum in veterinary medicine. J. Vet. Med. Educ. 33, 28-37.

Adamson, C., Kaufmann, M., Levine, D., Millis, D.L., Marcellin-Little, D.J., 2005. Assistive devices, orthotics, and prosthetics. Vet. Clin. N. Am.-Small Anim. Pract. 35, 1441-+.

Adell, R., Lekholm, U., Rockler, B., Branemark, P.I., 1981. A 15-YEAR STUDY OF OSSEOINTEGRATED IMPLANTS IN THE TREATMENT OF THE EDENTULOUS JAW. International Journal of Oral Surgery 10, 387-416.

Albrektsson, T., Branemark, P.I., Hansson, H.A., Lindstrom, J., 1981. OSSEOINTEGRATED TITANIUM IMPLANTS - REQUIREMENTS FOR ENSURING A LONG-LASTING, DIRECT BONE-TO-IMPLANT ANCHORAGE IN MAN. Acta Orthop. Scand. 52, 155-170.

Aschoff, H.H., Clausen, A., Hoffmeister, T., 2009. The Endo-Exo Femur Prosthesis - A New Concept of Bone-Guided, Prosthetic Rehabilitation Following Above-Knee Amputation. Z. Orthop. Unfallchir. 147, 610-615.

Aschoff, H.H., Juhnke, D.L., 2016. Endo-exo prostheses. Osseointegrated percutaneously channeled implants for rehabilitation after limb amputation. Unfallchirurg 119, 421-427.

Aschoff, H.H., Kennon, R.E., Keggi, J.M., Rubin, L.E., 2010. Transcutaneous, Distal Femoral, Intramedullary Attachment for Above-the-Knee Prostheses: An Endo-Exo Device. J. Bone Joint Surg.-Am. Vol. 92A, 180-186.

Baggot, J.D., Giguere, S., 2013. Principles of Antimicrobial Drug Bioavailability and Disposition. Blackwell Science Publ, Oxford.

Barnett, C., Vanicek, N., Polman, R., Hancock, A., Brown, B., Smith, L., Chetter, I., 2009. Kinematic gait adaptations in unilateral transtibial amputees during rehabilitation. Prosthetics and Orthotics International 33, 135-147.

Barr, A.E., Siegel, K.L., Danoff, J.V., McGarvey, C.L., Tomasko, A., Sable, I., Stanhope, S.J., 1992. BIOMECHANICAL COMPARISON OF THE ENERGY-STORING CAPABILITIES OF SACH AND CARBON COPY II PROSTHETIC FEET DURING THE STANCE PHASE OF GAIT IN A PERSON WITH BELOW-KNEE AMPUTATION. Phys. Ther. 72, 344-354.

Barrere, F., van der Valk, C.M., Meijer, G., Dalmeijer, R.A.J., de Groot, K., Layrolle, P., 2003. Osteointegration of biomimetic apatite coating applied onto dense and porous metal implants in femurs of goats. J. Biomed. Mater. Res. Part B 67B, 655-665.

Bateni, H., Maki, B.E., 2005. Assistive devices for balance and mobility: Benefits, demands, and adverse consequences. Arch. Phys. Med. Rehabil. 86, 134-145.

Benedetti, M.G., Merlo, A., Leardini, A., 2013. Inter-laboratory consistency of gait analysis measurements. Gait Posture 38, 934-939.

Bennett, B.C., Robert, T., Russell, S.D., Ieee, 2011. Angular Momentum: Insights into Walking and Its Control, 2011 Ieee/Rsj International Conference on Intelligent Robots and Systems. Ieee, New York, pp. 3969-3974.

Bentolila, V., Boyce, T.M., Fyhrie, D.P., Drumb, R., Skerry, T.M., Schaffler, M.B., 1998. Intracortical remodeling in adult rat long bones after fatigue loading. Bone 23, 275-281.
Berg, K.O., Wood-Dauphinee, S.L., Williams, J.I., Maki, B., 1992. Measuring balance in the elderly: validation of an instrument. Can J Public Health 83 Suppl 2, S7-11.
Beyaert, C., Grumillier, C., Martinet, N., Paysant, J., Andre, J.M., 2008. Compensatory mechanism involving the knee joint of the intact limb during gait in unilateral below-knee amputees. Gait Posture 28, 278-284.
Board, W.J., Street, G.M., Caspers, C., 2001. A comparison of trans-tibial amputee suction and vacuum socket conditions. Prosthetics and Orthotics International 25, 202-209.
Bothe, T.B., KE; Davenport, HA, 1940. Reaction of bone to multiple metallic implants. Surg Gynecol Obstet 71, 598-602.
Bowden, M.G., Balasubramanian, C.K., Neptune, R.R., Kautz, S.A., 2006. Anterior-posterior ground reaction forces as a measure of paretic leg contribution in hemiparetic walking. Stroke 37, 872-876.
Branemark, P.I., 1983. OSSEOINTEGRATION AND ITS EXPERIMENTAL BACKGROUND. J. Prosthet. Dent. 50, 399-410.
Branemark, R., Berlin, O., Hagberg, K., Bergh, P., Gunterberg, B., Rydevik, B., 2014. A novel osseointegrated percutaneous prosthetic system for the treatment of patients with transfemoral amputation A PROSPECTIVE STUDY OF 51 PATIENTS. Bone Joint J. 96B, 106-113.
Branemark, R., Branemark, P.I., Rydevik, B., Myers, R.R., 2001. Osseointegration in skeletal reconstruction and rehabilitation: A review. Journal of Rehabilitation Research and Development 38, 175-181.
Branemark, R., Thomsen, P., 1997. Biomechanical and morphological studies on osseointegration in immunological arthritis in rabbits. Scand J Plast Reconstr Surg Hand Surg 31, 185-195.
Brown, G.N., Sattler, R.L., Guo, X.E., 2016. Experimental studies of bone mechanoadaptation: bridging in vitro and in vivo studies with multiscale systems. Interface Focus 6, 12.
Bruijn, S.M., Meyns, P., Jonkers, I., Kaat, D., Duysens, J., 2011. Control of angular momentum during walking in children with cerebral palsy. Res Dev Disabil 32, 2860-2866.
Burr, D.B., Martin, R.B., Schaffler, M.B., Radin, E.L., 1985. Bone remodeling in response to in vivo fatigue microdamage. J Biomech 18, 189-200.
Burrows, M., Cullen, D.A., Dorosenko, M., Sutton, G.P., 2015. Mantises Exchange Angular Momentum between Three Rotating Body Parts to Jump Precisely to Targets. Curr. Biol. 25, 786-789.
Carberry, C.A., Harvey, H.J., 1987. OWNER SATISFACTION WITH LIMB AMPUTATION IN DOGS AND CATS. J. Am. Anim. Hosp. Assoc. 23, 227-232.
Chang, Y.H., Huang, H.W.C., Hamerski, C.M., Kram, R., 2000. The independent effects of gravity and inertia on running mechanics. J. Exp. Biol. 203, 229-238.
Chehroudi, B., Gould, T.R.L., Brunette, D.M., 1989. EFFECTS OF A GROOVED TITANIUM-COATED IMPLANT SURFACE ON EPITHELIAL-CELL BEHAVIOR INVITRO AND INVIVO. J. Biomed. Mater. Res. 23, 1067-1085.

Chen, G., Patten, C., Kothari, D.H., Zajac, F.E., 2005. Gait differences between individuals with post-stroke hemiparesis and non-disabled controls at matched speeds. Gait Posture 22, 51-56.
Chowdhary, R., Chowdhary, N., Mishra, S.K., 2011. Re-osseointegration of loosened implant in a splinted fixed prosthesis. Niger. J. Clin. Pract. 14, 102-105.
Corbee, R.J., Maas, H., Doornenbal, A., Hazewinkel, H.A.W., 2014. Forelimb and hindlimb ground reaction forces of walking cats: Assessment and comparison with walking dogs. The Veterinary Journal 202, 116-127.
Cowin, S.C., Mosssalentijn, L., Moss, M.L., 1991. CANDIDATES FOR THE MECHANOSENSORY SYSTEM IN BONE. J. Biomech. Eng.-Trans. ASME 113, 191-197.
Curtze, C., Hof, A.L., Postema, K., Otten, B., 2016. Staying in dynamic balance on a prosthetic limb: A leg to stand on? Medical Engineering & Physics 38, 576-580.
D'Andrea, S., Wilhelm, N., Silverman, A.K., Grabowski, A.M., 2014. Does Use of a Powered Ankle-foot Prosthesis Restore Whole-body Angular Momentum During Walking at Different Speeds? Clin. Orthop. Rel. Res. 472, 3044-3054.
Dalagiorgou, G., Basdra, E.K., Papavassiliou, A.G., 2010. Polycystin-1: Function as a mechanosensor. Int. J. Biochem. Cell Biol. 42, 1610-1613.
Dapunt, U., Radzuweit-Mihaljevic, S., Lehner, B., Haensch, G.M., Ewerbeck, V., 2016. Bacterial Infection and Implant Loosening in Hip and Knee Arthroplasty: Evaluation of 209 Cases. Materials 9, 10.
Day, K.V., Kautz, S.A., Wu, S.S., Suter, S.P., Behrman, A.L., 2012. Foot placement variability as a walking balance mechanism post-spinal cord injury. Clinical Biomechanics 27, 145-150.
Devan, H., Hendrick, P., Ribeiro, D.C., Hale, L.A., Carman, A., 2014. Asymmetrical movements of the lumbopelvic region: Is this a potential mechanism for low back pain in people with lower limb amputation? Med. Hypotheses 82, 77-85.
DeVita, P., Hortobagyi, T., Barrier, J., 1998. Gait biomechanics are not normal after anterior cruciate ligament reconstruction and accelerated rehabilitation. Med. Sci. Sports Exerc. 30, 1481-1488.
Dickerson, V.M., Coleman, K.D., Ogawa, M., Saba, C.F., Cornell, K.K., Radlinsky, M.G., Schmiedt, C.W., 2015. Outcomes of dogs undergoing limb amputation, owner satisfaction with limb amputation procedures, and owner perceptions regarding postsurgical adaptation: 64 cases (2005-2012). Journal of the American Veterinary Medical Association 247, 786-792.
Dimiskovski, M., Scheinfield, R., Higgin, D., Krupka, A., Lemay, M.A., 2017. Characterization and validation of a split belt treadmill for measuring hindlimb ground-reaction forces in able-bodied and spinalized felines. J. Neurosci. Methods 278, 65-75.
Dobkin, B., Apple, D., Barbeau, H., Basso, M., Behrman, A., Deforge, D., Ditunno, J., Dudley, G., Elashoff, R., Fugate, L., Harkema, S., Saulino, M., Scott, M., Grp, S., 2006. Weight-supported treadmill vs overground training for walking after acute incomplete SCI. Neurology 66, 484-492.
Drygas, K.A., Taylor, R., Sidebotham, C.G., Hugate, R.R., McAlexander, H., 2008. Transcutaneous tibial implants: A surgical procedure for restoring ambulation after amputation of the distal aspect of the tibia in a dog. Vet. Surg. 37, 322-327.

Dunlop, J.W.C., Hartmann, M.A., Brechet, Y.J., Fratzl, P., Weinkamer, R., 2009. New Suggestions for the Mechanical Control of Bone Remodeling. Calcif. Tissue Int. 85, 45-54.
Duysens, J., Clarac, F., Cruse, H., 2000. Load-regulating mechanisms in gait and posture: comparative aspects. Physiological reviews 80, 83-133.
Duysens, J., Pearson, K.G., 1998. From cat to man: basic aspects of locomotion relevant to motor rehabilitation of SCI. Neurorehabilitation 10, 107-118.
Ebersbach, G., Sojer, M., Valldeoriola, F., Wissel, J., Muller, J., Tolosa, E., Poewe, W., 1999. Comparative analysis of gait in Parkinson's disease, cerebellar ataxia and subcortical arteriosclerotic encephalopathy. Brain 122, 1349-1355.
Farrell, B.J., Bulgakova, M.A., Beloozerova, I.N., Sirota, M.G., Prilutsky, B.I., 2014a. Body stability and muscle and motor cortex activity during walking with wide stance. J. Neurophysiol. 112, 504-524.
Farrell, B.J., Bulgakova, M.A., Sirota, M.G., Prilutsky, B.I., Beloozerova, I.N., 2015. Accurate stepping on a narrow path: mechanics, EMG, and motor cortex activity in the cat. J Neurophysiol 114, 2682-2702.
Farrell, B.J., Prilutsky, B.I., Kistenberg, R.S., Dalton, J.F., Pitkin, M., 2014b. An animal model to evaluate skin-implant-bone integration and gait with a prosthesis directly attached to the residual limb. Clinical Biomechanics 29, 336-349.
Farrell, B.J., Prilutsky, B.I., Ritter, J.M., Kelley, S., Popat, K., Pitkin, M., 2014c. Effects of pore size, implantation time, and nano-surface properties on rat skin ingrowth into percutaneous porous titanium implants. J. Biomed. Mater. Res. Part A 102, 1305-1315.
FDA, 2015. FDA authorizes use of prosthesis for rehabilitation of above-the-knee amputations. U.S. Food and Drug Administration.
Fey, N.P., Klute, G.K., Neptune, R.R., 2011. The influence of energy storage and return foot stiffness on walking mechanics and muscle activity in below-knee amputees. Clinical Biomechanics 26, 1025-1032.
Fitzpatrick, N., Smith, T.J., Pendegrass, C.J., Yeadon, R., Ring, M., Goodship, A.E., Blunn, G.W., 2011. Intraosseous Transcutaneous Amputation Prosthesis (ITAP) for Limb Salvage in 4 Dogs. Vet. Surg. 40, 909-925.
Fliegel, O.F., S.G., 1966. Historical Development of Lower-Extremity Prostheses. Arch. Phys. Med. Rehabil. 47, 275-285.
Flier, J.S., 2002. Physiology - Is brain sympathetic to bone? Nature 420, 619-+.
Forster, L.M., Wathes, C.M., Bessant, C., Corr, S.A., 2010. Owners' observations of domestic cats after limb amputation. Vet. Rec. 167, 734-739.
Frossard, L., Haggstrom, E., Hagberg, K., Branemark, R., 2013. Load applied on bone-anchored transfemoral prosthesis: Characterization of a prosthesis-A pilot study. Journal of Rehabilitation Research and Development 50, 619-634.
Fuchs, A., Goldner, B., Nolte, I., Schilling, N., 2014. Ground reaction force adaptations to tripedal locomotion in dogs. Veterinary journal (London, England : 1997) 201, 307-315.
Gabler, C., Zietz, C., Gohler, R., Fritsche, A., Lindner, T., Haenle, M., Finke, B., Meichsner, J., Lenz, S., Frerich, B., Luthen, F., Nebe, J.B., Bader, R., 2014. Evaluation of Osseointegration of Titanium Alloyed Implants Modified by Plasma Polymerization. Int. J. Mol. Sci. 15, 2454-2464.

Gaffney, B.M., Murray, A.M., Christiansen, C.L., Davidson, B.S., 2016. Identification of trunk and pelvis movement compensations in patients with transtibial amputation using angular momentum separation. Gait Posture 45, 151-156.
Gagnon, D., Duclos, C., Desjardins, P., Nadeau, S., Danakas, M., 2012. Measuring dynamic stability requirements during sitting pivot transfers using stabilizing and destabilizing forces in individuals with complete motor paraplegia. J. Biomech. 45, 1554-1558.
Galindo-Zamora, V., von Babo, V., Eberle, N., Betz, D., Nolte, I., Wefstaedt, P., 2016. Kinetic, kinematic, magnetic resonance and owner evaluation of dogs before and after the amputation of a hind limb. BMC veterinary research 12, 20.
Galvez-Lopez, E., Maes, L.D., Abourachid, A., 2011. The search for stability on narrow supports: an experimental study in cats and dogs. Zoology 114, 224-232.
Gerritsen, M., Lutterman, J.A., Jansen, J.A., 2000. Wound healing around bone-anchored percutaneous devices in experimental diabetes mellitus. J. Biomed. Mater. Res. 53, 702-709.
Gillis, G.B., Bonvini, L.A., Irschick, D.J., 2009. Losing stability: tail loss and jumping in the arboreal lizard Anolis carolinensis. J. Exp. Biol. 212, 604-609.
Gregor, R.J., Smith, D.W., Prilutsky, B.I., 2006. Mechanics of slope walking in the cat: Quantification of muscle load, length change, and ankle extensor EMG patterns. J. Neurophysiol. 95, 1397-1409.
Gutierrez, G.M., Chow, J.W., Tillman, M.D., McCoy, S.C., Castellano, V., White, L.J., 2005. Resistance training improves gait kinematics in persons with multiple sclerosis. Arch. Phys. Med. Rehabil. 86, 1824-1829.
Hachisuka, K., Dozono, K., Ogata, H., Ohmine, S., Shitama, H., Shinkoda, K., 1998. Total surface bearing below-knee prosthesis: Advantages, disadvantages, and clinical implications. Arch. Phys. Med. Rehabil. 79, 783-789.
Hagberg, K., Branemark, R., 2009. One hundred patients treated with osseointegrated transfemoral amputation prostheses-Rehabilitation perspective. Journal of Rehabilitation Research and Development 46, 331-344.
Hagberg, K., Branemark, R., Gunterberg, B., Rydevik, B., 2008. Osseointegrated trans-femoral amputation prostheses: Prospective results of general and condition-specific quality of life in 18 patients at 2-year follow-up. Prosthetics and Orthotics International 32, 29-41.
Hagberg, K., Haggstrom, E., Uden, M., Branemark, R., 2005. Socket versus bone-anchored trans-femoral prostheses: Hip range of motion and sitting comfort. Prosthetics and Orthotics International 29, 153-163.
Haggstrom, E., Hagberg, K., Rydevik, B., Branemark, R., 2013a. Vibrotactile evaluation: Osseointegrated versus socket-suspended transfemoral prostheses. Journal of Rehabilitation Research and Development 50, 1423-1434.
Haggstrom, E.E., Hansson, E., Hagberg, K., 2013b. Comparison of prosthetic costs and service between osseointegrated and conventional suspended transfemoral prostheses. Prosthetics and Orthotics International 37, 152-160.
Hakansson, B., Tjellstrom, A., Rosenhall, U., Carlsson, P., 1985. The bone-anchored hearing aid. Principal design and a psychoacoustical evaluation. Acta Otolaryngol 100, 229-239.

Hall, C.W., 1974. Developing a permanently attached artificial limb. Bull Prosthet Res, 144-157.
Haraldson, T., Carlsson, G.E., 1977. BITE FORCE AND ORAL FUNCTION IN PATIENTS WITH OSSEOINTEGRATED ORAL IMPLANTS. Scandinavian Journal of Dental Research 85, 200-208.
Hernigou, P., 2013. Ambroise Pare IV: The early history of artificial limbs (from robotic to prostheses). Int. Orthop. 37, 1195-1197.
Herr, H., Popovic, M., 2008. Angular momentum in human walking. J Exp Biol 211, 467-481.
Herr, H.M., Grabowski, A.M., 2012. Bionic ankle-foot prosthesis normalizes walking gait for persons with leg amputation. Proc. R. Soc. B-Biol. Sci. 279, 457-464.
Hof, A.L., 2008. The 'extrapolated center of mass' concept suggests a simple control of balance in walking. Hum. Mov. Sci. 27, 112-125.
Hof, A.L., Gazendam, M.G.J., Sinke, W.E., 2005. The condition for dynamic stability. J. Biomech. 38, 1-8.
Hof, A.L., van Bockel, R.M., Schoppen, T., Postema, K., 2007. Control of lateral balance in walking - Experimental findings in normal subjects and above-knee amputees. Gait Posture 25, 250-258.
Hoy, M.G., Zernicke, R.F., 1985. MODULATION OF LIMB DYNAMICS IN THE SWING PHASE OF LOCOMOTION. J. Biomech. 18, 49-60.
Hurley, G.R.B., McKenney, R., Robinson, M., Zadravec, M., Pierrynowski, M.R., 1990. THE ROLE OF THE CONTRALATERAL LIMB IN BELOW-KNEE AMPUTEE GAIT. Prosthetics and Orthotics International 14, 33-42.
Isackson, D., McGill, L.D., Bachus, K.N., 2011. Percutaneous implants with porous titanium dermal barriers: An in vivo evaluation of infection risk. Medical Engineering & Physics 33, 418-426.
Jacobs, R., Branemark, R., Olmarker, K., Rydevik, B., Van Steenberghe, D., Branemark, P.I., 2000. Evaluation of the psychophysical detection threshold level for vibrotactile and pressure stimulation of prosthetic limbs using bone anchorage or soft tissue support. Prosthetics and Orthotics International 24, 133-142.
Jaegers, S., Arendzen, J.H., Dejongh, H.J., 1995. PROSTHETIC GAIT OF UNILATERAL TRANSFEMORAL AMPUTEES - A KINEMATIC STUDY. Arch. Phys. Med. Rehabil. 76, 736-743.
Jahn, K., Deutschlander, A., Stephan, T., Kalla, R., Hufner, K., Wagner, J., Strupp, M., Brandt, T., 2008. Supraspinal locomotor control in quadrupeds and humans, in: Kennard, C., Leigh, R.J. (Eds.), Using Eye Movements as an Experimental Probe of Brain Function - a Symposium in Honor of Jean Buttner-Ennever. Elsevier Science Bv, Amsterdam, pp. 353-362.
Jansen, J.A., Vanderwaerden, J., Degroot, K., 1990. WOUND-HEALING PHENOMENA AROUND PERCUTANEOUS DEVICES IMPLANTED IN RABBITS. J. Mater. Sci.-Mater. Med. 1, 192-197.
Jarrell, J.R.F., B.J.; Kistenberg, R.S.; Dalton, J.F., IV; Pitkin, M.; Prilutsky, B.I., 2014. Hindlimb kinetics of level and slope walking in the cat with a trans-tibial osseointegrated prosthesis, World Congress of Biomechanics, Boston, MA.
Jarrell, J.R.F., B.J.; Kistenberg, R.S.; Dalton, J.F., IV; Pitkin, M.; Prilutsky, B.I., 2016. Cat level and slope walking with a transtibial osseointegrated prosthesis, First

International Symposium on Innovations in Amputation Surgery and Prosthetic Technologies, Chicago, IL.
Jarrell, J.R.F., B.J.; Kistenberg, R.S.; Dalton, J.F., IV; Pitkin, M.; Prilutsky, B.I., 2017. Kinetics of quadrupedal level and slope walking in the cat with a unilateral transtibial prosthesis anchored to the bone via a porous titanium pylon, 7th International Conference on the Advances in Orthopaedic Osseointegration, Coronado, CA.
Jeans, K.A., Browne, R.H., Karol, L.A., 2011. Effect of Amputation Level on Energy Expenditure During Overground Walking by Children with an Amputation. J. Bone Joint Surg.-Am. Vol. 93A, 49-56.
Jeyapalina, S., Beck, J.P., Bachus, K.N., Chalayon, O., Bloebaum, R.D., 2014a. Radiographic Evaluation of Bone Adaptation Adjacent to Percutaneous Osseointegrated Prostheses in a Sheep Model. Clin. Orthop. Rel. Res. 472, 2966-2977.
Jeyapalina, S., Beck, J.P., Bachus, K.N., Williams, D.L., Bloebaum, R.D., 2012. Efficacy of a porous-structured titanium subdermal barrier for preventing infection in percutaneous osseointegrated prostheses. J. Orthop. Res. 30, 1304-1311.
Jeyapalina, S., Beck, J.P., Bloebaum, R.D., Bachus, K.N., 2014b. Progression of Bone Ingrowth and Attachment Strength for Stability of Percutaneous Osseointegrated Prostheses. Clin. Orthop. Rel. Res. 472, 2957-2965.
Jonsson, S., Caine-Winterberger, K., Branemark, R., 2011. Osseointegration amputation prostheses on the upper limbs: methods, prosthetics and rehabilitation. Prosthetics and Orthotics International 35, 190-200.
Juhnke, D.L., Aschoff, H.H., 2015. Endo-exo prostheses following limb-amputation. Orthopade 44, 419-425.
Kajrolkar, T., Yang, F., Pai, Y.C., Bhatt, T., 2014. Dynamic stability and compensatory stepping responses during anterior gait-slip perturbations in people with chronic hemiparetic stroke. J. Biomech. 47, 2751-2758.
Khiri, F., Karimi, M.T., Fatoye, F., Jamshidi, N., 2015. AN ASSESSMENT OF STABILITY, GAIT PERFORMANCE AND ENERGY CONSUMPTION IN INDIVIDUALS WITH TRANSFEMORAL AMPUTATION. J. Mech. Med. Biol. 15, 15.
Kirpensteijn, J., Van den Bos, R., Endenburg, N., 1999. Adaptation of dogs to the amputation of a limb and their owners' satisfaction with the procedure. Vet. Rec. 144, 115-118.
Kirpensteijn, J., Van den Bos, R., Van den Brom, W.E., Hazewinkel, H.A.W., 2000. Ground reaction force analysis of large breed dogs when walking after the amputation of a limb. Vet. Rec. 146, 155-159.
Koc, E., Tunca, M., Akar, A., Erbil, H., Demiralp, B., Arca, E., 2008. Skin problems in amputees: a descriptive study. Int. J. Dermatol. 47, 463-466.
Kramer, M.J., Tanner, B.J., Horvai, A.E., O'Donnell, R.J., 2008. Compressive osseointegration promotes viable bone at the endoprosthetic interface: retrieval study of Compress((R)) implants. Int. Orthop. 32, 567-571.
Kuntz, C.A., Asselin, T.L., Dernell, W.S., Powers, B.E., Straw, R.C., Withrow, S.J., 1998. Limb salvage surgery for osteosarcoma of the proximal humerus: Outcome in 17 dogs. Vet. Surg. 27, 417-422.

Lajoie, Y., Gallagher, S.P., 2004. Predicting falls within the elderly community: comparison of postural sway, reaction time, the Berg balance scale and the Activities-specific Balance Confidence (ABC) scale for comparing fallers and non-fallers. Arch. Gerontol. Geriatr. 38, 11-26.
Lammers, A.R., Zurcher, U., 2011. Torque around the center of mass: dynamic stability during quadrupedal arboreal locomotion in the Siberian chipmunk (Tamias sibiricus). Zoology 114, 95-103.
Lanyon, L.E., Rubin, C.T., 1984. STATIC VS DYNAMIC LOADS AS AN INFLUENCE ON BONE REMODELING. J. Biomech. 17, 897-905.
Lascelles, B.D.X., Dernell, W.S., Correa, M.T., Lafferty, M., Devitt, C.M., Kuntz, C.A., Straw, R.C., Withrow, S.J., 2005. Improved survival associated with postoperative wound infection in dogs treated with limb-salvage surgery for osteosarcoma. Ann. Surg. Oncol. 12, 1073-1083.
Laskomccarthey, P., Beuter, A., Biden, E., 1990. KINEMATIC VARIABILITY AND RELATIONSHIPS CHARACTERIZING THE DEVELOPMENT OF WALKING. Dev. Psychobiol. 23, 809-837.
Lavoie, S., McFadyen, B., Drew, T., 1995. A kinematic and kinetic analysis of locomotion during voluntary gait modification in the cat. Exp Brain Res 106, 39-56.
Lay, A.N., Hass, C.J., Gregor, R.J., 2006. The effects of sloped surfaces on locomotion: A kinematic and kinetic analysis. J. Biomech. 39, 1621-1628.
Lelas, J.L., Merriman, G.J., Riley, P.O., Kerrigan, D.C., 2003. Predicting peak kinematic and kinetic parameters from gait speed. Gait Posture 17, 106-112.
Liptak, J.M., Dernell, W.S., Ehrhart, N., Lafferty, M.H., Monteith, G.J., Withrow, S.J., 2006. Cortical allograft and endoprosthesis for limb-sparing surgery in dogs with distal radial osteosarcoma: A prospective clinical comparison of two different limb-sparing techniques. Vet. Surg. 35, 518-533.
Lu, J., Liong, M., Li, Z.X., Zink, J.I., Tamanoi, F., 2010. Biocompatibility, Biodistribution, and Drug-Delivery Efficiency of Mesoporous Silica Nanoparticles for Cancer Therapy in Animals. Small 6, 1794-1805.
Lu, T.-W., Chang, C.-F., 2012. Biomechanics of human movement and its clinical applications. The Kaohsiung Journal of Medical Sciences 28, S13-S25.
Lundberg, M., Hagberg, K., Bullington, J., 2011. My prosthesis as a part of me: a qualitative analysis of living with an osseointegrated prosthetic limb. Prosthetics and Orthotics International 35, 207-214.
Lundborg, G., Waites, A., Bjoerkman, A., Rosen, B., Larsson, E.M., 2006. Functional magnetic resonance imaging shows cortical activation on sensory stimulation of an osseointegrated prosthetic thumb. Scand. J. Plast. Reconstr. Surg. Hand Surg. 40, 234-239.
Lyon, C.C., Kulkarni, J., Zimerson, E., Van Ross, E., Beck, M.H., 2000. Skin disorders in amputees. J. Am. Acad. Dermatol. 42, 501-507.
Malgaigne, J.F., 2007. Double vertical fractures of the pelvis (Reprinted from Treatise on Fractures, pg 523, 1859). Clin. Orthop. Rel. Res., 17-19.
Manderson, R.D., 1972. EXPERIMENTAL INTRA-OSSEOUS IMPLANTATION IN JAWS OF PIGS. Dental Practitioner and Dental Record 22, 225-+.

Markin, S.N., Klishko, A.N., Shevtsova, N.A., Lemay, M.A., Prilutsky, B.I., Rybak, I.A., 2016. A Neuromechanical Model of Spinal Control of Locomotion. Springer, New York.
McFadyen, B.J., Lavoie, S., Drew, T., 1999. Kinetic and energetic patterns for hindlimb obstacle avoidance during cat locomotion. Exp Brain Res 125, 502-510.
McKay, J.L., Welch, T.D., Vidakovic, B., Ting, L.H., 2013. Statistically significant contrasts between EMG waveforms revealed using wavelet-based functional ANOVA. J Neurophysiol 109, 591-602.
Meulenbelt, H.E.J., Geertzen, J.H.B., Dijkstra, P.U., Jonkman, M.F., 2007. Skin problems in lower limb amputees: an overview by case reports. J. Eur. Acad. Dermatol. Venereol. 21, 147-155.
Mich, P.M., 2014. The Emerging Role of Veterinary Orthotics and Prosthetics (V-OP) in Small Animal Rehabilitation and Pain Management. Top. Companion Anim. Med. 29, 10-19.
Miller, W.C., Speechley, M., Deathe, B., 2001. The prevalence and risk factors of falling and fear of falling among lower extremity amputees. Arch. Phys. Med. Rehabil. 82, 1031-1037.
Mitchell, K.E., Boston, S.E., Kung, M., Dry, S., Straw, R.C., Ehrhart, N.P., Ryan, S.D., 2016. Outcomes of Limb-Sparing Surgery Using Two Generations of Metal Endoprosthesis in 45 Dogs With Distal Radial Osteosarcoma. A Veterinary Society of Surgical Oncology Retrospective Study. Vet. Surg. 45, 36-43.
Montanaro, L., Testoni, F., Poggi, A., Visai, L., Speziale, P., Arciola, C.R., 2011. Emerging pathogenetic mechanisms of the implant-related osteomyelitis by Staphylococcus aureus. Int. J. Artif. Organs 34, 781-788.
Morone, G., Annicchiarico, R., Iosa, M., Federici, A., Paolucci, S., Cortes, U., Caltagirone, C., 2016. Overground walking training with the i-Walker, a robotic servo-assistive device, enhances balance in patients with subacute stroke: a randomized controlled trial. J. NeuroEng. Rehabil. 13, 10.
Murphy, E.F., 1973. History and philosophy of attachment of prostheses to the musculo-skeletal system and of passage through the skin with inert materials. J Biomed Mater Res 7, 275-295.
Murray, M.P., Seireg, A.A., Sepic, S.B., 1975. NORMAL POSTURAL STABILITY AND STEADINESS - QUANTITATIVE ASSESSMENT. J. Bone Joint Surg.-Am. Vol. A 57, 510-516.
Nerlich, A.G., Zink, A., Szeimies, U., Hagedorn, H.G., 2000. Ancient Egyptian prosthesis of the big toe. Lancet 356, 2176-2179.
Nott, C.R., Neptune, R.R., Kautz, S.A., 2014. Relationships between frontal-plane angular momentum and clinical balance measures during post-stroke hemiparetic walking. Gait Posture 39, 129-134.
Oddsson, L.I.E., Wall, C., McPartland, M.D., Krebs, D.E., Tucker, C.A., 2004. Recovery from perturbations during paced walking. Gait Posture 19, 24-34.
Olney, S.J., Griffin, M.P., Monga, T.N., McBride, I.D., 1991. WORK AND POWER IN GAIT OF STROKE PATIENTS. Arch. Phys. Med. Rehabil. 72, 309-314.
Ortiz-Catalan, M., Hakansson, B., Branemark, R., 2014. An osseointegrated human-machine gateway for long-term sensory feedback and motor control of artificial limbs. Sci. Transl. Med. 6, 8.

Pai, Y.C., Patton, J., 1997. Center of mass velocity-position predictions for balance control. J. Biomech. 30, 347-354.
Palmquist, A., Jarmar, T., Emanuelsson, L., Branemark, R., Engqvist, H., Thomsen, P., 2008. Forearm bone-anchored amputation prosthesis - A case study on the osseointegration. Acta Orthop. 79, 78-85.
Pan, Y.T., Yoon, H.U., Hur, P., 2017. A Portable Sensory Augmentation Device for Balance Rehabilitation Using Fingertip Skin Stretch Feedback. IEEE Trans. Neural Syst. Rehabil. Eng. 25, 28-36.
Park, H., Mehta, R., DeWeerth, S.P., Prilutsky, B.I., Year Modulation of input from paw cutaneous afferents and quadriceps-sartorius stretch afferents differentially affects lateral static and dynamic stability during cat split-belt locomotion. In Society for Neuroscience Meeting. San Diego, CA.
Park, H.M., R.; DeWeerth, S.P.; Prilutsky, B.I.,, 2017. Modulation of input from paw cutaneous afferents and quadriceps-sartorius stretch afferents differentially affects lateral static and dynamic stability during cat split-belt locomotion, Society for Neuroscience Meeting, San Diego, CA.
Pearson, K.G., 2008. Role of sensory feedback in the control of stance duration in walking cats. Brain Res. Rev. 57, 222-227.
Pearson, O.M., Lieberman, D.E., 2004. The aging of Wolff's "Law": Ontogeny and responses to mechanical loading in cortical bone, in: Stinson, S. (Ed.), Yearbook of Physical Anthropology, Vol 47. Wiley-Liss, Inc, New York, pp. 63-99.
Peebles, A.T., Reinholdt, A., Bruetsch, A.P., Lynch, S.G., Huisinga, J.M., 2016. Dynamic margin of stability during gait is altered in persons with multiple sclerosis. J. Biomech. 49, 3949-3955.
Pendegrass, C.J., Goodship, A.E., Blunn, G.W., 2006a. Development of a soft tissue seal around bone-anchored transcutaneous amputation prostheses. Biomaterials 27, 4183-4191.
Pendegrass, C.J., Goodship, A.E., Price, J.S., Blunn, G.W., 2006b. Nature's answer to breaching the skin barrier: an innovative development for amputees. J. Anat. 209, 59-67.
Pendegrass, C.J., Gordon, D., Middleton, C.A., Sun, S.N.M., Blunn, G.W., 2008. Sealing the skin barrier around transcutaneous implants - In vitro study of keratinocyte proliferation and adhesion in response to surface modifications of titanium alloy. J. Bone Joint Surg.-Br. Vol. 90B, 114-121.
Perry, E.L., Beck, J.P., Williams, D.L., Bloebaum, R.D., 2010. Assessing Peri-Implant Tissue Infection Prevention in a Percutaneous Model. J. Biomed. Mater. Res. Part B 92B, 397-408.
Pickle, N.T., Wilken, J.M., Whitehead, J.M.A., Silverman, A.K., 2016. Whole-body angular momentum during sloped walking using passive and powered lower-limb prostheses. J. Biomech. 49, 3397-3406.
Pitkin, M., 2013. Design features of implants for direct skeletal attachment of limb prostheses. J. Biomed. Mater. Res. Part A 101, 3339-3348.
Pitkin, M., Cassidy, C., Muppavarapu, R., Edell, D., 2012a. Recording of electric signal passing through a pylon in direct skeletal attachment of leg prostheses with neuromuscular control. IEEE transactions on bio-medical engineering 59, 1349-1353.

Pitkin, M., Pilling, J., Raykhtsaum, G., 2012b. Mechanical properties of totally permeable titanium composite pylon for direct skeletal attachment. J. Biomed. Mater. Res. Part B 100B, 993-999.
Pitkin, M., Raykhtsaum, G., Pilling, J., Galibin, O.V., Protasov, M.V., Chihovskaya, J.V., Belyaeva, I.G., Blinova, M.I., Yudintseva, N.M., Potokin, I.L., Pinaev, G.P., Moxson, V., Duz, V., 2007. Porous composite prosthetic pylon for integration with skin and bone. Journal of Rehabilitation Research and Development 44, 723-738.
Pitkin, M., Raykhtsaum, G., Pilling, J., Shukeylo, Y., Moxson, V., Duz, V., Lewandowski, J., Connolly, R., Kistenberg, R.S., Dalton, J.F., Prilutsky, B., Jacobson, S., 2009. Mathematical modeling and mechanical and histopathological testing of porous prosthetic pylon for direct skeletal attachment. Journal of Rehabilitation Research and Development 46, 315-330.
Pitkin, M.R., G., 2012. Skin integrated device, in: Office, U.P. (Ed.).
Pontzer, H., Raichlen, D.A., Rodman, P.S., 2014. Bipedal and quadrupedal locomotion in chimpanzees. Journal of Human Evolution 66, 64-82.
Potocanac, Z., Pijnappels, M., Verschueren, S., van Dieen, J., Duysens, J., 2016. Two-stage muscle activity responses in decisions about leg movement adjustments during trip recovery. J Neurophysiol 115, 143-156.
Prilutsky, B.I., Klishko, A.N., 2011. Control of locomotion: Lessons from whole-body biomechanical analysis, in: Danion, F., Latash, M.L. (Eds.), Motor control: Theories experiments and applications. Oxford University Press, Oxford, pp. 197-218.
Prilutsky, B.I., Maas, H., Bulgakova, M., Hodson-Tole, E.F., Gregor, R.J., 2011. Short-term motor compensations to denervation of feline soleus and lateral gastrocnemius result in preservation of ankle mechanical output during locomotion. Cells, tissues, organs 193, 310-324.
Prilutsky, B.I., Sirota, M.G., Gregor, R.J., Beloozerova, I.N., 2005. Quantification of motor cortex activity and full-body biomechanics during unconstrained locomotion. J Neurophysiol 94, 2959-2969.
Proske, U., Gandevia, S.C., 2012. THE PROPRIOCEPTIVE SENSES: THEIR ROLES IN SIGNALING BODY SHAPE, BODY POSITION AND MOVEMENT, AND MUSCLE FORCE. Physiological reviews 92, 1651-1697.
Rajan, S., 2012. Skin and soft-tissue infections: Classifying and treating a spectrum. Clevel. Clin. J. Med. 79, 57-66.
Ramstrand, N., Nilsson, K.A., 2009. A comparison of foot placement strategies of transtibial amputees and able-bodied subjects during stair ambulation. Prosthetics and Orthotics International 33, 348-355.
Raphel, J., Holodniy, M., Goodman, S.B., Heilshorn, S.C., 2016. Multifunctional coatings to simultaneously promote osseointegration and prevent infection of orthopaedic implants. Biomaterials 84, 301-314.
Redfern, M.S., Cham, R., Gielo-Perczak, K., Gronqvist, R., Hirvonen, M., Lanshammar, H., Marpet, M., Pai, C.Y., Powers, C., 2001. Biomechanics of slips. Ergonomics 44, 1138-1166.
Robert, T., Bennett, B.C., Russell, S.D., Zirker, C.A., Abel, M.F., 2009. Angular momentum synergies during walking. Exp. Brain Res. 197, 185-197.

Robling, A.G., Castillo, A.B., Turner, C.H., 2006. Biomechanical and molecular regulation of bone remodeling. Annu. Rev. Biomed. Eng. 8, 455-498.
Rudy, R.J., Levi, P.A., Bonacci, F.J., Weisgold, A.S., Engler-Hamm, D., 2008. Intraosseous anchorage of dental prostheses: an early 20th century contribution. Compend Contin Educ Dent 29, 220-222, 224, 226-228 passim.
Ruff, C., Holt, B., Trinkaus, E., 2006. Who's afraid of the big bad wolff? "Wolff is law" and bone functional adaptation. Am. J. Phys. Anthropol. 129, 484-498.
Saunders, M.M., Brecht, J.S., Verstraete, M.C., Kay, D.B., Njus, G.O., 2012. Lower Limb Direct Skeletal Attachment. A Yucatan Micropig Pilot Study. J. Invest. Surg. 25, 387-397.
Segal, A.D., Orendurff, M.S., Mute, G.K., McDowell, M.L., Pecoraro, J.A., Shofer, J., Czerniecki, J.M., 2006. Kinematic and kinetic comparisons of transfemoral amputee gait using C-Leg (R) and Mauch SNS (R) prosthetic knees. Journal of Rehabilitation Research and Development 43, 857-869.
Segers, V., De Smet, K., Van Caekenberghe, I., Aerts, P., De Clercq, D., 2013. Biomechanics of spontaneous overground walk-to-run transition. J. Exp. Biol. 216, 3047-3054.
Sheehan, R.C., Beltran, E.J., Dingwell, J.B., Wilken, J.M., 2015. Mediolateral angular momentum changes in persons with amputation during perturbed walking. Gait Posture 41, 795-800.
Shelton, T.J., Beck, J.P., Bloebaum, R.D., Bachus, K.N., 2011. Percutaneous osseointegrated prostheses for amputees: Limb compensation in a 12-month ovine model. J. Biomech. 44, 2601-2606.
Shevtsov, M.A., Yudintceva, N., Blinova, M., Pinaev, G., Galibin, O., Potokin, I., Popat, K.C., Pitkin, M., 2015. Application of the skin and bone integrated pylon with titanium oxide nanotubes and seeded with dermal fibroblasts. Prosthetics and Orthotics International 39, 477-486.
Shin, Y.G., Kim, S.Y., Lee, H.K., Jeong, C.M., Lee, S.H., Huh, J.B., 2016. Effect of Double Screw on Abutment Screw Loosening in Single-Implant Prostheses. Int. J. Prosthodont. 29, 445-447.
Silverman, A.K., Fey, N.P., Portillo, A., Walden, J.G., Bosker, G., Neptune, R.R., 2008. Compensatory mechanisms in below-knee amputee gait in response to increasing steady-state walking speeds. Gait Posture 28, 602-609.
Silverman, A.K., Neptune, R.R., 2011. Differences in whole-body angular momentum between below-knee amputees and non-amputees across walking speeds. J. Biomech. 44, 379-385.
Silverman, A.K., Wilken, J.M., Sinitski, E.H., Neptune, R.R., 2012. Whole-body angular momentum in incline and decline walking. J Biomech 45, 965-971.
SilverThorn, M.B., Steege, J.W., Childress, D.S., 1996. A review of prosthetic interface stress investigations. Journal of Rehabilitation Research and Development 33, 253-266.
Smith, D.G., Ehde, D.M., Legro, M.W., Reiber, G.E., del Aguila, M., Boone, D.A., 1999. Phantom limb, residual limb, and back pain after lower extremity amputations. Clin. Orthop. Rel. Res., 29-38.

Sundfeldt, M., Carlsson, L.V., Johansson, C.B., Thomsen, P., Gretzer, C., 2006. Aseptic loosening, not only a question of wear - A review of different theories. Acta Orthop. 77, 177-197.
Sutherland, D.H., 2001. The evolution of clinical gait analysis part l: kinesiological EMG. Gait Posture 14, 61-70.
Szewczyk, M., Lechowski, R., Zabielska, K., 2015. What do we know about canine osteosarcoma treatment? - review. Vet. Res. Commun. 39, 61-67.
Tami, A.E., Nasser, P., Verborgt, O., Schaffler, M.B., Tate, M.L.K., 2002. The role of interstitial fluid flow in the remodeling response to fatigue loading. J. Bone Miner. Res. 17, 2030-2037.
Thi, M.M., Kojima, T., Cowin, S.C., Weinbaum, S., Spray, D.C., 2003. Fluid shear stress remodels expression and function of junctional proteins in cultured bone cells. Am. J. Physiol.-Cell Physiol. 284, C389-C403.
Thurston, A.J., 2007. Pare and prosthetics: The early history of artificial limbs. ANZ J. Surg. 77, 1114-1119.
Tillander, J., Hagberg, K., Hagberg, L., Branemark, R., 2010. Osseointegrated Titanium Implants for Limb Prostheses Attachments: Infectious Complications. Clin. Orthop. Rel. Res. 468, 2781-2788.
Tjellstrom, A., Hakansson, B., Granstrom, G., 2001. Bone-anchored hearing aids - Current status in adults and children. Otolaryngol. Clin. N. Am. 34, 337-+.
Torcasio, A., van Lenthe, G.H., Van Oosterwyck, H., 2008. THE IMPORTANCE OF LOADING FREQUENCY, RATE AND VIBRATION FOR ENHANCING BONE ADAPTATION AND IMPLANT OSSEOINTEGRATION. Eur. Cells Mater. 16, 56-66.
Tranberg, R., Zugner, R., Karrholm, J., 2011. Improvements in hip- and pelvic motion for patients with osseointegrated trans-femoral prostheses. Gait Posture 33, 165-168.
Tsikandylakis, G., Berlin, O., Branemark, R., 2014. Implant Survival, Adverse Events, and Bone Remodeling of Osseointegrated Percutaneous Implants for Transhumeral Amputees. Clin. Orthop. Rel. Res. 472, 2947-2956.
Tuan, R.S., 2011. Role of Adult Stem/Progenitor Cells in Osseointegration and Implant Loosening. Int. J. Oral Maxillofac. Implants 26, 50-62.
Van de Meent, H., Hopman, M.T., Frolke, J.P., 2013. Walking Ability and Quality of Life in Subjects With Transfemoral Amputation: A Comparison of Osseointegration With Socket Prostheses. Arch. Phys. Med. Rehabil. 94, 2174-2178.
Verghese, J., Holtzer, R., Lipton, R.B., Wang, C., 2009. Quantitative gait markers and incident fall risk in older adults. J Gerontol A Biol Sci Med Sci 64, 896-901.
Vistamehr, A., Kautz, S.A., Bowden, M.G., Neptune, R.R., 2016. Correlations between measures of dynamic balance in individuals with post-stroke hemiparesis. J. Biomech. 49, 396-400.
von Recum, A.F., 1984. Applications and failure modes of percutaneous devices: a review. J Biomed Mater Res 18, 323-336.
Vonrecum, A.F., 1984. APPLICATIONS AND FAILURE MODES OF PERCUTANEOUS DEVICES - A REVIEW. J. Biomed. Mater. Res. 18, 323-336.

Wanntorp, H., 1960. STUDIES ON CHEMICAL DETERMINATION OF WARFARIN AND COUMACHLOR AND THEIR TOXICITY FOR DOG AND SWINE. Acta Pharmacologica Et Toxicologica 16, 1-123.
Weinbaum, S., Cowin, S.C., Zeng, Y., 1994. A MODEL FOR THE EXCITATION OF OSTEOCYTES BY MECHANICAL LOADING-INDUCED BONE FLUID SHEAR STRESSES. J. Biomech. 27, 339-360.
Weishaupt, M.A., Wiestner, T., Hogg, H.P., Jordan, P., Auer, J.A., 2004. Compensatory load redistribution of horses with induced weightbearing hindlimb lameness trotting on a treadmill. Equine Vet J 36, 727-733.
Whelan, P.J., 1996. Control of locomotion in the decerebrate cat. Prog. Neurobiol. 49, 481-515.
White, A., Wallis, G., 2001. Endochondral ossification: A delicate balance between growth and mineralisation. Curr. Biol. 11, R589-R591.
Wilson, A.B., 1970. Limb Prosthetics - 1970. Artificial Limbs 14, 1-52.
Winter, D.A., Sienko, S.E., 1988. Biomechanics of below-knee amputee gait. J Biomech 21, 361-367.
Winter, G.D., 1974. Transcutaneous implants: reactions of the skin-implant interface. J Biomed Mater Res 8, 99-113.
Withrow, S.J., Hirsch, V.M., 1979. OWNER RESPONSE TO AMPUTATION OF A PETS LEG. Veterinary Medicine & Small Animal Clinician 74, 332-&.
Witso, E., Kristensen, T., Benum, P., Sivertsen, S., Persen, L., Funderud, A., Magne, T., Aursand, H.P., Aamodt, A., 2006. Improved comfort and function of arm prosthesis after implantation of a Humerus-T-Prosthesis in trans-humeral amputees. Prosthetics and Orthotics International 30, 270-278.
You, J., Yellowley, C.E., Donahue, H.J., Zhang, Y., Chen, Q., Jacobs, C.R., 2000. Substrate deformation levels associated with routine physical activity are less stimulatory to bone cells relative to loading-induced oscillatory fluid flow. J. Biomech. Eng.-Trans. ASME 122, 387-393.
You, L.D., Cowin, S.C., Schaffler, M.B., Weinbaum, S., 2001. A model for strain amplification in the actin cytoskeleton of osteocytes due to fluid drag on pericellular matrix. J. Biomech. 34, 1375-1386.
You, L.D., Temiyasathit, S., Lee, P.L., Kim, C.H., Tummala, P., Yao, W., Kingery, W., Malone, A.M., Kwon, R.Y., Jacobs, C.R., 2008. Osteocytes as mechanosensors in the inhibition of bone resorption due to mechanical loading. Bone 42, 172-179.
Zarb, G.A., Symington, J.M., 1983. OSSEOINTEGRATED DENTAL IMPLANTS - PRELIMINARY-REPORT ON A REPLICATION STUDY. J. Prosthet. Dent. 50, 271-276.
Zhang, M., Turner-Smith, A.R., Tanner, A., Roberts, V.C., 1998. Clinical investigation of the pressure and shear stress on the trans-tibial stump with a prosthesis. Medical Engineering & Physics 20, 188-198.
Zhang, M., TurnerSmith, A.R., Roberts, V.C., Tanner, A., 1996. Frictional action at lower limb prosthetic socket interface. Medical Engineering & Physics 18, 207-214.

VITA

JOSHUA R. JARRELL

Josh was born and raised in Richmond, Virginia. After graduating from the Mathematics and Science High School in Chesterfield County, Virginia, he enlisted in the Army Reserves, completed his basic training, and then began his undergraduate degree at Auburn University. He graduated with a B.S. in Applied Mathematics in 2005 and enlisted into Special Forces, the Army Green Berets, as a medical sergeant. In 2012 Josh moved to Atlanta to begin his pre-doctoral studies in Applied Physiology at the Georgia Institute of Technology. Outside of his research work, Josh stays very active with his National Guard unit, and with this wife and their three young children.